Alma Mater Studiorum - Università di Bologna

DOTTORATO DI RICERCA IN

CHIMICA

Ciclo XXVIII

Settore concorsuale di afferenza: 03/C2

Settore scientifico disciplinare: CHIM/04

SUSTAINABLE CATALYTIC PROCESS FOR THE SYNTHESIS OF NIACIN

Presentata da

Massimiliano Mari

Coordinatore dottorato

Prof. **Aldo Roda**

Relatore

Prof. **Fabrizio Cavani**

Esame finale anno 2016

Niacin

Nicotinates production

2-methylglutaronitrile

β-picoline oxidation

Vanadia-zirconia catalyst

Zirconium pyrovanadate

Vanadyl pyrophosphate

in-situ Raman spectroscopy

Abstract

Nicotinic acid (niacin) is an important vitamin of the B group, with an annual production close to 40,000 tons. It is used in medicine, food industry, agriculture and in production of cosmetics. Older industrial processes have drawbacks such as a low atomic efficiency and the use of toxic catalysts or stoichiometric oxidants. Several studies were carried out during latest years on new technologies for the synthesis of niacin and nicotinate precursors, such as 3-picoline and pyridine-3-nitrile. This thesis reports about the results of three different research projects; the first was aimed at the study of the one-step production of pyridine-3-nitrile starting from 2-methylglutaronitrile, the second at acetaldehyde/acetonitrile condensation for 3-picoline synthesis, and the third at investigating the reactivity of supported vanadium oxide catalysts for the direct gas-phase oxidation of 3-picoline with air; this process would be more sustainable compared to both older ones and some of those currently used for niacin production. For the first two research projects, a catalysts screening was carried out; however, results were not satisfactory. The third project involved the preparation, characterisation and reactivity testing of different zirconia-supported V_2O_5 catalysts. The effect of parameters, such as the Vanadium oxide loading and specific surface area, on catalytic performance were studied. Operative conditions such as temperature, contact time and feed composition were optimized. Yields to nicotinic acid close to the best ones reported in the literature were achieved; moreover, catalysts based on V_2O_5/ZrO_2 were found to be remarkably active. Catalysts were characterized by means of XRD and in-situ Raman spectroscopy in the aim of finding correlations between catalytic performances and physic-chemical properties. In some cases, ZrV_2O_7 formed during the reaction.

Vanadyl-pyrophosphate was also tested as the catalyst for 3-picoline oxidation, but its performance was lower compared to that one shown by V_2O_5/ZrO_2.

Summary

Summary

1 Introduction

Over the past few years, environmental problems such as climate change and air pollution have become more and more important due to their effect on the human being wellness and the future sustainability of Earth resources. Because of these reasons, the application of the "green chemistry" principles has become the driving force for the development of new industrial catalytic processes, in order to reduce human activities footprint and consumption of natural resources such as mineral feedstock, energy, water, air and soil for waste disposal.

At the same time, the market is creating the conditions for the application of the green chemistry principles; the increase of feedstock prices is setting a new challenge for more feedstock-intensive processes, in the context of a worldwide market competition.

Many governments, especially in the EU, are setting a new economical challenge for less polluting processes, for example with the application of "green taxes" [1-2].

All chemical processes, in the future, will have to follow these rules; obviously, the bigger the size of the chemical plant, the higher are the problems to deal with, but also small plants, typically used for fine chemicals production, have to deal with the same problems, related, for instance, to the large amount of waste produced or to highly pollutant reactants they make use of.

One the most impressive example of chemical processes which has been undergoing remarkable changes over the latest 20 years, toward more sustainable, albeit economically viable, technologies is the synthesis of niacin. Many processes for niacin production have been developed during the latest decades, and most of them will be analysed in detail later in this thesis. More importantly, only few of them fit the green chemistry principles.

Therefore, with the aim of exploring new synthetic and more sustainable routes for niacin production, we decided to investigate on alternative technologies. This thesis reports about the results of my research work aimed at the study of innovative synthetic approaches.

1.1 Uses and market of niacin

The term niacin commercially indicates nicotinic acid and/or a mixture of nicotinic acid and nicotinic amide; indeed, nicotinic acid cannot be directly converted into nicotinamide, and both compounds, in vivo, are precursors of the coenzymes nicotinamide adenine dinucleotide (NAD) and nicotinamide adenine dinucleotide phosphate (NADP), which participate in oxidation–reduction cycles in living cells [3].

Nicotinic acid can be synthesized by human cells using the essential aminoacid tryptophan but with a very low yield, anyway a balanced and varied diet can ensure the total intake of RDA. In the past, especially poor people could not have a diversified diet; in countries where the diet was based on corn, as in northern Italy, France and Spain, pellagra disease was endemic; also in the USA it caused more than 100.000 deaths between 1900 and 1940. In 1937, Dr. Spies and Dr. Frostig [4] discovered that the lack of niacin was the cause for pellagra and the disease was defeated; the number of deaths due to the niacin deficiency disease pellagra dropped in the US from over 7500 to 70 from 1929 to 1956 [5]. Nowadays pellagra is no more present in developed countries unless few cases in patients that have severe alcoholism problems.

For this reason, the substance was first known as vitamin PP (pellagra preventer) and only more recently as vitamin B3.

Niacin is naturally present in foodstuff, high levels are contained in liver, beef and fish, and in yeast and wheat too. Corn also contains good level of niacin but, unfortunately, it is unavailable for human beings.

Nowadays, at least in developed countries, nutritional deficiency is not a problem, many illnesses are related to the opposite problem, the excess of nutrition, but niacin is still valuable for our health, being used for the treatment of hypercholesterolemia [6-7-8]. Niacin acts as an inhibitor of cyclic adenosine monophosphate (cAMP) synthesis, which is responsible for the breakdown of fat in adipose tissues, and the free fatty acids formed are metabolized in the liver to form triglycerides and low density lipoprotein (LDL cholesterol) [9-10]. Nicotinic acid also exhibits an action increasing high density lipoprotein (HDL cholesterol), but the mechanism is still under investigation. It's widely used in medicine also for the insulin-mimetic effect.

The purposes above mentioned are the most important in terms of impact over human life but not of absolute quantity used; from this point of view more relevant are the uses in agriculture, namely as additive for animal feed and as plant growth stimulator.

The market for nicotinates, word that indicates nicotinic acid, nicotinamide and their derivatives, mainly used as drugs with modified release, still is increasing despite market world crisis in 2009. The production was 8.500 metric tons in 1980's, grown up until 22.000 in 1995 and 40.000 metric tons in 2006 [11]. It still presents a growth from 3% to 5% per year.

1.2 Past and present technologies for niacin and nicotinates derivatives production

Pyridine and its derivatives have long been investigated since their discovery in 1846. In 1876 the first synthesis of pyridine was reported by Ramsay [12], passing acetylene and hydrogen cyanide through a red-hot tube. More useful for the production of nicotinic acid and derivatives were the works carried out by Hantzsch (1882) [13], and Chichibabin (1905) [14]. The former investigated the reaction between formaldehyde, 2 equivalents of a β-ketoester such as ethylacetoacetate and a nitrogen donor, such as ammonium acetate

or ammonia. The initial reaction product was dihydropyridine which could be oxidized in a subsequent step to pyridine. The driving force for this second reaction step is aromatization. The latter is a method for synthesizing pyridine rings. In its general form, the reaction can be described as a condensation reaction of aldehydes, ketones, α,β-Unsaturated carbonyl compounds, or any combination of the above, with ammonia or ammonia derivatives. These reactions are useful especially for the production of intermediates for niacin synthesis, but unfortunately they show poor selectivity.

1.2.1 Liquid-phase oxidation of nicotine with permanganate, chromic acid etc.

The classic method for the preparation of nicotinic acid is by oxidation of nicotine with potassium dichromate. This was discovered over a hundred years ago. Although no longer relevant today, this reaction serves as an excellent example when considering green technologies.

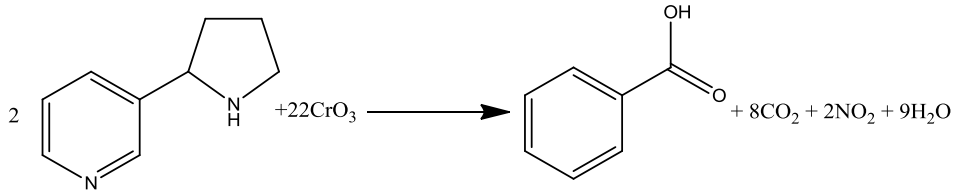

Figure 1 Nicotine oxidation with chromic acid

In those days, the use of nicotine extracted from tobacco as a cheap starting material was chosen because synthetic alkylpyridine was too expensive, since the market and technologies still were not developed.

Chromic acid (CrO_3) is carcinogenic and environmentally threatening. Chromic (III) oxide, on the other hand, is extensively used in the tanning industry, and has a higher present value on the market than its precursor. Assuming an ideal chemical reaction (100% yield), the above reaction gives the following figures:

Nicotine /ton nicotinic acid:	1.32 tons
Chromic acid:	9.02 tons
CO2 produced:	1.43 tons
NOx (calculated as NO2):	0.37 tons
Chromic oxide:	6.80 tons

Thus almost 9 tons of hazardous by-products are produced for 1 ton of the desired product. As seen, this process is quite far from the green chemistry principles: it has low atomic efficiency and a high production of toxic waste, even though the starting material is renewable.

1.2.2 Liquid-phase oxidation of 3-picoline with permanganate, chromic acid or nitric acid

The oxidation of 3-picoline (β-picoline) with permanganate or chromic acid suffers from the same drawbacks, albeit in a lesser form, as for nicotine.

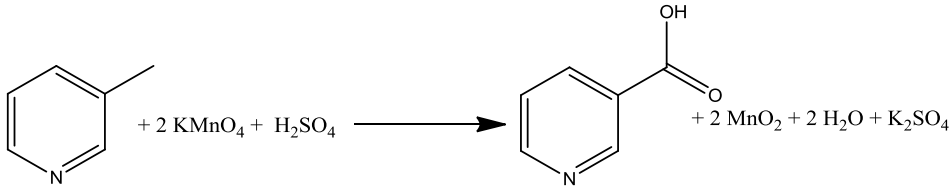

Figure 2 The permanganate oxidation of 3-picoline

For 1 ton of nicotinic acid, 2.8 tons of inorganic material are produced as waste. With chromium trioxide (neglecting any inorganic acid involved to produce the required chromic acid), 1.24 tonnes of Cr_2O_3 are produced/ton of nicotinic acid. This calculation assumes stoichiometric quantities of oxidant and quantitative yields, both of which are in practice unrealistic. A stoichiometric excess of 50 to 100% oxidant is usual, and molar yields of 80-90% are generally not exceeded. Thus, the inorganic waste for the permanganate process would probably lie around 4 tons/ton of niacin produced, and for chromium oxide between 1.7 and 2.0 tons/ton. From an ecological standpoint, this situation is clearly unsustainable. Even though chromium (III) sulphate can be utilised in the

leather industry as a tanning agent, there are several factors which are against this type of process, even if it appears to be economically attractive:

1. The combination of two processes, each one with its economic constraints, into a single one requires that both end products (chromic oxide and nicotinic acid) can be sold. Thus the success of the process is dependent on the demand for both products being sustained. A decline of market demand for one of the two will lead to the process as a whole being unsustainable.
2. The energy required for the production of chromic acid (or permanganate) is considerable. Chromite ore is roasted with sodium carbonate at temperatures around 1000°C to produce the common starting material for most chromium compounds, namely sodium chromate.
3. The environmental problems in the leather industry due to chromium pollution can be solved, but are expensive and the alternatives are not without their own problems.

As explained before, niacin is used as a feed and food additive. The presence of even small quantities of chromium, albeit beneficial (chromium is an essential trace metal in the human metabolism), is not accepted by today's stringent legislation. Removal of last traces of Cr impurity is possible by recrystallization, but this increases the number of unit operations, is expensive and energy consuming, and the problem remains as to what to do with the chromium-containing mother liquors.

1.2.3 Liquid-phase oxidation of MEP with nitric acid

This process has been running for the past 40 years and is very selective. Continuous development and improvement of this process over the years have led to a high-quality product.

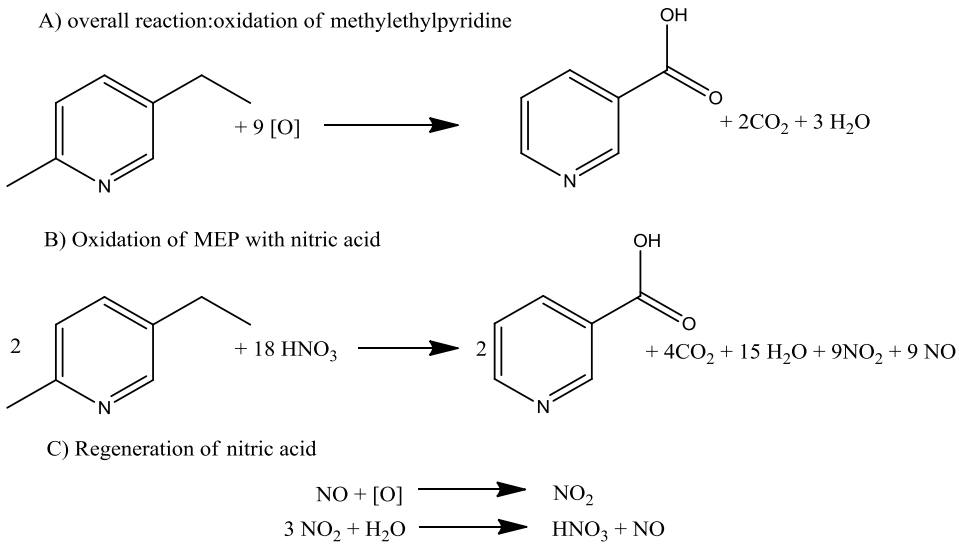

Figure 3 Traditional Process for Preparation of Nicotinic Acid (>15000 tons/year)

Despite the many improvements and developments made to this process, it intrinsically holds some disadvantages, when considered from the "greenness" stand-point:

1. Safety: using nitric acid at high temperatures and pressures requires a well-conceived safety concept, using advanced reaction technology.
2. Ecology (carbon dioxide and nitric oxides): although nitric oxide fumes can be largely regenerated to nitric acid, some nitric oxide (NO) is present in the off-gases, which then have to be catalytically treated to remove the last traces of NOx. Carbon dioxide is vented to the atmosphere. In today's process, over 1 ton of CO_2 is produced per ton of niacin.
3. Downstream processing: in order to produce a compound of quality acceptable for today's standards, extensive processing in the form of recrystallization and decolourising is necessary. Recrystallization is an energy and labour intensive process.
4. Starting-material: although MEP is produced from cheap starting-materials (ammonia and paraldehyde), the process itself

produces considerable quantities of by-products and/or waste material, which have to be separated and suitably treated to avoid environmental pollution. Additionally, the carbon efficiency of the MEP conversion to niacin is at best only 0.75 (2 carbon atoms are burnt off during oxidation), so that from the environmental standpoint, MEP is not the ideal starting material.

Even though also 3-picoline is produced with the Chicibabin reaction (like MEP), there are several reasons for this choice. MEP is synthetized in the liquid phase starting from acetaldehyde and ammonia in a dedicated process, while 3-picoline is produced along with pyridine in a gas-phase process involving acetaldehyde, formaldehyde and ammonia. The process for the liquid-phase synthesis of MEP is more selective (around 70%) then the traditional picoline/pyridine process where 3-picoline comes as a by-product with selectivity around 20%-40%; the economics of the major product (pyridine) determine the price and availability of 3-picoline on the market [15].

The reaction of MEP with nitric acid is selective (>80%), and the resulting nitric oxide gases are recycled and reacted with air and water to reconstitute nitric acid.

1.2.4 Niacinamide process

In order to overcome the disadvantages listed above, a new technology was developed to take over many of the green chemistry principles.

The target of this process is niacinamide, but the latter can be easily converted into nicotinic acid in vivo or with acid hydrolysis.

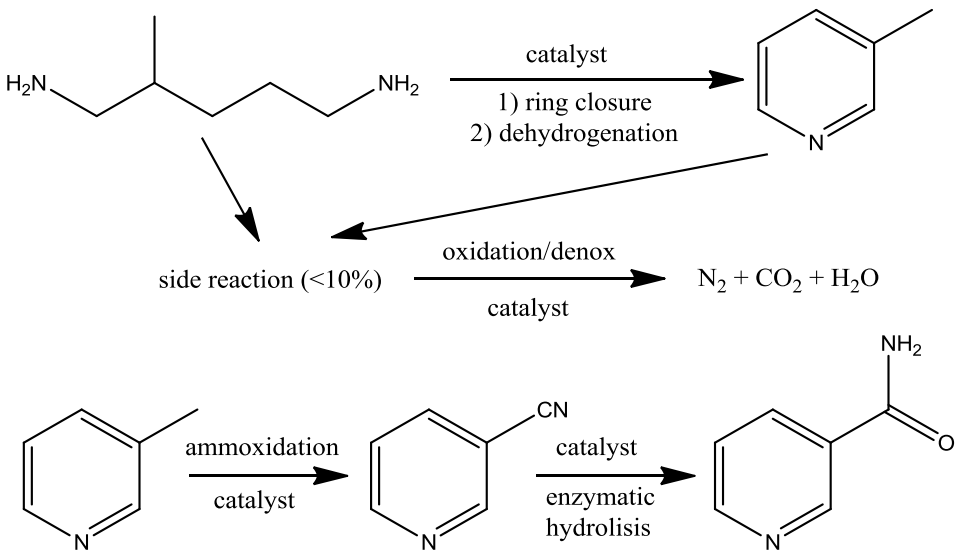

Figure 4 Nicotinamide Process (Guangzhou China)

The advantages of 3-picoline as a starting material and the disadvantages of the main manufacturing method have been described above. In order to avoid the mentioned drawbacks, a 2-stage alternative process has developed starting from 2-methylpentanediamine (MPDA). MPDA is readily obtained by hydrogenation of 2-methylglutaronitrile, the major by-product in the adiponitrile process and, as such, a readily available starting-material (~105 mtpa). In the first stage, MPDA is cyclised to methyl piperidine, which is then dehydrogenated to 3-picoline.

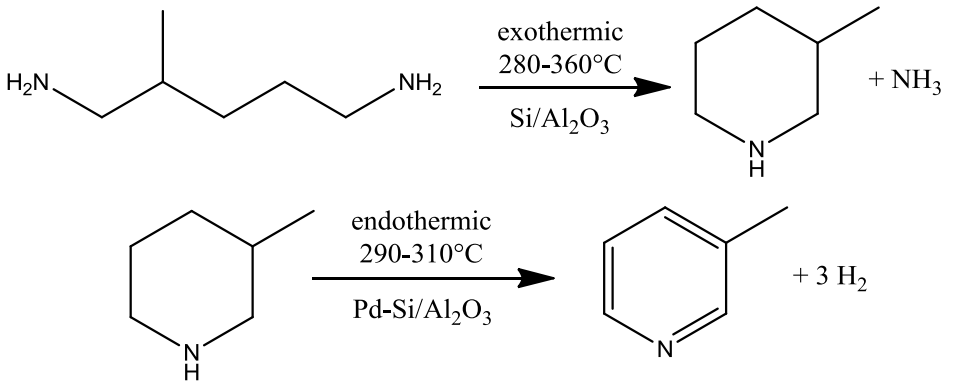

Figure 5 Alternative process for 3-picoline manufacture

Although this route has the same weakness of being coupled to another product (adiponitrile), the foreseeable future of nylon 6,6 and the route to its manufacture (hydrogen cyanide addition to butadiene) seem assured for the next decades. Several advantages, relevant to green chemistry principles, are apparent in this route:

1. The 3-picoline produced has a very high isomeric purity;
2. Picoline is produced in a 2-stage catalytic process which is practically energetically neutral: an endothermic (ring closure) and an exothermic (dehydrogenation) reaction;
3. Ammonia is liberated during the ring closure which can be utilised in a following process;
4. Utilisation of a waste-product; in fact, 2-methylglutaronitrile can be used as a co-monomer in the production of other polyamides, but the end-product niacin has an intrinsically much higher value;

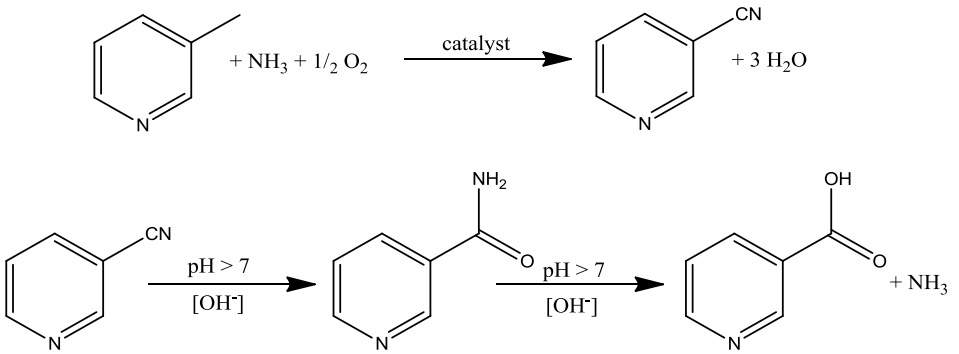

Figure 6 Ammoxidation of 3-picoline and hydrolysis of cyanopyridine to niacinamide and niacin

The process is also a nice example of how in order to reduce the amount of waste produced in a reaction, a starting material of the highest quality is desirable, since any by-product would have to be removed later in the process.

The ammonia co-produced in the cyclization step of MPDA is utilised in the ammoxidation step. This is an example of recycling a by-product that would otherwise require disposal.

The ammoxidation of 3-picoline utilises a catalyst which selectively converts the reactant in the presence of oxygen and ammonia to 3-cyanopyridine (nicotinonitrile). Even at elevated reaction temperatures, deep oxidation contributes marginally, and the heat generated by the reaction is recuperated and utilised elsewhere in the process.

Cyanopyridine generated by ammoxidation is hydrolysed to the amide using an enzymatic catalyst with practically quantitative yields. This efficient procedure avoids the consecutive hydrolysis reaction to nicotinic acid, which here is a by-product.

Starting from MPDA, an overall yield for the process of around 90% is obtained, which means that the carbon efficiency (ratio of C in product to C in reactants) and the overall atom efficiency (yield ratio of molecular weight of product to reactants) are 90% and 99%, respectively. The waste and any toxic by-products generated from the process are catalytically treated to give nitrogen, water and low quantities of carbon dioxide (about 200 kg/ ton nicotinamide).

The energy-neutral picoline route and the recovery and use of energy generated in the exothermic ammoxidation contribute to the low-energy requirements in the process.

Therefore, the green principles observed in the process can be effectively summarised as follows:

1. Waste is prevented by a highly selective process over 4 chemical or bio-chemical steps;
2. The atom and carbon efficiencies are high (90 -100%);
3. The reagents used (3-picoline, water, air) are not particularly toxic (picoline LD50 = 420 mg/kg). The ammonia necessary for the ammoxidation is predominantly obtained as a by-product in the production of 3-picoline. Any toxic by-products are catalytically converted.

4. Benign solvents are used (water and toluene for extraction of cyanopyridine). Toluene is practically 100% recycled.
5. The energy requirements are largely covered by the exothermic nature of the main reaction.
6. Catalysis is used in every step to increase the efficiency of reaction and reduce energy requirements. Six catalyst types are employed in the process.
7. Hazardous materials are avoided. Apart from a relatively small quantity of carbon dioxide there is no environmental waste.

1.2.5 Advances in 3-picoline and 3-cyanopyridine manufacture

Many companies have described processes for producing nicotinates precursor utilising 2-methylglutaronitrile (MGN) or its hydrogenated product MDPA [15]; the Lonza process utilises Al oxide and/or Si oxide catalyst (zeolite) in the cyclization step to 3-methylpiperidine and a catalytic dehydrogenation to 3-picoline in the second step. The Mitsubishi process hydrogenates MGN directly to 3-methylpiperidine with a Rhodium catalyst in the presence of ammonia. Ammonia prevents the formation of polyamines, which otherwise would poison the Rhodium catalyst. Reilly have taken this idea one step further and have developed a method for the production of 3-cyanopyridine directly from MDPA, with yields that however do not exceed the 20% [16]. Main drawback of this process is the high number of steps. A process starting from MGN would require five reactors with a separation apparatus after every reactor, resulting in high costs for plant construction. A patent from BASF in 1981 claimed a process for dinitrile cyclization to produce substituted and unsubstituted pyridine using a platinum or palladium based catalyst [17].

In two papers published in 1996 by Lanini and Prins [18-19], the authors reported about a study of the process for the direct production of 3-picoline from MGN. Silica-supported Palladium catalyst was found to be active for this

reaction. MGN was fed along with hydrogen at a ratio H_2/MGN=7, pressure was 6 bar. Initial picoline yields higher than 75% was achieved, but catalyst rapidly deactivated after few hours on stream. In the process, MGN is partially hydrogenated to an amine-imine intermediate, then intramolecular amine-imine condensation occurs and 2-amino-3-methylpiperidine is formed; this molecule spontaneously releases ammonia and forms 3-methyl-1,2-dehydropiperidine, the latter is then dehydrogenated to β–picoline. Reaction pathways are reported in Figure .

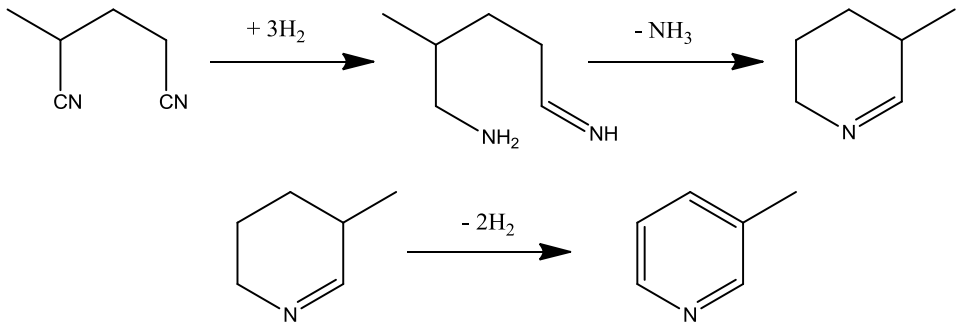

Figure 7 Reaction pathways for MGN dehydrocyclization over Pd/SiO_2 catalyst

The main limitation to the industrial application of this process is the very low lifetime of the catalyst; deactivation occurs mainly because of intermolecular condensation that forms resin-like compounds that stick over the catalyst surface. By varying the feed composition, it is possible to reduce resins formation, but a sudden decrease in selectivity is observed.

Further improvements in the aim of process simplification is reported in a patent from Standard Oil Company [20]. A process for the one-step oxidative cyclization of MGN to 3-cyanopiridine is therein claimed. Multi-metallic molybdate catalysts containing up to nine elements such as Cs, K, Ni, Co, Fe, Mn, Bi, Cr, V and P are reported. In this process, MGN is vaporized and fed along with oxygen and a diluting agent (usually N_2) over the catalyst; the typical composition of the inlet stream is 2%mol MGN/2.5%mol O_2/95.5%N_2. Yield of

3.6% is reported in the patent; despite the very low price of MGN, such low yield poses several problems for a possible industrial application, because of the low overall productivity, and the high costs for 3-cyanopyridine recovery from a very diluted solution.

1.2.6 Liquid-phase oxidation of 3-picoline with oxygen

Direct oxidation of 3-picoline with oxygen or air offers the most logical route to nicotinic acid, although the reaction technology is not as simple as the ammoxidation. Many Japanese companies such as Daicel [21-22], Mitsubishi [23-24-25-26], and Nissan [27-28] have developed processes based on the catalytic liquid-phase oxidation where picoline can be selectively oxidised to niacin [29]. A catalyst combination such as cobalt and manganese acetate and/or bromide is used in an acetic acid medium, and the air-oxidation takes place under elevated temperatures and pressures. The disadvantages of this process are the following:

1. The product must be efficiently separated from the reaction solution. In practice the two goals show contrasting solutions; if the product is clean, then relevant quantities remain in the solution and vice-versa.
2. In practice, additional cleaning and/or processing steps are necessary to ensure the desired purity and physical properties of the product.
3. The mother liquor contains metallic catalysts which must be recycled for process efficiency. Recycling of the reaction solution usually entails considerable effort in working-up and cleaning. In fact, the spent solution contains water, tar, and/or high boilers and of course the metal catalyst salts in addition to acetic acid [15].

In spite of these inherent difficulties, some plants in commercial scale were practiced especially from Reilly in the US in the 1970s.

Some of the above-mentioned Japanese companies have studied some development, but their conversion to technical or commercial process remains to be seen.

1.3 A “greener” technology for niacin production

The oxidation of picoline with stoichiometric or excess of the oxidising agent, such as permanganate, nitric acid or chromic acid, has been discussed above. The most logical and direct method of producing nicotinic acid is to oxidize 3-picoline with air. In fact, the direct gas-phase oxidation of 3-picoline using vanadium oxide catalyst has been known for over 60 years [30] but, only in the last 20 years, serious efforts have been made to develop a commercial process based on this technology. There are some difficulties that limit the application of this gas-phase reaction, first the need of a selective and efficient catalyst. In the absence of ammonia, the direct oxidation reaction proceeds slowly than the ammoxidation and, in contrast to the latter, 3-pyridinecarbaldehyde is also formed. The total oxidation of the intermediate, of picoline and of the product can reduce severely the selectivity.

In addition, nicotinic acid is less stable than 3-cyanopyridine and decarboxylates rapidly at temperatures normally encountered in the gas-phase reaction. Furthermore, nicotinic acid easily de-sublimates at temperature below 200°C, and can create plugging problems in the equipment.

Nowadays, 3-cyanopyridine is considered equivalent or even better than nicotinic acid, because of the easy and selective hydrolysis to nicotinic acid; moreover, it is obviously preferred when the target molecule is niacinamide.

Although nicotinic acid presents this disadvantage in comparison to 3-cyanopiridine and nicotinamide, both Lonza [31] and the Boreskov Institute of Catalysis [32] have developed pilot processes for niacin production by catalytic gas-phase oxidation of 3-picoline. The main difference between the two technologies is the method used for niacin removal from the reaction mixture:

Boreskov's process uses a de-sublimation technology while Lonza's one is based on a spray-drying technology of a concentrated solution of nicotinamide.
The choice between the two methods also depends on reaction conditions; for example, in Lonza's conditions ammonia is formed as a side-product from total oxidation rather than hydrogen cyanide.
There are many "green" advantages for this process:

1. Replacement of a stoichiometric oxidising agent with air.
2. Use of a catalyst to promote the reaction.
3. Reaction carried out at atmospheric pressure.
4. Heterogeneous catalyst, which allows intrinsic separation of the catalyst from the reactant-products stream.
5. Energy recover from the exothermal reaction.
6. Few operation units.
7. Water as unique solvent.
8. Ammonia is recycled.
9. Minimization of waste by a highly selective reaction.
10. High conversion, with more efficient use of equipment, energy and materials.

These advantages make this process very interesting for future industrial application, although productivity is still an issue related to the low concentration of picoline needed in order to obtain high selectivity.

1.3.1 Catalysts for 3-picoline oxidation

In literature many catalysts are reported for the oxidative transformation of nitrogen-containing alkyl heterocycles. Typically, these catalysts are based on vanadium oxide either in combination with Molybdenum, Phosphorus and Tin, or in the form of Vanadium oxide on various supports.

Since Cislak, who first claimed the use of elements of group V and VI for gas-phase 3-picoline oxidation with oxygen in 1944 [30], many different catalyst compositions have been tested.

In 1969, Suvorov et al. [33] reported the use of fused Tin and Titanium vanadates as catalyst for 3–picoline oxidation with air in the presence of steam; main products were pyridine-3-carbaldehyde and nicotinic acid with a total selectivity of 76%. On Tin-vanadate, 35% yield to nicotinic acid was achieved at a temperature of 410-420°C, whereas on Titanium vanadate yield was 50% at 360°C. Vanadium-Aluminium [34] and Tin-Vanadium [35] catalysts gave lower yields. In 1976, Järås and Lundin reported yields higher than 50% on vanadia-titania catalyst [36-37].

More recently, different research groups have focused their attention on simple vanadia-titania catalysts. A group from the Boreskov Institute of Catalysis improved 3–picoline oxidation over the V-Ti-O catalyst, resulting in a breakthrough in performance and an 85% yield to nicotinic acid [32]. Hölderich reported an astonishingly high value of nicotinic acid yield, as high as 96% [38] on a similar catalyst.

Again the Boreskov Institute of Catalysis [39] and Chang Chun Petrochemicals [40] claimed a ternary catalyst based on V-Ti-O but using Molybdenum, Tellurium, Tin, Cerium or Zirconium as promoters; these elements increased the activity of the catalyst but had only small effect on selectivity. Oxides of Chromium, Iron and Tungsten were additionally used in catalysts with lower Vanadium oxide content (5%-10%), and nicotinic acid yield reached the 90% [40]. Promoted vanadia-titania catalysts showed similar selectivity between 90% and 93%, but with lower yields. Increasing the Vanadium content until 25%, or doping it with Chromium reduced the yields down to 77% [41]. The comparison of the catalysts reported in the literature leads to the conclusion that the efficiency of V-Ti-O catalysts decreases when the Vanadium oxide

content is increased from 5% to 25%; however, data reported are not sufficient to select the optimum Vanadium content for this type of catalyst.

For niacin production, also metal vanadates have been considered a promising class of catalysts by Takehira et al. in the last years. Vanadates of Cr, Y, Bi, Mn, Fe and Co [42-43-44] have been tested; the best result, 50% nicotinic acid yield [43], was obtained with monoclinic Chromium vanadate. The addition of a ternary component, namely Aluminium or Phosphorus, increased the yields. On a Cr/V/P/O catalyst, niacin yields reached the 78% with a selectivity of 84% [42], a value still lower than that one reported for vanadia-titania systems. The latter showed higher activity and nicotinic acid yield at a temperature which was 100°C lower than the best one registered with metal vanadate catalysts.

More recently a group from Kazakhstan studied the reactivity of modified V_2O_5, doped with Ti, Sn, Zr, Nb and Al oxides [45-46]. These catalysts were not supported, because were prepared by intimate mixing of the powders of the two oxides (in different proportion), followed by calcination at 650°C-800°C for 2h. It was shown that mixed oxides were more active and selective than the two pure phases, regardless of the proportions used for each compound. Proton affinity of active oxygen bonded to Vanadium was calculated by quantum-chemical method, and a relationship was found with activity; however, yields were quite far away from those reported for supported catalysts.

1.3.2 Acid-base properties of the catalysts

It is well known that alkylpyridine holds the same basic properties as pyridine, that is tipically used as a probe molecule for acidity measurement. Also all the other heterocycle molecules above mentioned present the same functionality; moreover, niacin also presents the acid feature related to the carboxylic group. Because of this, acid-base properties play a crucial role in the behaviour of catalysts for picoline oxidation.

Studies report that the oxidation of methyl heteroaromatics to their aldehydes is strongly related to the nature, strength and concentration of acid and basic superficial sites of the catalyst [47]. Similar investigation on heterocycle aldehydes oxidation shows that acid-base properties can remarkably affect the selectivity to the corresponding acid and deep oxidation products [48-49]. Thereby, it is expected that an increase of surface acidity has no effect on the adsorption of an acid compound; on the other hand, the absorption-desorption equilibrium of basic components, namely 3-picoline and pyridine-3-carbaldehyde, may be heavily affected. In fact, alkali cations added as dopants to Vanadium oxide catalyst results in an accelerated aldehyde desorption, with an higher selectivity to this product [47]. Addition of sulphate ions enhances the acidity of vanadia-titania catalysts, with development of stronger bonds for surface complexes of 3-picoline and pyridine-3-carbaldehyde, that may lead to oxidative decomposition.

A study on vanadia-titania catalysts with different sulphates content for nicotinic acid oxidation showed that different acid strength had no effect on niacin oxidation [50]; however, a decrease of nicotinic acid yield was reported, with sulphated catalysts [38], probably due to the strong adsorption of 3-picoline and pyridine-3-carbaldehyde, which led to their overoxidation.

1.3.3 Active Vanadium species for 3-picoline gas-phase oxidation

Because of the several applications of Vanadium oxide catalysts, the nature of active species in these catalysts has long been investigated. From the literature, it is known that different Vanadium oxide species are found on titania (in the anatase form), depending on Vanadium content, surface area of the support and temperature of calcination. Monomeric isolated (VO_x), polymeric $(VO_x)_n$, amorphous and bulk phases of V_2O_5 can be found [51-52-53-54-55]. It is also known that monolayer Vanadium species are more active and selective than bulk Vanadium oxide [53-54-55] in the oxidation of many molecules such as

o-xylene, formaldehyde, toluene as well as in β–picoline ammoxidation [56-57-58-59].

In ref [60], Al'kaeva et al. studied the catalytic performance of V_2O_5/TiO_2 in 3-picoline oxidation with oxygen in the presence of steam. The binary system was two times more active than titania and much more selective, while pure vanadia showed similar selectivity but lower activity compared to V-Ti-O catalysts.

For binary systems, it was shown that selectivity to nicotinic acid increased from 75% until 90% when Vanadium oxide content was raised from 5% to 20%; at the same time, the rate of 3-picoline oxidation became three times higher, while a further rise in Vanadium content had only a small effect on selectivity and activity. The performances of these catalysts were similar in a wide range of Vanadium oxide content because of two opposite contributions: increasing the amount of Vanadium oxide, more coherent intergrowth boundaries of V_2O_5 crystallites and TiO_2 were formed; the extent of these boundary phases was strictly related to activity because titania stabilized specific oxidation states of Vanadium ions. On the other hand, also the amount of inactive V_2O_5 increased.

Studies were also carried out in order to understand the role of the monolayer Vanadium oxide: a sample containing a high Vanadium content was washed with 10% vol solution of nitric acid in water, that selectively dissolved bulk V_2O_5 while strongly bound monomeric and polymeric Vanadium species were left untouched. For the treated catalyst, the rate of β–picoline oxidation was five times higher than that shown by the untreated one, if compared on Vanadium amount [61]; a slight decrease of selectivity was observed due to the small fraction of uncovered TiO_2 surface after the acid treatment, because titania was more selective for deep oxidation.

The same authors report in other papers [62] that the appearance of the rutile phase (catalyst with >30% V_2O_5 content, calcined at over 550°C) reduced catalytic activity but had no effect on selectivity.

Active catalysts are produced either when Vanadium oxide is supported in the form of a monolayer [53], or when higher amounts lead to the presence of coherent interphase boundaries [60], or even when the catalyst is prepared via solid state reaction [45-46]. This allows to state that V-O-Ti bonds are the active species, irrespective of the synthesis methodology used. It is interesting to note that for 3-picoline ammoxidation, that shows, as already seen, many analogies with 3-picoline oxidation, catalysts made of vanadia-titania supported over alumina or silica gel have been proposed, whereby Titanium dioxide is not considered a support but a component of the active phase.

Sirnivas et al. showed a relationship between catalysts oxidation activity and concentration of tetrahedral (monomeric and polymeric) Vanadium species, identified by means of Diffuse Reflectance UV-vis spectroscopy (DRUV-vis) [63].

In Chromium Aluminium vanadate and Chromium Vanadium phosphate, the active species are the tetrahedral Vanadium sites; the addition of Aluminium and Phosphorus, that replace Cr or V, modifies both redox and acidic properties [42-43-44].

Overall, the reactivity of all catalysts mentioned is due to Vanadium oxide. However, interaction of Vanadium with the support or other elements inside the structure of the catalyst, is beneficial for catalytic performance.

1.3.4 Reaction pathways and proposed mechanism for Vanadium oxide based catalysts

With all catalysts, 3-picoline oxidation in the presence of steam proceeds in a temperature range from 250°C to 500°C [60-64-65]. Vanadia-titania catalysts are usually more selective in the bottom part of this range, i.e., from 250°C to 300°C. Conversely, Vanadium-Tin oxide catalysts are active only at higher temperature, namely 400°C-500°C [35], while modified Chromium Vanadium oxide works in the middle part of the temperature range (300°C-360°C) [42-43-44].

Catalytic tests are usually performed by feeding a mixture of 3-picoline, water vapour and oxygen or air. Major by-products identified are nicotinic acid, pyridine-3-carbaldehyde (also named nicotinic aldehyde), CO and CO_2, other minor by-products commonly found are pyridine and 3-cyanopyridine [15-35-42-43-44-60-64-65-66]. In few works only, the formation of hydrogen cyanide [35-66] and ammonia [15] is reported.

From the study of selectivity in function of 3-picoline conversion, it was possible to determine the pathway of the reaction. Ovchinnikova et al in [64-65] reported data for a 20% V_2O_5/TiO_2 catalyst. Increasing 3-picoline conversion, the selectivity to nicotinic acid increased while that to pyridine-3-carbaldehyde decreased, a clear indication that the aldehyde is an intermediate in nicotinic acid formation.

They claimed also a direct route from 3-picoline to nicotinic acid, but data were not enough to quantify the contribution of the two parallel routes. The experiment was repeated in [63] by Srinivas et al. at low picoline conversion (1-2%); this confirmed the presence of the two parallels ways, and extrapolation to zero conversion was possible: 60% of niacin was produced as the consecutive product of pyridine-3-carbaldehyde oxidation, while the remaining 40% was formed directly from 3-picoline [61].

By-products such as CO_x, pyridine and 3-cyanopyridine were produced mainly via consecutive routes, but a small contribution of parallel reactions was also present (lower than 3%) [61]. By feeding directly nicotinic acid in mixture with oxygen and steam, it was shown that mainly CO_x and 3-cyanopyridine were produced as consecutive products of oxidative decomposition [50]. In the same way, the oxidation of aldehyde to CO_x was proved [34].

The formation of N-containing molecules, namely 3-cyanopyridine and, in lower amount, HCN and NH_3, derives from surface fragments remaining after the deep oxidation of pyridine ring [64-67]. Several papers investigate the mechanism of formation of nitriles during picoline oxidation [68-69-70]; it was

assumed that these compounds form by reaction of oxygenated molecules with surface N-containing complexes formed by pyridine ring fragmentation.
The reaction pathway was assumed to be the same also for Cr/V/O catalysts.
For sintered V_2O_5/SnO_2 catalysts, no test aimed at the identification of reaction pathways was carried out, but nicotinic acid and pyridine-3-carbaldehyde yield variation in function of temperature indicated that nicotinic acid derives mainly from the consecutive oxidation of the aldehyde; in this case, the contribution of the parallel pathway was reduced compared to vanadia-titania catalysts.
The complete pathway is reported in figure 8

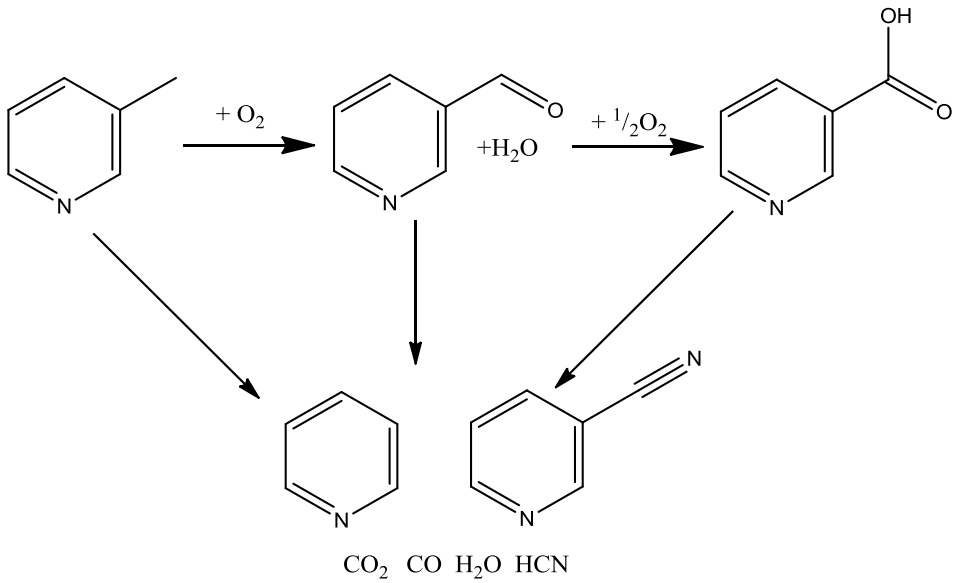

Figure 8 Reaction pathways for 3-picoline oxidation over vanadium based catalysts.

Many studies were carried out in order to elucidate the mechanism of nicotinic acid formation [35-44-71-72]. The mechanism was found to be very similar for all catalyst types; 3-picoline is first adsorbed over acid surface sites, mainly of Brønsted type but also of Lewis type. The interaction of protons and carbon atoms of the methyl group with the oxygen ion of the catalyst forms an aldehyde-type surface complex. This complex is in equilibrium with the gas-phase compound, so freepyridine-3-aldehyde is formed; if the aldehyde complex reacts immediately with catalyst oxygen (O^{2-}) without desorbing into

the gas-phase, the direct way from picoline to niacin takes place. If instead the aldehyde desorbs and then re-adsorbs again, niacin is formed through the consecutive pathway. The main difference between the mechanisms occurring with vanadia-titania and $CrV_{1-x}P_xO$ catalysts is in desorption equilibria for nicotinate formation.

In vanadia-titania catalysts, absorbed niacin forms only in the presence of gas-phase oxygen; in its absence, only the nicotinate complex is formed. With the $CrV_{1-x}P_xO$ catalyst, molecular nicotinic acid is formed in both cases, resulting from the Mars-Van Krevelen mechanism, where the substrate is oxidised by the V ion, and ionic oxygen is delivered to the substrate with formation of anionic vacancies; later on, ionic oxygen is restored by molecular oxygen reduction, with recovery of the original oxidation state of Vanadium. On the other hand, V_2O_5/TiO_2 catalysts show an associative mechanism with a combined stage of oxygen adsorption and acid desorption.

This theory is supported also by DFT calculations for vanadia-titania catalysts; the heat of desorption for nicotinic acid from reduced and oxidized superficial sites was also calculated [73]. The value for reduced sites was found to be twice as much that one for oxidized sites; this results in reduced sites with strongly bound nicotinates species that are more easily desorbed when V sites are reoxidized.

TPR analysis was used to get additional qualitative information about ionic oxygen mobility and oxygen bond strength. In fact, the temperature of the peak in hydrogen-TPR profile can provide information about the nature of V-O bonds. From literature, it is known that a correlation exists between the reducibility of Vanadium species and the activity in hydrocarbons partial oxidation [56-57-74-75-76-77-78].

The TPR profile of vanadia-titania catalysts usually presents two peaks; the first one between 470°C and 520°C is due to the reduction of monomeric and polymeric Vanadium species, and the second one at ca 550°C is related to bulk

V_2O_5. In ref [58], it was shown that catalysts with higher concentration of easily reducible species or showing a low reduction temperature for monomeric species are more active in picoline oxidation. Also for $CrV_{1-x}P_xO_4$ catalysts, in ref [44] a correlation was found between the low-temperature of reduction in the TPR profile and the high activity in the reaction.

1.3.5 Effect of inlet feed composition

The ratio between the three main components of the reaction mixture is a crucial parameter for catalytic performance; it has been studied in several patents and papers [32-34-35-37-38-39-42-43-79-80]. In analogy with other reactions such as the oxidation and ammoxidation of hydrocarbons [34-68] that are carried on with similar catalysts, also 3-picoline oxidation needs a large excess of oxygen. Data from literature report a beneficial effect when high O_2/3-picoline ratios are used. Niacin selectivity higher than 85% is obtained with O_2/3-picoline molar ratio higher than 15, and a sharp decline of selectivity is observed when this value is decreased. Low oxygen concentrations oddly result in high CO_x selectivity. This supports the theory reported in paragraph 1.3.4 about nicotinic acid desorption, i.e., the lower is the oxygen concentration in the gas phase, the lower is the oxidation state of Vanadium in steady state conditions, and this finally results in a difficult desorption of the desired product and a high selectivity to deep oxidation products.

In the same way, high O_2/3-picoline ratios are beneficial for modified $CrVO_4$ catalysts, because a high oxidation state for Vanadium species assists the desorption of nicotinic acid and prevents it from further oxidation.

The presence of steam significantly changes catalyst behaviour; its influence has been deeply investigated in several papers [35-42-43-44-64-65]. With all types of catalysts above mentioned, steam increases dramatically the niacin yield and selectivity.

Takehira et al. in [42-81] reported that over modified $CrVO_4$ catalysts, water vapour is effective because it converts superficial Lewis acid sites into Brønsted sites, that can activate 3-picoline and simultaneously accelerate the desorption of nicotinic acid saving it from deep oxidation and finally increasing selectivity. The same authors calculated the activation energy in the presence and absence of steam; the value turned out to be substantially unchanged (54±2 kJ/mol). This implies that the nature of the active site is unaffected by steam, and only their concentration is increased in the presence of water.

With V_2O_5/TiO_2 catalysts, Andrushkevich et al. in [64] reported the rate of product formation and selectivity in function of water concentration at two different 3-picoline conversions (28% and 82%). At low conversion, when parallel reactions are more relevant, steam has a positive effect for the formation rate of all products, and has a positive effect also for pyridine-3-carbaldehyde transformation into nicotinic acid. In fact, the rate of aldehyde formation is increased in the presence of steam, but its selectivity is decreased because of the higher niacin selectivity.

At high 3-picoline conversion, when nicotinic acid concentration is high while that of 3-picoline is low, and consecutive reactions are predominant, water has practically no effect; only a small effect is observed in niacin formation rate while its selectivity is unchanged. From this it follows that water does not influence overoxidation of nicotinic acid, pyridine-3-carbaldehyde and 3-cyanopyridine.

Andrushkevich and co-workers concluded that water increases the selectivity by accelerating aldehyde and niacin formation and not by suppressing overoxidation.

The authors also noticed that water has an impact on catalyst stability, reducing the heterocycle irreversible adsorption and resins formation. Studies were carried out in order to clarify the mechanism of activation by water; in [82], it is reported that steam promotes dynamic reversible dispersion of bulk V_2O_5. It is

also reported how water hydrolyses V-O-V bonds in bulk vanadia, generating mobile and active species. Other papers [83-84] report that water modifies the ratio between monomeric and polymeric VO_x species in supported vanadia catalysts. Domain size and coordination environment are modified at the same time.

The presence of water also enhances oxygen exchange, terminal V=O and V-O-V bridges exchange the oxygen atom with water but not with molecular oxygen [85]. The intermediate for this oxygen exchange is the hydroxyl species, the Brønsted acid sites that are claimed to be those responsible for 3-picoline adsorption.

1.4 Supported Vanadium oxide catalysts

As widely reported in the previous paragraph, V_2O_5/TiO_2 shows the best performance in 3-picoline oxidation. Similarities with alkylaromatics ammoxidation were also reported.

It is also worth noting that zirconia-supported Vanadium oxide catalysts have been reported to give better performance in ammoxidation reactions, specifically for toluene and picoline [86-87-88]. The same type of catalyst is also used in several oxidation reactions, such as ethanol to acetaldehyde [89-90], methanol to formaldehyde [91-92-93] and alkane oxidehydrogenation to olefins [94-95-96-99-103-107-108]. Moreover, various catalysts based on supported Vanadium oxide have been described for ethanol oxidation [97-98-99-100-101].

The role of the support in Vanadium oxide catalysts has been highlighted by several authors in the literature [102-103-104-105]. Tian et al. reported that for various supported vanadia catalysts used for alkane oxidation, the support cation is a potent ligand that directly influences the reactivity of the bridging V-O-support bond, the catalytic active site, by controlling its basic character via the electronegativity of the support [106]. Even the acid-basic features of the

support can affect reactivity. For example, Enache et al. [107-108] reported that in ethane oxidation over titania and zirconia supported Vanadium oxides, the greater selectivity to acetic acid observed with the former system is due to the stronger retention of acetic acid over the more basic zirconia support.

Significantly higher degrees of reduction of VO_x species were observed with TiO_2- than with ZrO_2-supported catalysts in steady conditions. Wachs et al. [104] compared different supported vanadia catalysts for *n*-butane oxidation. With V_2O_5/ZrO_2, the Raman intensities of the terminal V=O and polymeric vanadate functionalities decreased somewhat due to the reduced surface Vanadium oxide species, while bulk Vanadium oxide was not affected. Conversely, in the case of V_2O_5/TiO_2, the Raman intensities of surface Vanadium oxide functionalities decreased at all temperatures. Burcham et al. [91] reported that upon the introduction of a methanol/O_2/He gas stream, both the terminal V=O and bridging V–O–V bands decreased in intensity and shifted to lower wavenumbers for all supported vanadia catalysts. Su and Bell [109] reported that for V_2O_5/ZrO_2, the partial reduction of the dispersed Vanadium oxide increases the absorbance of vanadia and alters the Raman spectra while increasing the intensity of zirconia bands compared to those of vanadia.

It is known from [106] that for catalysts with surface coverage below the monolayer, the nature of the support strongly influences the ratio between monomeric and polymeric VO_x species.

All the features above listed, especially the tendency to work in steady state at high Vanadium oxidation state, make V_2O_5/ZrO_2 a promising catalyst for 3-picoline oxidation.

1.5 Bulk Vanadium oxide-based catalysts

Shishido et al. in [42-43-44] reported that metal vanadates are catalysts showing good performance in 3-picoline oxidation. Due to its natural tendency to form polymorphs, Vanadium species can be found in several arrangements.

Vanadyl pyrophosphate is known to be one of the best performing catalysts for mild oxidation reactions [110-111-112-113-114-115-116]. Besides being used in industry for the oxidation of *n*-butane to maleic anhydride [111--117-118-119-120-121-122-123], it gives good performance also in other reactions, such as the oxidation of *n*-pentane to maleic and phthalic anhydrides [124-125-126-127-128-129-130], the oxidation of propane [131-132-133-134], the ammoxidation of alkylaromatics [135-136-137-138-139-140], but also in liquid-phase oxidations with H_2O_2 or alkylhydroperoxides as oxidants for various organic substrates (*p*-cymene, cyclohexane) [141-142-143-144-145].

Some recent applications take advantage of its intrinsic bifunctional (both acid and redox) properties, such as the oxidative dehydration of glycerol to acrylic acid [146-147-148-149-150], and the oxidative dehydration of 1-butanol to maleic anhydride [151]. Also in the case of oxidation reactions, it is believed that surface acidity plays an important role in the reaction mechanism [152-153-154-155-156-157].

Indeed, this catalyst has also been used for reactions which require acid sites only [146-147-158]. The presence of Brønsted acid sites formed by P-O-P bond hydrolysis and the possibility to tune Vanadium redox properties by selecting the proper dopant make vanadyl pyrophosphate an interesting catalyst for 3-picoline oxidation.

1.6 Aim of the thesis

During the three years of my PhD different lines of research, all of them related to nicotinates production processes, have been investigated. The third line took two years while the remaining one-year time was equally dedicated to the first two projects.

The first project (Project A) dealt with the direct cyclisation of MGN into a mono-unsaturated 3-cyanopiperidine over bifunctional acid-base catalysts, followed by the dehydrogenation of the piperidine into 3-cyanopyridine.

The two steps might be conducted simultaneously (one-pot reaction) on a system containing also a noble metal for the second step. As reported in paragraph 1.2.5, some attempts were done in this direction, but many further efforts should be done in order to develop a suitable catalyst.

The target of the second project (Project B) was the synthesis of 3-picoline in a multi-molecular condensation as in Hantzsch [13] and Chichibabin [14] processes, still used in industry. The objective was a process in which acetaldehyde was made react with acetonitrile:

$$2\ CH_3CHO + CH_3CN \rightarrow 3\text{-picoline} + 2\ H_2O$$

In this way it would have been possible to avoid the use of free ammonia with several benefits in the aim of intrinsic safety and green chemistry principles application.

The reaction is an acid-base-catalyzed condensation which occurs because of the acidity of the α-C-H atom in acetaldehyde, which may condense with another molecule of acetaldehyde and one molecule of acetonitrile (thus, instead of a condensation with water elimination, might be a sort of multi-aldol condensation).

The third project (Project C) carried out during my thesis dealt with the gas-phase 3-picoline oxidation to niacin; despite the several advantages listed in paragraph 1.4, zirconia-supported Vanadium catalyst has never been tested before for this reaction. We also decided to test a Vanadium oxide catalyst supported over Titania-Zirconia, in order to gain a deeper insight on the behavior of zirconia as a support for Vanadium oxide.

The reaction has also been studied using a vanadyl pyrophosphate (VPP) catalyst, in order to find whether this well-known catalyst might be an efficient system also for this reaction.

Characterization of the catalysts by porosimetry, XRD and Raman spectroscopy material was carried out in order to correlate catalyst structural properties with catalytic performances.

2 Experimental part

All catalysts prepared were in the form of powder with dimension lower than 0,125mm. Before catalytic tests the powder was pressed and ground again to a dimension between 0,595mm and 0,250mm, in order to form granules suited to fill in the reactor while avoiding high pressure drop and clogging of the reactor due to carbon deposit.

2.1 Synthesis of the catalysts for Projects A (MGN cyclisation) and B (C_2 condensation)

Commercial supports or catalysts, when available, were used for Projects A and B; the experimental procedure for the synthesis of catalysts not available in the commercial form are described in the following Sections.

2.1.1 Magnesium oxide and mixed Mg/Me oxide support

Magnesium oxide has long been known as a very basic catalyst. In order to obtain a material with high specific surface area, an “hydrotalcite-like” co-precipitation synthesis [159] was chosen. The details of the procedure are described below.

500 mL of a solution 0,5M of $Mg(NO_3)_2$ was added dropwise (1 drop every 3 seconds) to 500mL of a solution 0,5M of Na_2CO_3 vigorously stirred and kept at 50°C. The pH was adjusted at 10.50 before starting the addition and was kept at this value by adding NaOH 6M. Then the precipitate was aged for 2h, vacuum filtered with a Buckner funnel and then washed with 2L of warm water every gram of solid, in order to remove sodium ion. The wet paste was dried overnight at 120°C and grinded to obtain a dry powder of magnesium hydroxy-carbonate; after calcination at 450°C in a muffle oven, high-surface-area MgO was produced.

Catalysts made of Mg/Al/O, Mg/Fe/O and Mg/Cr/O were also synthesized; the procedure was identical to the previous one, except that the solution of Mg^{2+} was replaced by a mixed solution of the two cations Mg^{2+}/Me^{3+} (Me = Al, Fe, Cr), with concentration equal to 0.167M and 0.333M, respectively.

These materials were used either as catalysts or as supports for the noble metal. From literature [18-19], it is known that palladium gives the best results while nickel and platinum catalysts either are inactive or produce heavy compounds, respectively; therefore we chose Pd as the active component. The impregnation was carried out by means of the incipient wetness method. The precursor of palladium (palladium acetylacetonate, $Pd(C_5H_7O_2)_2$) was weighed in such an amount to obtain 1% $^{w}/_{w}$ content of Pd over the support; then it was dissolved in the volume of toluene required for a full series of successive impregnations, two or three depending on the porosity of the support. The catalyst was then dried at 120°C for 2h and calcined at 400°C for 4h in order to remove the organic precursor. Before the catalytic tests, the impregnated catalyst was pre-reduced in situ with an H_2 flow (50%mol in nitrogen) at 350°C for 2h, with a contact time of 2s.

2.1.2 Other catalysts

Other catalysts with acidic features were tested.

The γ-AI_2O_3 used was a commercially available material produced by BASF, with a specific surface area of 190m^2/g. It was used either as such or impregnated by means of wet impregnation with 20% $^{w}/_{w}$ of cobalt or 20% $^{w}/_{w}$ of cobalt and 3% of nickel. Details on the procedure adopted can be find in [160].

The Zeolite used was a commercial Y sample in the hydrogen form, with a silica-to-alumina (SAR) ratio of 10; also this H-Y was used either as a catalyst or as a support. Palladium was supported by ion exchange, as reported in [161]; as in the case of the Pd/MgO catalyst, before the reactivity test the catalyst was pre-reduced using the same procedure as described above. For Project A, some

tests were carried out by co-feeding oxygen as reported in the literature [20]. For these experiments, a commercial oxidation catalyst, namely a multi-metallic molybdate, and a catalyst made of V_2O_5 supported over zirconia, were used.

The multi-metallic molybdate was the well-known C-41 catalyst, employed in industry for propene ammoxidation; it contains Mo, Bi, alkali and alkaline earth metals, Ni, Fe, Co, P, As and Sb.

2.2 Synthesis of catalysts for Project C (3-picoline oxidation)

All catalysts used for picoline oxidation were based on Vanadium oxide, supported over zirconia or over a mixed titania/zirconia support. A commercial vanadyl pyrophosphate, $(VO_2)_2P_2O_7$ catalyst, shaped in microspheres, supplied by Du Pont was also used.

Two different types of zirconia support were used, a commercial one supplied by Carlo Erba (ACS grade, 99%), and a home-made one, synthetized starting from zirconium oxonitrate. For this latter sample, the synthesis procedure was the following: 50g of $ZrO(NO_3)_2$ was dissolved in 300mL of water and heated at 40°C, while continuously stirring. Concentrated ammonia (25% $^w/_w$) was added until pH 9,5 was reached; a white $ZrO(OH)_2$ precipitate was produced. While keeping the pH between 8 and 10, 100mL of ammonium hydrate (25% $^w/_w$) was slowly added in order to complete the precipitation of zirconium oxohydroxide. The slurry was kept stirring overnight for the ageing of the precipitate, then it was vacuum filtered and washed with cold water until water was neutral.

The solid obtained was dried at 120°C for 8h, grinded and then calcined in a muffle oven at 550°C in order to decompose $ZrO(OH)_2$ to ZrO_2. The zirconia was also calcined at increasing temperatures in order to decrease its specific surface area down to the desired value. With both types of zirconia support, three different amounts of V_2O_5 were deposited, namely 2%, 4% and 7% $^w/_w$.

Ammonium metavanadate was used as the precursor for the Vanadium species, and was supported by means of wet impregnation. The required

amount of NH_4VO_3, depending on the desired nominal loading in the final catalyst, was dissolved in 100mL of water; the same weight of oxalic acid was then added in order to completely dissolve ammonium metavanadate. The solution was heated at 50°C and zirconia was added to the solution. The slurry was stirred vigorously for one hour and then dried in a vacuum rotating evaporator until a barely dry powder was formed.

This powder was then dried overnight at 120°C, grinded and calcined in a muffle oven at 500°C in order to decompose the V salt and form V_2O_5 while releasing ammonia and water.

2.3 Characterization techniques

2.3.1 XRD

XRD powder patterns of the catalysts were recorded with Ni-filtered Cu Kα radiation (λ = 1.54178 Å) on a Philips X'Pert vertical diffractometer equipped with a pulse height analyzer and a secondary curved graphite-crystal monochromator. The range of analysis was 5°<2θ<80° with a scanning rate of 0,05°/s and Time-per-step=1s. The interpretation of the patterns was made by using a software from PANalytical Company using the ICSD Database FIZKarlsruhe library. The scheme of the instrument is shown in figure 9.

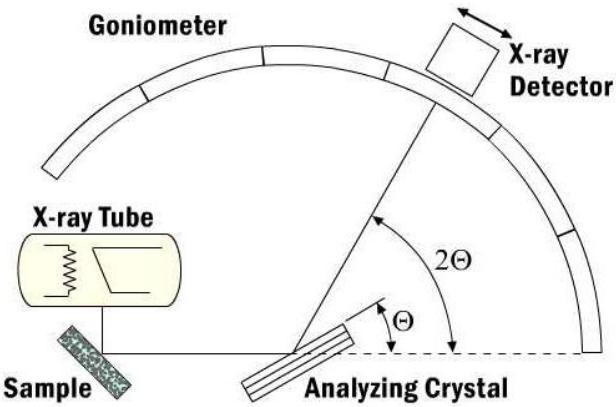

Figure 9. scheme of X-ray diffraction spectroscopy

2.3.2 Porosimetry and specific surface area measurement

In the introduction, the relationship between the Vanadium oxide species and the support surface area is described; therefore, specific surface area plays a crucial role in catalyst design and characterization. Different analytical methods are available, the most used are based on Brauner-Emmet-Teller model of gas adsorption [162-163].

Specific surface area and porosimetry analysis of the calcined catalysts were carried out in a Micromeritics ASAP2 020 instrument (Accelerated Surface Area and Porosimetry System). Each analysis requires 0,2-0,3 grams of powders; nitrogen is used as adsorbate molecule.

The sample is pre-treated under vacuum while heating it up to 150°C, until a pressure of 30mmHg is reached; then it is kept 30min at this temperature and finally heated up to 250°C and maintained at this temperature for 30min. This pretreatment is carried out in order to eliminate all the impurities that can be absorbed on the surface of the sample. Afterwards the N_2 adsorption is carried out, subsequent steps of adsorption and then desorption are performed at constant temperature, equal to N_2 liquefaction temperature (77 K). The instrument measures the adsorption and desorption isothermal curve at 77 K from the volume of adsorbed/desorbed N_2, in function of the relative pressure (via multi point method).

The value of surface area is calculated on the basis of the Brauner-Emmet-Teller (BET) equation:

$$\frac{P}{V(P_0 - P)} = \frac{C - 1}{V_m \cdot C} \cdot \frac{P}{P_0} + \frac{1}{V_m \cdot C}$$

Where:

P_0= saturation pressure;

V= gas volume adsorbed per gram of solid at a pressure P;

V_m= gas volume adsorbed per gram of solid in the formation of a monolayer on the surface;

C = BET constant, function of gas-surface interaction, mainly of the heat of adsorption.

The range of linearity of the equation is defined in 0.05<P/P0<0.35 interval. Inside this range, from the values of the intercept and the slope of the isotherm curves, it is possible to calculate V_m and C, and through the equation below reported it is possible to calculate the specific BET surface area of the sample expressed in m^2/g_{cat}.

$$S_{BET} = \frac{V_m}{V_{mol}} \cdot \frac{N_A s}{g_{cat}}$$

Where:

S_{BET} = surface area calculated through the BET model;

V_m= N_2 Volume adsorbed for the formation of the monolayer;

V_{mol} = molar volume of the adsorbed gas;

N_A = Avogadro number;

g_{cat}= weight of the analysed catalyst;

s = cross section of the adsorbing molecule.

For samples with a low surface area, full porosimetry was carried out, while samples with higher surface area (>10m^2/g) were analysed with a simpler and faster instrument. In this case, the instrument used for the specific surface area measurement was the Carlo Erba Sorpty 1700, based on the simplified BET model, with the measurement carried out based on a single point. This is possible because of the approximate form of the BET equation above reported, where the C constant is assumed to be very high compared to other variables; so, it is possible to simplify the above equation in this way:

$$\frac{P}{V(P_0 - P)} = \frac{1}{V_m} \cdot \frac{P}{P_0}$$

After this approximation, the BET equation becomes linear and passes through the origin, so with a single measurement it is possible to calculate the specific surface area.

The percent error that derives from these approximations is about 5% for surface area values over 3 m^2.

2.3.3 Raman spectroscopy

Raman is a spectroscopic technique based on the inelastic scattering of monochromatic light, usually from a laser source. Inelastic scattering means that the frequency of photons in monochromatic light changes upon interaction with the sample. Photons of the laser are absorbed by the sample and then re-emitted. Frequency of the re-emitted photons is shifted up or down with respect to the original monochromatic frequency, which is called the Raman effect. This shift provides information about vibrational, rotational, and other low frequencies transition in molecules. Through this analysis it is possible to identify the substances or compounds present in the sample, recognizing not only their chemical composition but also different molecular and crystalline structures. Raman spectroscopy is more sensible for probing structural defects present in a crystalline network, so allowing, for instance, the identification of a particular distorted phases which is not detectable by means of XRD analysis. The simplified working principle of a Raman spectrophotometer is showed in figure 10.

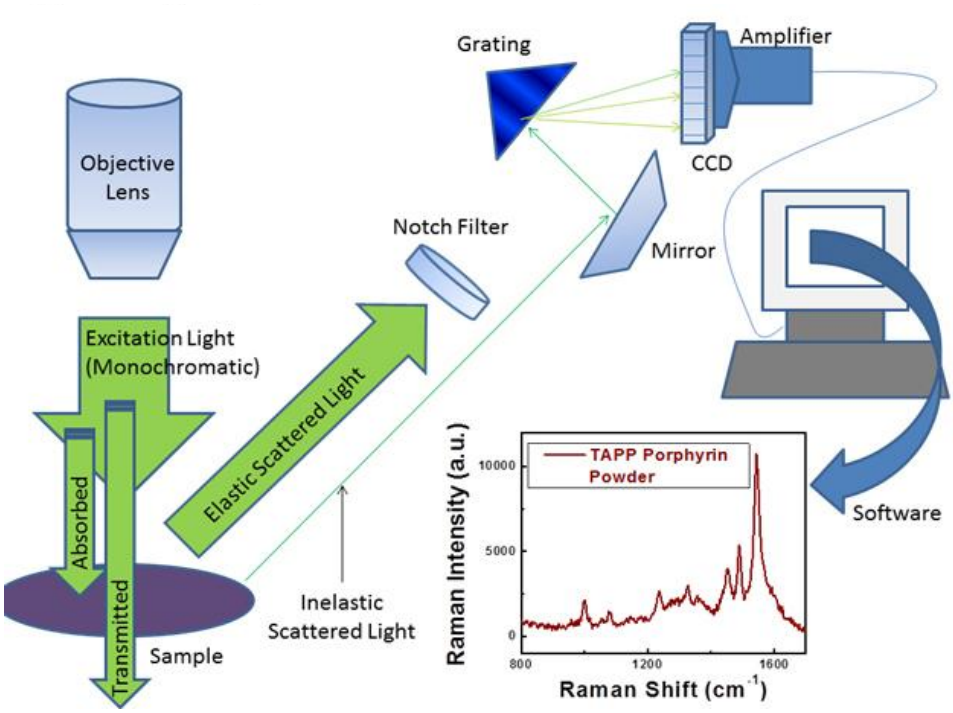

Figure 10. Scheme of a Raman spectroscopy

Raman analysis were carried out using a Renishaw Raman System RM1000 instrument, equipped with a Leica DLML confocal microscope, with 5x, 20x and 50x objectives, video camera, CCD detector and laser source Argon ion (514 nm) with power 25 mW. In order to eliminate the Raleygh scattering, the system is equipped with a notch filter. The network is a monochromator with a pass of 1200lines/mm. Generally, the parameters of spectrum acquisition were: 5 accumulations, 10 seconds, 50x objective.

The maximum spatial resolution is 0.5 µm and the spectral resolution is 1 cm^{-1}. For each sample a wide number of spectra were recorded changing the laser spot on different positions.

In-situ analysis

"*In-situ"* analysis was performed using a commercial Raman cell (Linkam Instruments TS1500). The quantity of sample used for the analysis was about 5-10 mg. The gas flow, fed from the beginning of the experiment, was about

20 mL/min. Spectra were recorded at room temperature (rt), while increasing temperature (heating rate generally equal to 10°C/min, up to the desired temperature), and during the isotherm period as well. The acquisition parameters were: 5 accumulations, 10 s each; the objective used was 20x.

Different temperature ramps were used, as shown in figures 11-12-13

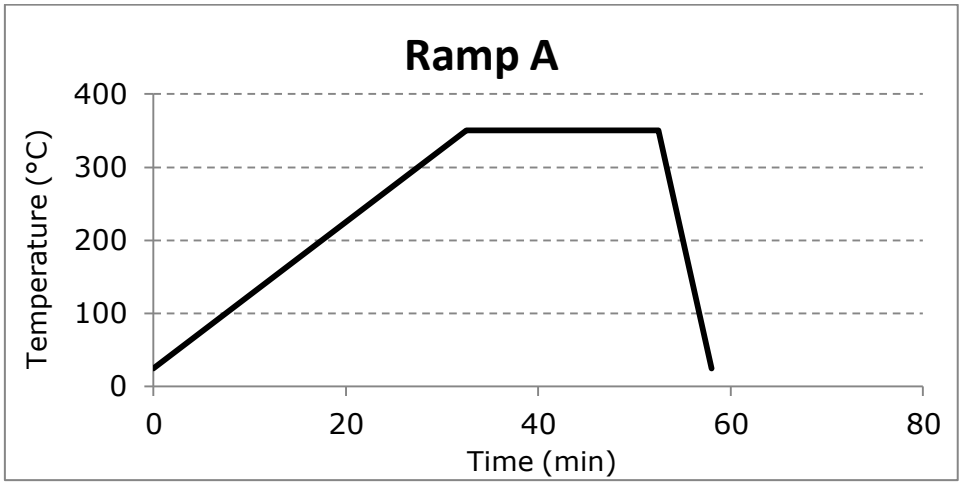

Figure 11. Temperature profile for experiment A

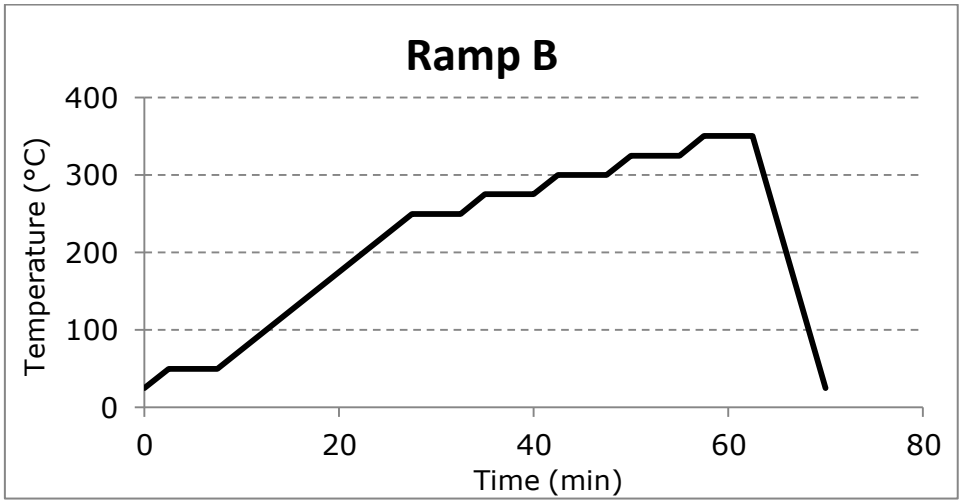

Figure 12. Temperature profile for experiment B

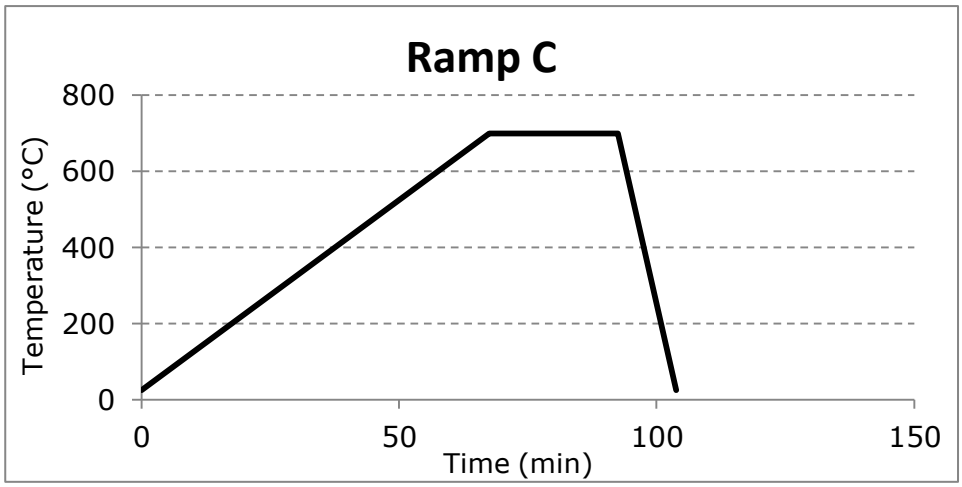

Figure 13. Temperature profile for experiment C

2.4 Catalytic tests

Catalytic tests were performed in a bench-scale apparatus. The glass reactor [A] was the same for the three different Projects; it has a catalytic zone with a diameter of 12.7mm and a porous quartz septum to hold the catalyst bed; before and after the bed, the reactor diameter is 7mm in order to have a higher flow speed and minimize contributions from gas-phase reactions. A coaxial stainless steel thermocouple holder is inserted from the top of the reactor in order to measure the real temperature of the catalyst bed. A vertical tubular furnace (Carbolite MTF 12/25/250) and its controller provide the heat necessary to the reaction. All the pipes and connections before and after the reactor are made of AISI 316L steel with 1/8" external diameter. Gas flow (reactants or inert) are controlled by means of Brooks gas flow meters. An auxiliary inert gas is controlled by a needle valve and a four port valve allows to choose the gas to convey to the reactor in order to have an inert flow over the heated catalyst or while heating up or cooling down the reactor. Liquid reactants are fed with a syringe and an infusion pump (KDS scientific, KDS-100-CE). After the introduction of the liquids, an evaporator-mixing section is present, made of a steel pipe of 150mm length with an external diameter of

25.4mm, internally filled with quartz Raschig rings in order to have a better mixing of vapours and gas. The heat necessary to vaporize the liquid reactants is provided by a caulked resistance; also the gas stream is pre-heated before being put in contact with the liquid stream.

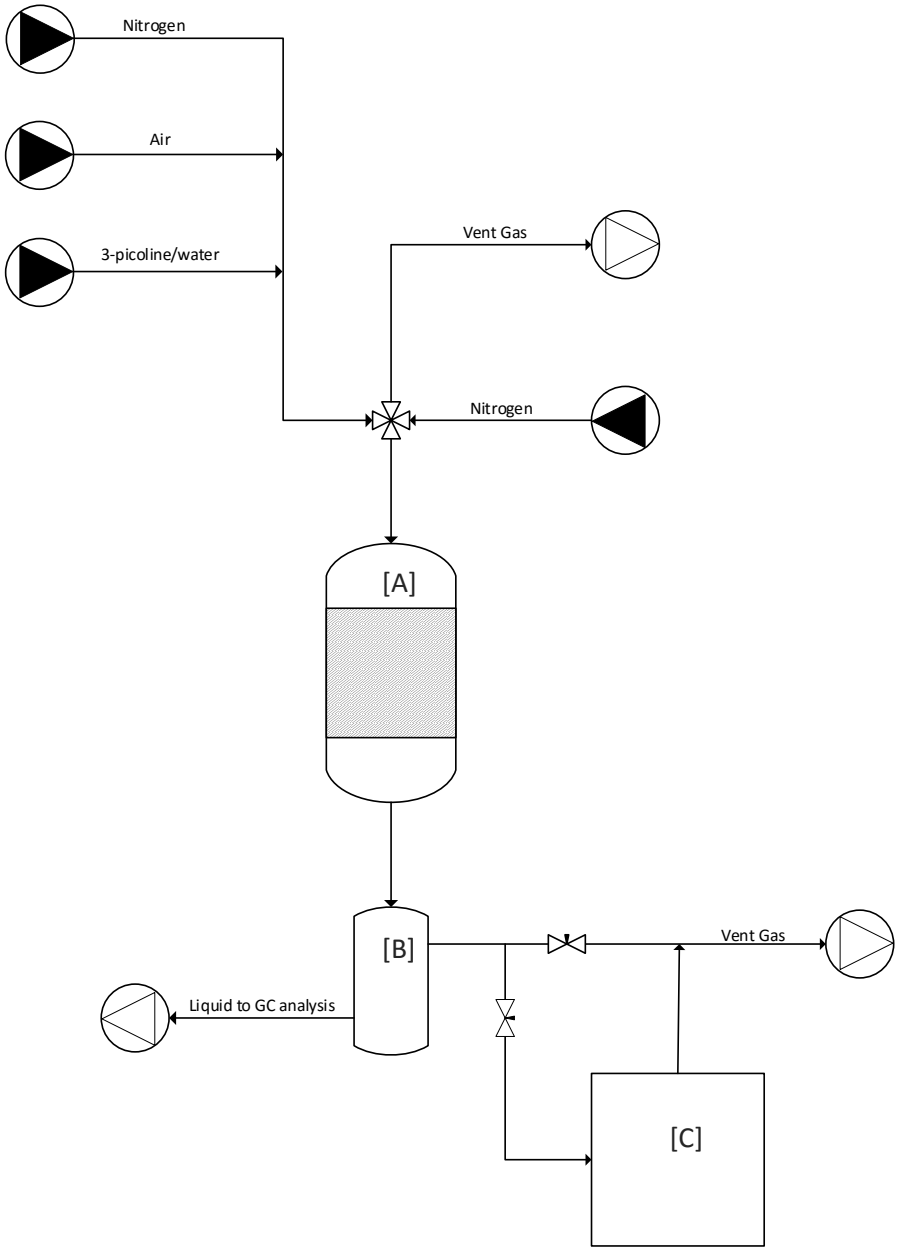

Figure 14. Scheme of experimental set-up for Project C (picoline oxidation)

While the feeding zone is the same for all research studies carried out (Projects A, B and C), the downstream zone was different.

For Project A (MGN cyclisation) and B (C_2 condensation) the bottom part of the reactor was heated by a caulked resistance in order to avoid any condensation of liquid products, and a cold trap filled with acetone was directly connected to it. The gaseous cold stream was sent to the vent system. The acetone solution of liquid products was analyzed by means of gas-chromatography using an external standard; more details on the analytical set-up are given later in this Chapter.

For Project C (picoline oxidation) a cold trap [B] was fitted at the end of the reactor (figure 14). In this case, however, the trap was kept at a temperature of -20°C, in order to avoid the stripping of volatile liquid compounds such as pyridine and 3-picoline. The flow containing gas-phase products was splitted into two streams, one sent directly to the vent system, the other one to an on-line sampling system [C] for analysis, and finally sent to the vent.

2.4.1 GC analytical system

Conversion of reactants and products yields were evaluated by means of gas-chromatography. For Project A (MGN cyclisation) and B (C_2 condensation), the same analytical set-up was used and only the liquid solutions containing the condensable products were analyzed.

The GC-analysis was performed with a HP 5890 instrument equipped with a DB-5ms column and a FID detector; the carrier used was helium. The acetone contained in the cold trap was added with more acetone used for the cleaning of the bottom part of the reactor, where condensation of heavy compounds may occur; then a precise quantity of the internal standard, namely decane, was added, and finally the solution was analyzed.

In the case of Project C (picoline oxidation), the procedure for samples preparation was more complicated, because carboxylic acids are typically

difficult to analyze by GC, and usually are esterified prior to injection. A paper [164] from the Russian team of the Boreskov Institute of Catalysis reports the successful use of a column packed with Chromosorb WAW + 10wt% FFAP. We also installed this column, and the same analytical conditions as those reported in the literature were used. However, nicotinic acid was not eluted in a reasonable time frame. Therefore, we decided to install a DB-5ms column, which provided a good separation of main products, but with a partial overlap of 3-pyridinecarbaldehyde and 3-piridinenitrile peak. However, by tuning the carrier gas flow it was possible to obtain a reasonable separation of the two peaks. The analytical set-up was the same as that used for Projects A and B, but the internal standard used was undecane in this case.

The above cited paper also reports on the use of an on-line sampling system for GC analysis. Some attempts were done to apply this tool, but after few hours on stream, pipes and sampling loop became completely clogged. After several attempts, we decided to collect samples by means of the cold trap system, more reliable than on-line sampling. After the trap, the stream containing gaseous products, such as CO and CO_2, was conveyed to the on-line sampling system; the calibrated volume of gas was analyzed by means of a packed column 3m x 1/8" filled with Carbosieve SII (Supelco). The carrier gas was helium, and the detector was a TCD.

2.4.2 Data elaboration: conversion, yield and selectivity

The values of conversion, yield and selectivity to products were determined using the following equations:

$$Conversion = \frac{n^{\circ}\, mols\ of\ converted\ reactant}{n^{\circ} mols\ of\ fed\ reactant} \times 100$$

$$Yield = \frac{n° \, mols \, of \, product/stoichiometric \, coeff.}{n° \, mols \, of \, fed \, reactant/stoichiometric \, coeff.} \times 100$$

$$Selectivity = \frac{Yield}{Conversion} \times 100$$

$$C \, balance = \frac{\sum Yields}{Conversion} \approx 100$$

3 2-methylglutaronitrile cyclization to 3-cyanopyridine

This section deals with the results of catalytic tests on 2-methylglutaronitrile (MGN) cyclisation to 3-cyanopyridine (Project A).

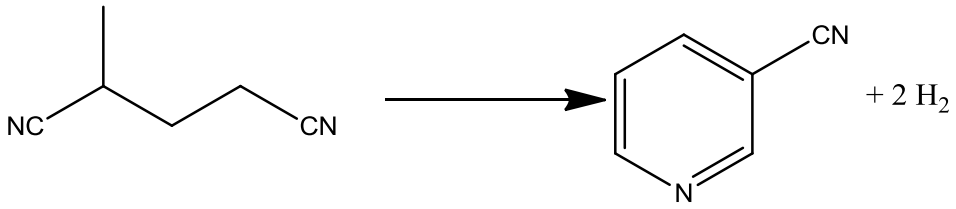

Figure 15. *MGN cyclization to 3-cyanopyridine.*

3.1 Reaction in the absence of oxygen

Some authors already investigated this reaction in the past, as reported in paragraph 1.2.5. However, the approach used during my research work was different, because we operated in the absence of oxygen. Because of this, we decided to use both catalysts different from those reported in the literature and different conditions as well.

For all experiments, 5 mol% of MGN was fed using nitrogen as carrier gas; contact time was 0,5s. In fact, a low MGN concentration is preferable, because a low coverage of the catalyst surface implies a lower probability of occurrence of intermolecular condensation reactions, while intramolecular cyclisation and subsequent dehydrogenation with aromatic ring formation might be more preferred. The MGN concentration chosen was twice as much that one reported in literature for the oxidative approach, while the contact time was similar; however, our catalysts had specific surface area higher than that one of the multi-metallic molybdate catalyst reported in the literature [20].

Prior to catalytic experiments, blank tests were performed by replacing the catalyst with corundum, in order to check for any contribution deriving from

reactions occurring in the gas-phase or over the reactor wall. For these experiments, conversion lower than 4% was registered in the whole range of temperature investigated.

Some experiments were also carried out in order to evaluate the catalytic behaviour of the basic (MgO) and acidic-basic (Mg/M/O) supports; another aim was to check for the possible formation of 3-cyanodehydropiperidine, the expected intermediate of the reaction. Also these tests gave low MGN conversion, below 6% in the whole range of temperature investigated, and no 3-cyanodehydropiperidine was detected.

3.1.1 Pd/Magnesium oxide catalysts

Because of its basic feature, MgO was chosen as the support. Preliminary tests with 1%Pd/MgO showed high MGN conversion, compared to pure MgO, whereas only traces of the desired product were detected. Several by-products formed, which were identified by means of GC-MS, and also calibrated for a quantitative determination. Main products obtained are shown in figure 16.

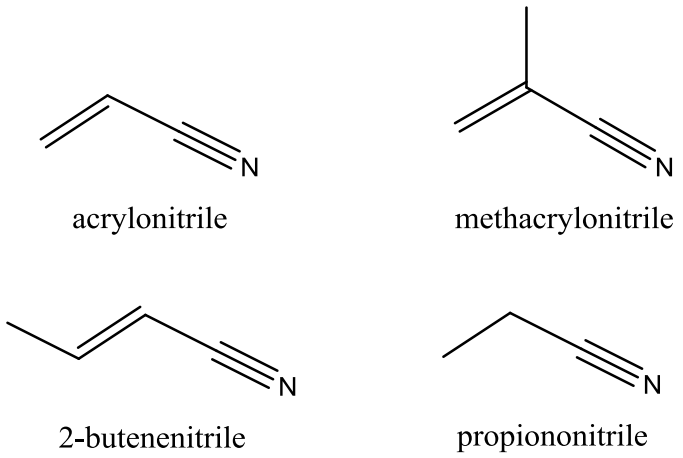

Figure 16. Main products obtained during MGN cyclization in the absence of oxygen

Other products such as isobutyronitrile, butanenitrile, 2-pentenenitrile, 2-methylbutanenitrile, 3-picoline and benzonitrile were detected in minor or trace amount.

Yields of major products and MGN conversion with the 1%Pd/MgO catalyst are plotted in figure 17 in function of temperature.

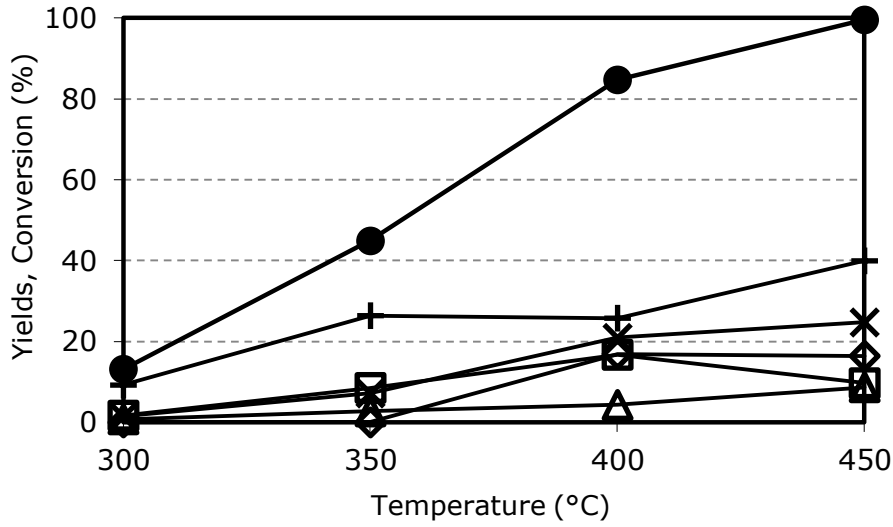

Figure 17. Effect of temperature on MGN conversion and on yield to products. Reaction conditions: feed composition (molar %): MGN/inert=5/95; contact time 0.5s. Symbols: MGN conversion (●), yield to: acrylonitrile (◇), metacrylonitrile (◘), crotylonitrile (△), propanenitrile (✖), and carbon loss (✚). Catalyst 1%Pd/MgO.

Conversion raised from 13% up to 100% by increasing temperature from 300°C to 450°C. The selectivity to main liquid products showed similar trends in function of temperature.

MGN decomposed into smaller fragments containing one nitrile moiety only. The carbon loss was more relevant than yields to any other product. This was due to both the presence of some unquantified minor products and, mainly, to carbonaceous compounds deposition. In fact, from GC-ms no other by-products were found, whereas the spent catalyst was black because of the carbonaceous material which had accumulated after 2-3 hours on stream.

It is known [159] that mixed oxides in the form MgX_2O_4 (where X is a trivalent cation), show both acidic and basic properties. By changing the nature of the trivalent cation it is possible to tune the strength of the basic sites. In order to study how basicity influences reactivity, three different supports were

prepared: Al^{3+}, Fe^{3+} and Cr^{3+} were precipitated as hydroxycarbonates along with Mg^{2+} following the procedure described above. Preliminary tests with 1%Pd/$MgAl_2O_4$ gave a distribution of products similar to that one obtained with 1%Pd/MgO; results are shown in figure 18.

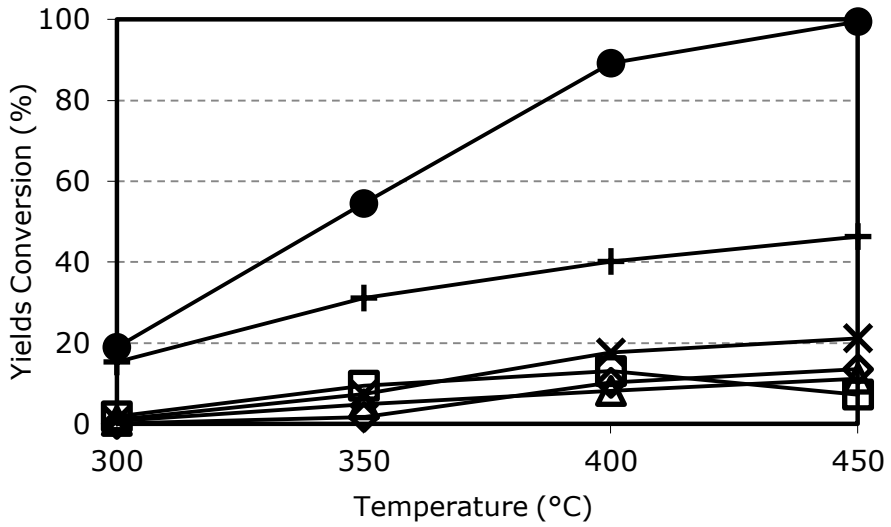

Figure 18. Effect of temperature on MGN conversion and on yield to products. Reaction conditions: feed composition (molar %): MGN/inert=5/95; contact time 0.5s. Symbols: MGN conversion (●), yield to: acrylonitrile (◇), methacrylonitrile (□), crotylonitrile (△), propanenitrile (✕), and carbon loss (+). Catalyst 1%Pd/$MgAl_2O_4$.

In the whole temperature range, conversion was slightly higher for this catalyst than for 1%Pd/MgO, but unfortunately this did not correspond to higher yields to any valuable product. The selectivity to liquid products was lower compared to that one achieved with 1%Pd/MgO, while an increase in carbon deposit was observed.

The same experiment carried out with Pd/$MgFe_2O_4$ and Pd/$MgCr_2O_4$ gave similar results, with an increased selectivity to carbon deposits compared to the MgO supported catalyst.

Unfortunately, no cyanopyridine formed, a clear indication that radicalic fragmentation was more preferred than cyclisation.

3.1.2 Pd/Zeolite catalyst

From the previous results, it is clear that the basic component of the catalyst, used as the support for Pd, may be one reason for the poor catalytic behavior shown. Therefore, we decided to use an acid support, a HY zeolite with a silica-to-alumina ratio of 10. Moreover, an advantage of the Pd/zeolite system might be that one of achieving a better palladium dispersion, because of the method used for the deposition of the metal, by ion exchange of Pd^{2+} instead of impregnation.

Results of catalytic tests carried out in the same conditions as for the basic supported catalyst are reported in figure 19. GC-ms analysis demonstrated that the same products already observed with the basic systems were obtained also in this case.

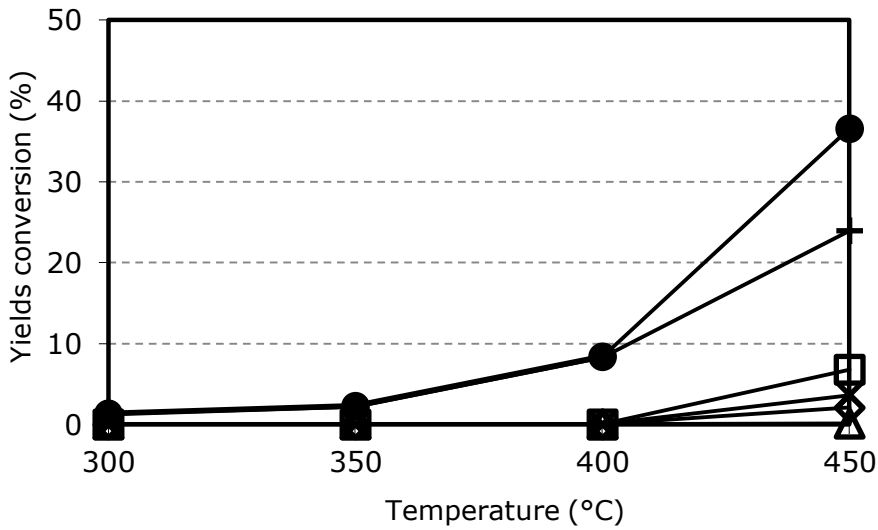

Figure 19. Effect of temperature on MGN conversion and on yield to products. Reaction conditions: feed composition (molar %): MGN/inert=5/95; contact time 0.5s. Symbols: MGN conversion (●), yield to: acrylonitrile (◇), methacrylonitrile (□), crotylonitrile (△), propanenitrile (✕), and carbon loss (✚). Catalyst 1%Pd/HY-SAR10.

This catalyst was less active than those based on MgO; in fact, conversion was lower. Significant carbon deposits were also noticed at all temperatures, in higher amount than with Pd/MgO. Yields to liquid products were much lower if

compared to previous tests, and reached a maximum value of 6.8% only for methacrylonitrile at 450°C. No formation of 3-cyanopyridine was observed.
This behaviour might be explained by taking into account diffusional problems of the reactant which could not reach the Pd active sites located inside the zeolite pores; it is possible that the rapid formation of carbonaceous deposits (coke) hindered the access of MGN to the pores.

3.1.3 Transition metal oxides based catalysts

Considering the previous results, we decided to test other catalysts containing an active phase different from Pd. Oxides of transition metals, such as Cobalt and Nickel, are known to be active in dehydrogenation reactions. We decided to prepare catalysts based on these elements, supported over a less acidic support, namely alumina, in order to limit cracking phenomena and coke formation.

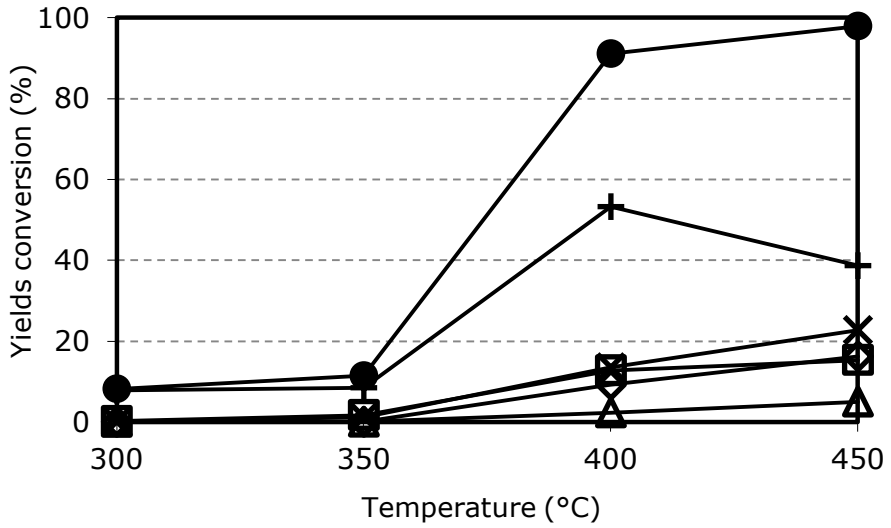

Figure 20. Effect of temperature on MGN conversion and on yield to products. Reaction conditions: feed composition (molar %): MGN/inert=5/95; contact time 0.5s. Symbols: MGN conversion (●), yield to: acrylonitrile (◇), methacrylonitrile (◘), crotylonitrile (△), propanenitrile (✕), and carbon loss (✚). Catalyst 20%CoO/Al_2O_3.

Preliminary tests carried out with the plain alumina support gave a conversion slightly higher compared to that achieved with MgO. GC-ms analysis showed again the formation of the same products.

In figure 20 are reported yields and conversion in function of temperature for the 20%$^{w}/_{w}$CoO/Al_2O_3 catalyst.

With this catalyst, the reaction showed a light-on effect between 350°C and 400°C. Carbon deposits still formed in remarkable amount, with a C loss (52%) even higher than that observed with Mg/M/O-supported catalysts; however, by increasing the temperature, a decrease of carbon deposits was observed, while liquid products formation increased. However, also in this case no 3-cyanopyridine formed.

A catalyst with an active phase composed of 20%$^{w}/_{w}$ of CoO and 3%$^{w}/_{w}$ of NiO was tested in the same reaction conditions; results are presented in figure 21.

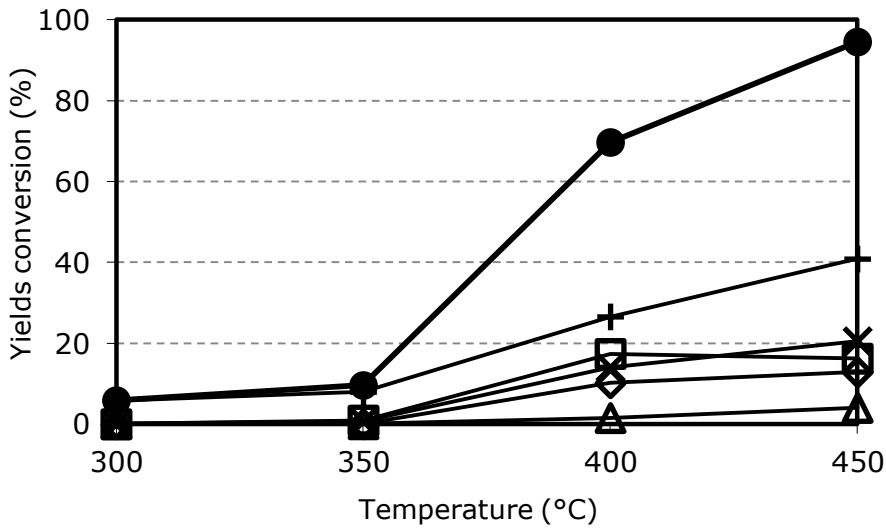

Figure 21. Effect of temperature on MGN conversion and on yield to products. Reaction conditions: feed composition (molar %): MGN/inert=5/95; contact time 0.5s. Symbols: MGN conversion (●), yield to: acrylonitrile (◇), methacrylonitrile (□), crotylonitrile (△), propanenitrile (✕), and carbon loss (✚). Catalyst 20%CoO/3%NiO/Al_2O_3.

In the presence of Nickel oxide, the light-on effect on conversion was less pronounced; moreover, the catalyst was slightly less active than the CoO-based

one. An additional effect of Ni was that the decrease of coke formation previously observed at high temperature, was now suppressed; on the other hand, the catalyst appeared to be more selective to liquid products at low temperature but, also in this case, no 3-cyanopyridine was detected.

3.1.4 Supported Vanadium oxide catalyst

Vanadium oxide is widely used as a mild oxidation catalyst, as reported in the introduction of this thesis. It is also known for its mild acidic features and for its oxidative dehydrogenation properties; in its reduced form, is also able to catalyse dehydrogenation and disproportionation reactions. A catalyst made of 7% V_2O_5 supported over zirconia was prepared and tested; results are reported in figure 22.

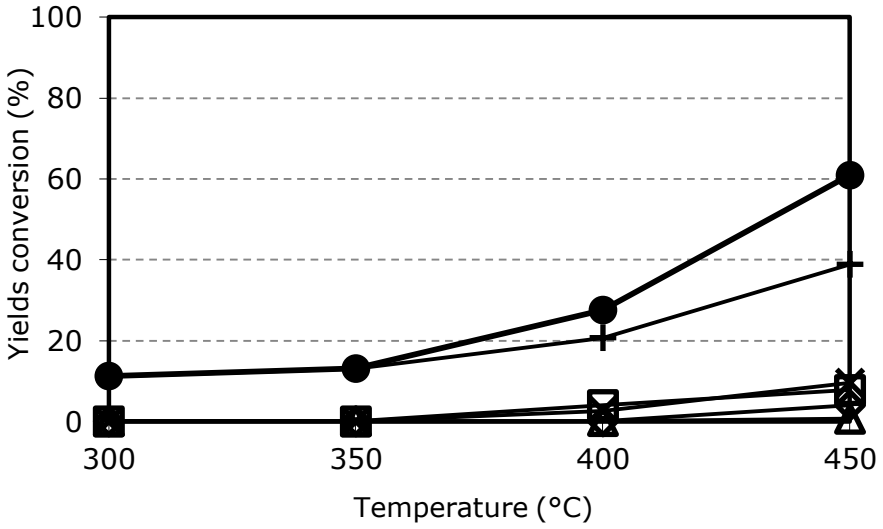

Figure 22. Effect of temperature on MGN conversion and on yield to products. Reaction conditions: feed composition (molar %): MGN/inert=5/95; contact time 0.5s. Symbols: MGN conversion (●), yield to: acrylonitrile (◇), methacrylonitrile (◻), crotylonitrile (△), propanenitrile (✕), and carbon loss (✚). Catalyst 7%V_2O_5/ZrO_2.

This catalyst showed a low activity, and the selectivity to liquid products was lower than with the other catalysts tested; coke was the major product, and no 3-cyanopyridine was produced.

3.2 Reaction in the presence of oxygen

In all the above reported experiments, no 3-cyanopyridine was produced; the largely preferred reaction was that one leading to reactant fragmentation into shorter-chain nitriles. By means of DFT calculation, we found a positive free Gibbs energy for the cyclisation reaction at temperature below 550 K (figure 23). This calculation took into account the co-production of two H_2 molecule (dehydrocyclisation). This means that in order to have cyclisation, it is necessary to operate at temperature no lower than 280°C. On the other hand, results obtained so far indicate that the kinetics of the reaction necessitates temperatures which are higher than 350°C, conditions at which, however, C-C thermolysis is also highly favoured. In other words, it seems that in order to allow cyclisation to become both kinetically and thermodynamically preferred over other undesired reactions, it is necessary to change completely the reaction strategy; for example, it is necessary to co-feed oxygen, in order to make the cyclisation even more favoured at lower temperature (because of the co-production of H_2O, and of reaction exothermicity) and use oxidation catalysts which are active at mild conditions.

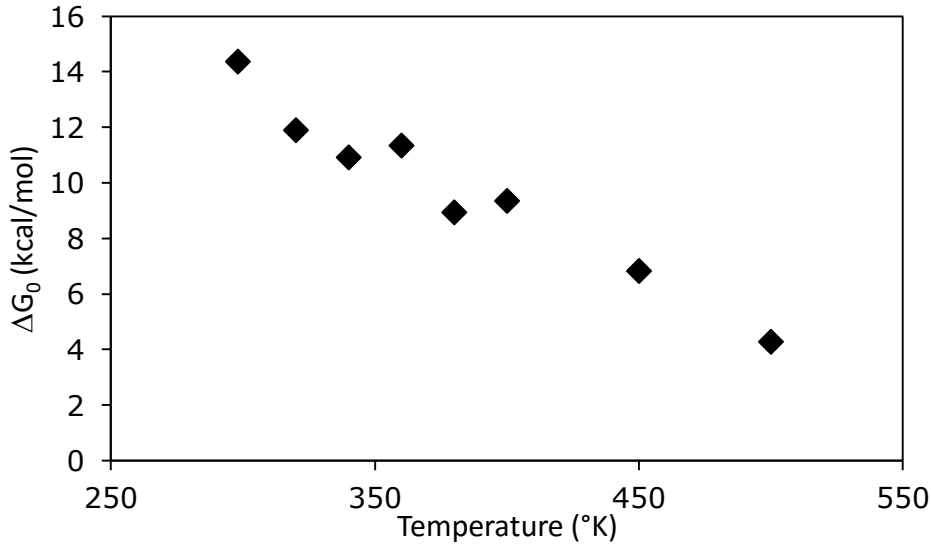

Figure 23. Free Gibbs energy for MGN cyclization in absence of oxygen (DFT calculation)

Reactivity tests in the presence of oxygen were carried out using two different inlet feed compositions; one feed was made of air and 5%mol MGN, the second one of 5% MGN with air and nitrogen as inert, in order to achieve a lower oxygen concentration, namely the same partial pressure as for MGN. The contact time used was the same as for tests carried out in the absence of oxygen (0.5 s). Blank tests, carried out without catalyst, gave MGN conversion below 6%, with no formation of liquid products. GC-ms analysis of the gaseous stream showed the formation of CO_x and traces of HCN.

3.2.1 Multi-metallic molybdate catalyst

A patent [20] issued by Standard Oil Company claims the production of 3-cyanopyridine with a multimetal molybdate catalyst under conditions close to those used for our catalytic tests.

From the GC-ms analysis of the outlet stream during a preliminary catalytic test, it was possible to determine that the reaction products were totally different from those obtained in the absence of oxygen. Main products were CO_x, carbon deposit and glutaronitrile, but in this case no C_3-C_4 nitriles were found. Other by-products obtained are reported in figure 24.

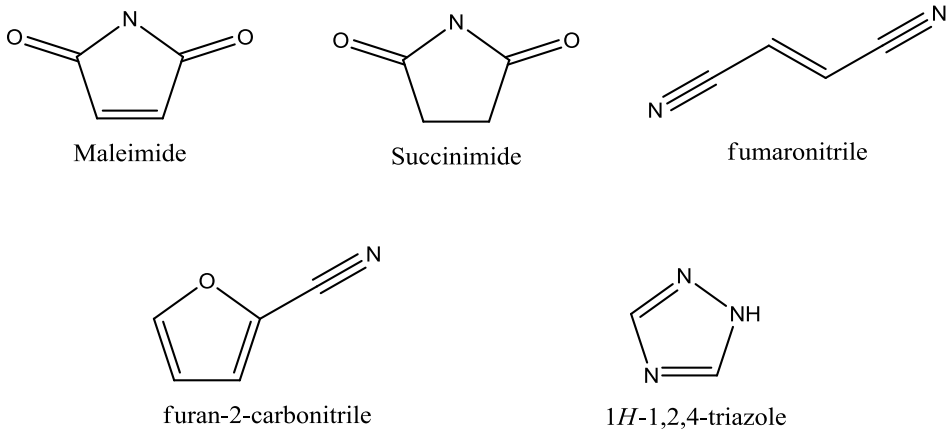

Figure 24 Main by-products for MGN cyclization in the presence of oxygen.

The demethylation of MGN to glutaronitrile is an interesting reaction because it is a cheap and clean way to produce pentanediamine, is a monomer for nylon

5,5. The demand for this polymer is growing not so much for the fibre market but mainly as a technoplastic material for the automotive sector. Polymerisation of glutaric acid and pentanediamine, the latter alone or in mixture with hexanediamine, makes possible to tune the properties of the resulting polymer. Selective production of glutaronitrile starting from cheap MGN might meet this market trend.

First tests with the multi-metallic molybdate catalyst were carried out by feeding MGN in mixture with air; results are reported in figure 25.

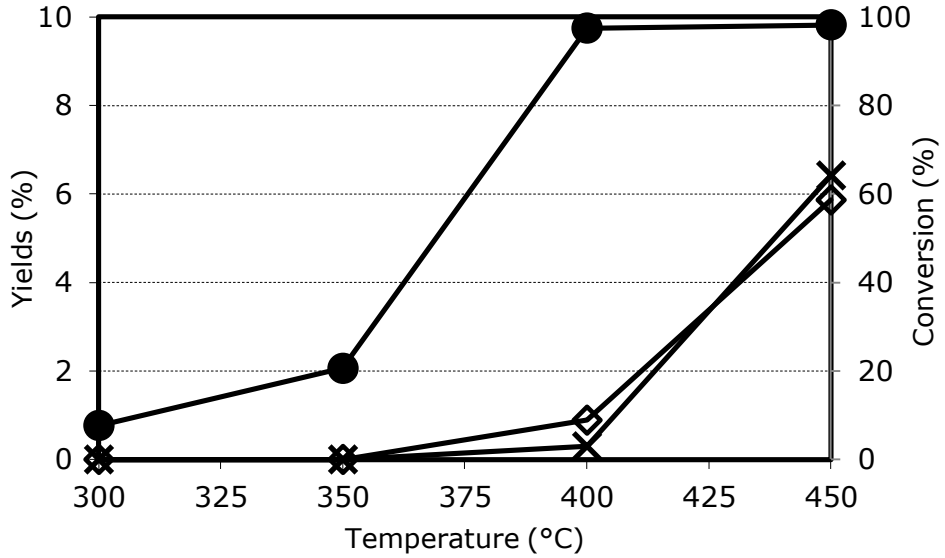

Figure 25. Effect of temperature on MGN conversion and on yield to products. Reaction conditions: feed composition (molar %): MGN/air=5/95; contact time 0.5s. Symbols: MGN conversion (●), yield to: succinimide and maleimide (◇), glutaronitrile (✘). Catalyst Multi-metallic molybdate.

It is possible to see how, despite a high MGN conversion, yields to valuable products were below 7%. The major products were CO_x (not quantified); therefore, we decided to carry out experiments with lower oxygen concentration in feed. Results are reported in figure 26.

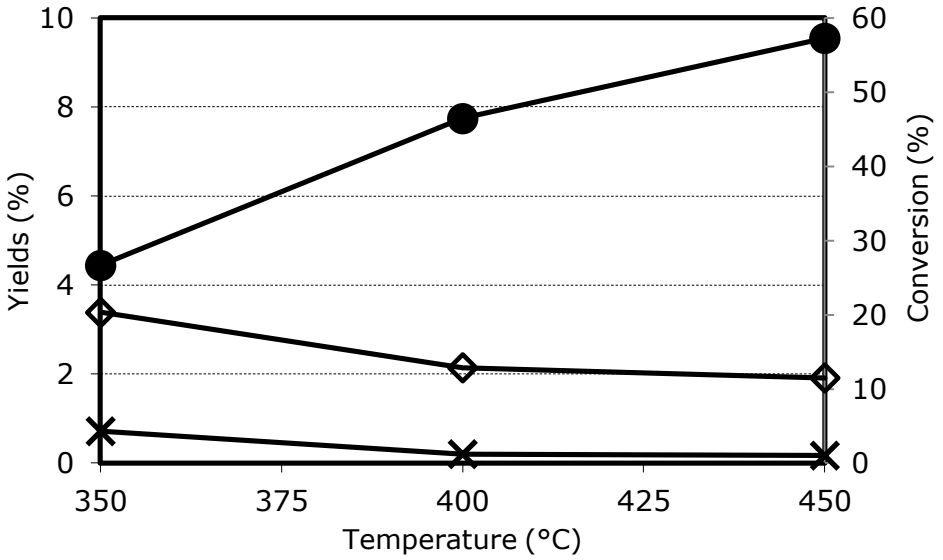

Figure 26. Effect of temperature on MGN conversion and on yield to products. Reaction conditions: feed composition (molar %): MGN/O_2/nitrogen=5/5/90; contact time 0.5s. Symbols: MGN conversion (●), yield to: succinimide and maleimide (◇), glutaronitrile (✖). Catalyst Multi-metallic molybdate.

Data obtained with 5 mol% O_2 concentration in feed showed lower MGN conversion values; yields to liquid products decreased with temperature, which is the opposite trend of that one observed previously with an O_2-richer inlet feed. This is probably due to the fact that adsorbed species are barely desorbed from a more reduced active site, with an enhanced coke formation and finally lower liquid products yields.

In no case 3-cyanopyridine production was noticed, and the low glutaronitrile yield achieved makes unlikely an industrial application of this reaction, despite the low MGN price.

3.2.2 Supported Vanadium oxide catalyst

Results obtained demonstrate that MGN cyclization in the presence of oxygen over multimetallic molybdate produces mainly CO_x, and yields to valuable products are low. Supported V_2O_5 catalysts are known to be selective in mild oxidation, therefore we tested a 7% V_2O_5/ZrO_2 catalyst for the reaction of MGN

cyclization to 3-cyanopyridine and MGN demethylation to glutaronitrile. Results of these experiments are shown in figure 27.

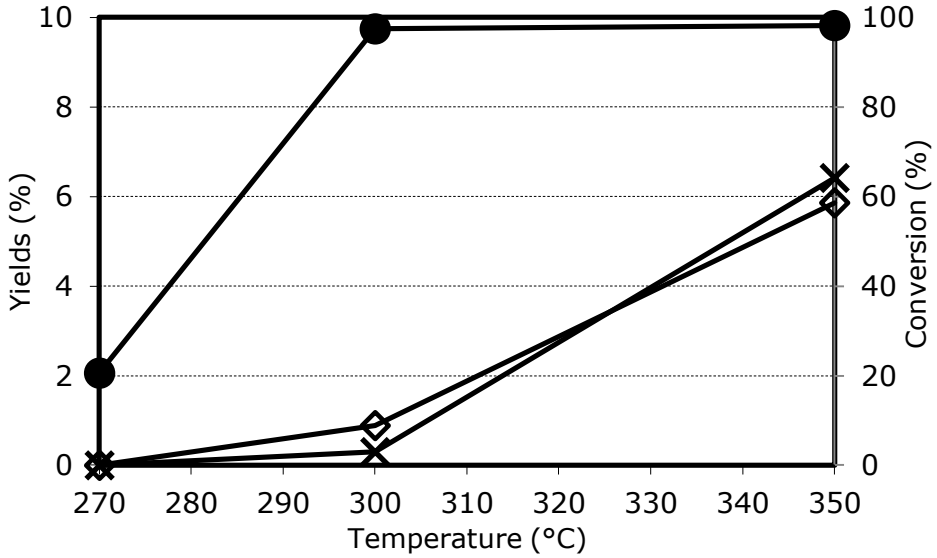

Figure 27 Effect of temperature on MGN conversion and on yield to products. Reaction conditions: feed composition (molar %): MGN/air=5/95; contact time 0.5s. Symbols: MGN conversion (●), yield to: succinimide and maleimide (◇), glutaronitrile (✖). Catalyst 7%V_2O_5/ZrO_2.

Conversion was much higher than with the molybdate catalyst, since it reached values close to 100% at the temperature of 300°C, at which the molybdate was barely active.

Yields to liquid products followed the same trend as with the molybdate catalyst; a similar yield of 6% was achieved for both glutaronitrile and maleimide plus succinimide.

Concluding, it is possible to say that the reaction of 2-methylglutaronitrile cyclisation cannot be carried out neither under anaerobic nor aerobic conditions, because other undesired reactions are kinetically more preferred. Specifically, under non-oxidative conditions, radical-type fragmentation leads to the formation of shorter-chain nitriles and to coke. In the presence of oxygen, preferred products are heavy compounds and COx, with minor formation of glutaronitrile and imides.

4 Acetonitrile and acetaldehyde condensation to 3-picoline

Results and discussion on the feasibility of a process in which acetaldehyde reacts with acetonitrile to produce 3-picoline, avoiding the use of ammonia, will be presented in this section (Project B).

$$2\ CH_3CHO + CH_3CN \rightarrow 3\text{-picoline} + 2\ H_2O$$

For preliminary tests, a low reactants concentration was chosen in order to reduce the extent of acetaldehyde self-condensation, namely a 5%mol total organic compounds in the N_2 stream. A contact time of 0.5s was chosen. As reported in paragraph 1.6, we decide to use of a basic catalyst for the activation of both acetaldehyde and acetonitrile. Preliminary experiments demonstrated that when a stoichiometric feed (acetaldehyde/acetonitrile 2:1) was used, with both basic (MgO) and acid (HY SAR 10) systems the only compound which reacted was the aldehyde, with negligible conversion of acetonitrile. GC-ms analysis revealed the formation of substituted and unsubstituted aromatic compounds and their isomers, such as benzene, toluene, xylenes, trimethylbenzenes, naphthalene and so on, along with carbon deposit.

Therefore, we decided to use an excess of acetonitrile, in order to push the adsorption and conversion of the nitrile, and to slow down the reaction of acetaldehyde self-condensation. In any case, a moderate conversion of acetonitrile was foreseen, with limited formation of picoline, and the formation of large amounts of by-products due to the side reactions occurring on acetaldehyde.

Experiments carried out by feeding acetaldehyde and acetonitrile in a molar ratio 1:5 showed now a small, but non negligible, acetonitrile conversion to

N-containing products, namely 2-butenenitrile and traces of 2-picoline and 4-picoline, but no formation of 3-picoline. The production of hetero-aromatics, albeit in trace amount, proved that this route is feasible, but the undesired isomers formed, as indeed it might be expected based on the mechanism for the condensation between acetonitrile and two molecules of acetaldehyde.
In order to overcome this problem, the reacting mixture was changed, introducing formaldehyde, that reacting with acetonitrile and acetaldehyde should produce picoline with the methyl group in β position (3-picoline).

4.1 Acid catalyst

The results achieved so far suggest that an acid catalyst might be more efficient in acetonitrile activation; therefore, we decided to investigate on the reactivity of the HY zeolite.

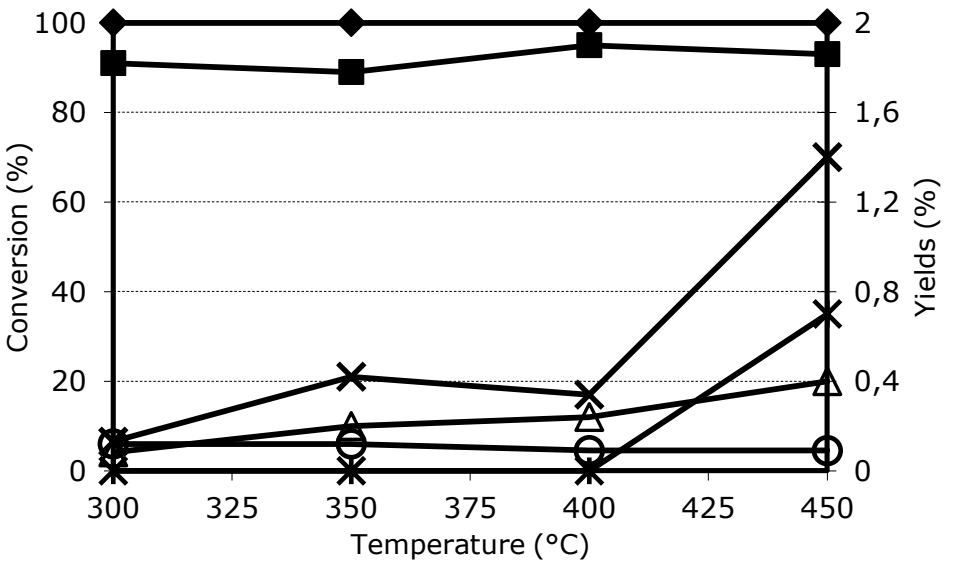

Figure 28. Effect of temperature on reactant conversion and on yield to products. Reaction conditions: feed composition (molar ratio): formaldehyde/acetaldehyde/acetonitrile=2/1/5; total organic 5mol%; contact time 0.5s. Symbols: Formaldehyde conversion(◆) acetaldehyde conversion(■), acetonitrile conversion (△); yields to: crotylonitrile (✘), 3-picoline (O), pyridine (✱). Catalyst HY-SAR10.

Formaldehyde and acetaldehyde were co-fed in the stoichiometric ratio 2:1, while a five-fold excess of acetonitrile was fed

(formaldehyde/acetaldehyde/acetonitrile = 2:1:5, 5mol% of organic compounds in N_2). Conversion and yields obtained are plotted in function of temperature in figure 28.

Conversion achieved was total for formaldehyde in the whole range of temperature investigated, and was about 90% for acetaldehyde. Acetonitrile conversion reached a maximum value of 20% at 450°C. Despite this, selectivity to N-containing products was very low; 3-picoline yield was ca 0.1% at all temperatures. Increasing the temperature, a slight increase of crotylonitrile yield was registered. Prevailing products were aromatic compounds and coke. This test showed that a catalyst containing only an acidic feature is not enough active and selective to facilitate acetonitrile activation. Therefore, a bi-functional catalyst was used, containing a hydrogenation metal; our aim was to co-feed also H_2, and activate acetonitrile through hydrogenation of the nitrile group to the more reactive imine.

4.2 Bifunctional catalyst

With the aim of performing acetonitrile activation by hydrogenation of the nitrile group, bifunctional (acid and hydrogenating) catalysts, already used also for MGN cyclization, were tested, namely 1%Pd/HYSAR10, 20%CoO-3%NiO /Al_2O_3 and 20%CoO-3%NiO/SiO_2 (concentration of the active phase is expressed as $\%^w/_w$). Hydrogen was co-fed with a molar ratio H_2/acetaldehyde equal to 8:1.

Conversions and yields in function of temperature are reported in figure 29 for the Pd-Zeolite catalyst. Before the experiments, the catalyst was activated with the above mentioned procedure. The comparison of results for this experiment with those for the experiment carried out in the absence of hydrogen, shows that the behaviour was similar in the two cases; in fact, the conversion of the reagents followed similar trends and yield to 3-picoline was not affected by hydrogen co-feeding. Probably this behaviour was due to zeolite pore blocking, an event which occurred after a short time-on-stream due to coke deposition;

therefore, acetonitrile could not reach Pd sites inside zeolite cavities. Moreover, hydrogenation of the cyano group probably requires higher pressure and lower temperature.

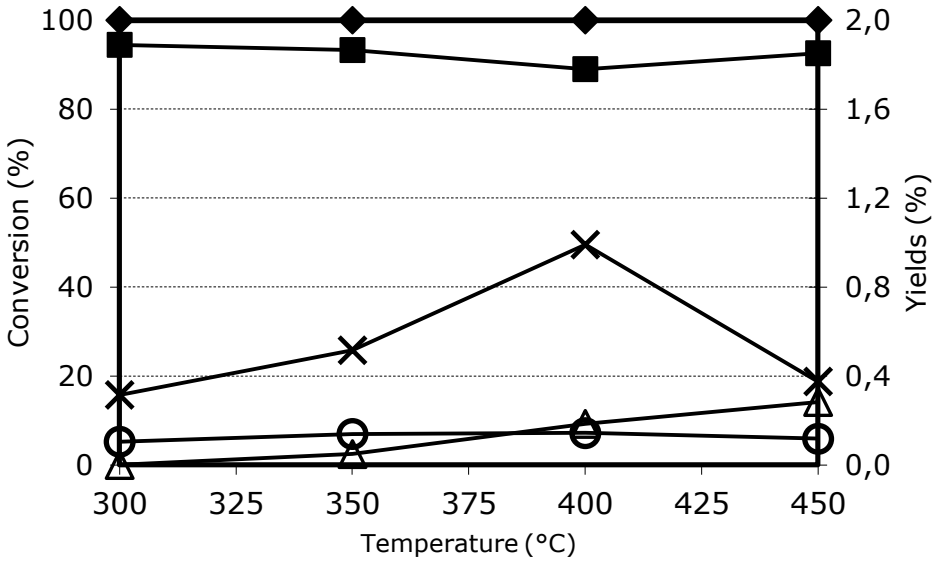

Figure 29. Effect of temperature on reactant conversion and on yield to products. Reaction conditions: feed composition (molar ratio): formaldehyde/acetaldehyde/ACN/H_2=2/1/5/8; total organic 5mol%; contact time 0.5s. Symbols: Formaldehyde conversion(◆) acetaldehyde conversion(■), acetonitrile conversion (△); yields to: crotylonitrile(✘), 3-picoline (O). Catalyst 1%Pd/HY-SAR10.

We then tested the reactivity of Co oxide supported over alumina and silica. Conversions and yields are plotted in function of temperature in figures 30 and 31.

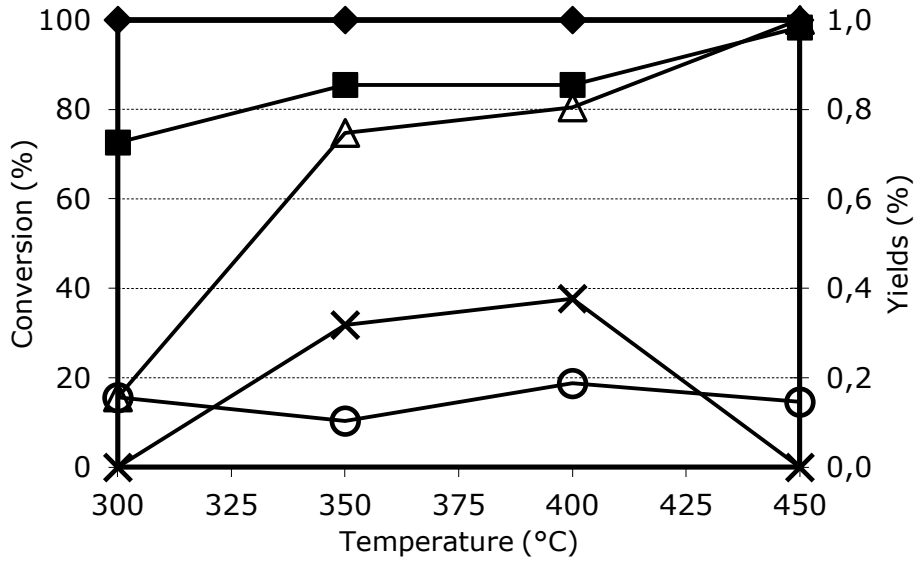

Figure 30. Effect of temperature on reactant conversion and on yield to products. Reaction conditions: feed composition (molar ratio): formaldehyde/acetaldehyde/acetonitrile/H_2=2/1/5/8; total organic 5mol%; contact time 0.5s. Symbols: Formaldehyde conversion(◆) acetaldehyde conversion(■), acetonitrile conversion (△); yields to: crotylonitrile(✘), 3-picoline (O). Catalyst 20%CoO-3%NiO/γ-alumina.

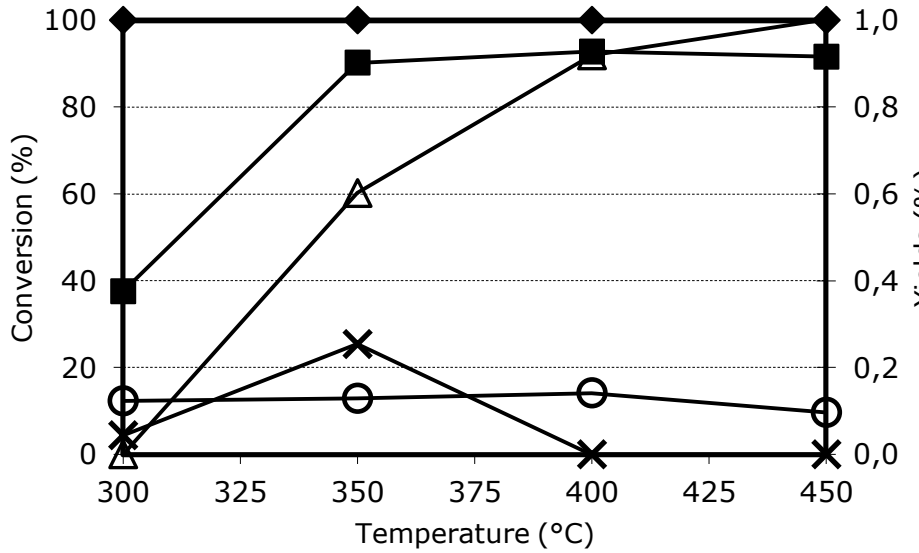

Figure 31. Effect of temperature on reactant conversion and on yield to products. Reaction conditions: feed composition (molar ratio): formaldehyde/acetaldehyde/acetonitrile/H_2=2/1/5/8; total organic 5mol%; contact time 0.5s. Symbols: Formaldehyde conversion(◆) acetaldehyde conversion(■), acetonitrile conversion (△); yields to: crotylonitrile(✘), 3-picoline (O). Catalyst 20%CoO-3%NiO/Silica.

Acetonitrile was activated with this catalyst type; in fact, its conversion was total in both cases at 450°C, and in the case of the alumina supported catalyst, acetonitrile conversion was non-negligible even at 300°C.

However, also with these catalysts 3-picoline formed in trace amount only.

The other N-containing compound, 2-butenenitrile, formed with yield below 1%. In all the experiments, both aldehydes were converted mainly to aromatic compounds.

The high excess of aldehyde needed and the very low yield to 3-picoline achieved make a possible future industrial application of this process highly unlikely.

5 The oxidation of 3-picoline with V_2O_5/ZrO_2 catalysts

This Chapter deals with the characterization of catalysts and results of catalytic experiments for Project C (3-picoline oxidation).

5.1 Catalysts preparation and characterization

The support, ZrO_2, was prepared three times using the same procedure; however, the samples obtained showed some differences in the value of surface area. This might be attributed to slight variations in the method adopted (e.g., the time of aging of the precipitate), or to some other unknown factor. The three zirconia samples obtained will be referred as 1st, 2nd and 3rd stock-UniBO (see table 1).

In some case, ZrO_2 was calcined also at temperature higher than 550°C, in order to decrease its surface area value; for example, in order to have a surface area close to 20-25 m^2/g, we calcined 1st and 2nd stock zirconia at 650°C, whereas the 3rd stock zirconia had to be calcined at 700°C.

We also used a commercial ZrO_2 support, supplied by Aldrich, characterized by a low surface area (4.2 m^2/g). This support is referred to as "commercial zirconia" (table 1). The crystalline structure was the same as that of the home-prepared zirconia samples (see Figures showing XRD patterns).

Table 1 summarizes the surface area values of the different supports used for catalysts preparation.

The impregnation of supports was carried out with the method reported in Experimental; finally, the sample was dried and calcined again at 550°C. Table 2 summarizes the samples prepared, with the corresponding codes used in the thesis.

Sample code	Origin	T of calcination (°C)	Surface area (m^2/g)
ZU1H	1st stock UniBO	550	Nd
ZU2H	2nd stock UniBO	550	68±3
ZU3H	3rd stock UniBO	550	50±3
ZU1M	1st stock UniBO	650	24±2
ZU2M	2nd stock UniBO	650	23.4
ZU3M	3rd stock UniBO	700	25±2
ZU3L	3rd stock UniBO	950	10.5
ZC	Commercial	Unknown	4.2

Table 1. Supports used for the preparation of catalysts; H stands for high surface area; M stands for medium surface area; L stands for low surface area.
**Surface areas determined with the single-point BET method are given without decimal digits; surface areas measured by porosimetry are given with one decimal unit.*

Sample code	V_2O_5 content (wt%) – support	Catalyst surface area, m^2/g*
2VZ	2 - ZU3M	25±2
4VZ	4 - ZU1M	23±2
7VZ	7 - ZU1M	25±2
2VZH	2 - ZU1H	67±3
2VZL	2 - ZU3L	10.5
2VZT	2 - ZU2H**	26±2
2VZC	2 – ZC	4.8
4VZC	4 – ZC	5.0
7VZC	7 – ZC	5.4

*Table 2. Catalysts prepared using supports listed in Table 1. *Surface areas determined with the single-point BET method are given without decimal digits; surface areas measured by porosimetry are given with one decimal unit. ** This sample was prepared by calcination at 700°C of the catalyst prepared by deposition of 2 wt% V_2O_5 over the ZU2H support.*

Catalysts were characterised by means of XRD and Raman spectroscopy.

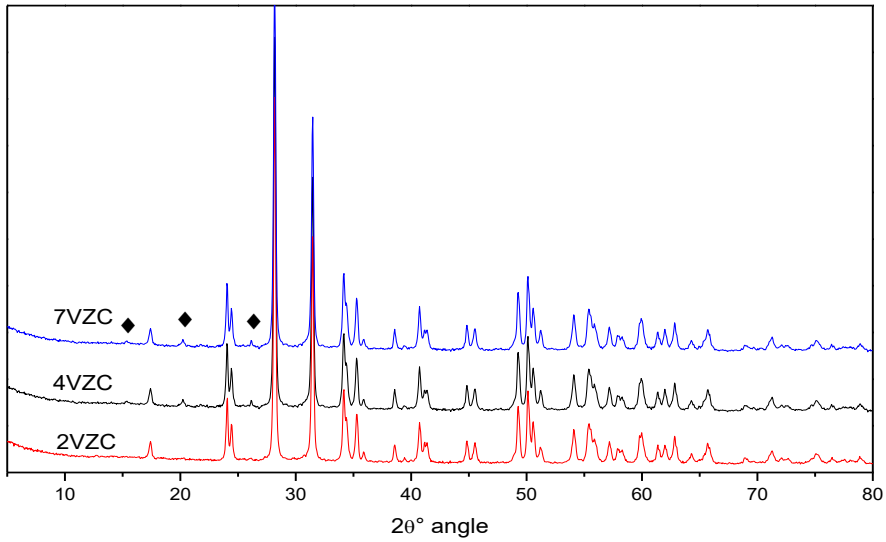

Figure 32. XRD pattern of catalysts with different V_2O_5 content supported over commercial zirconia (indexed with ◆ are reflections of crystalline V_2O_5).

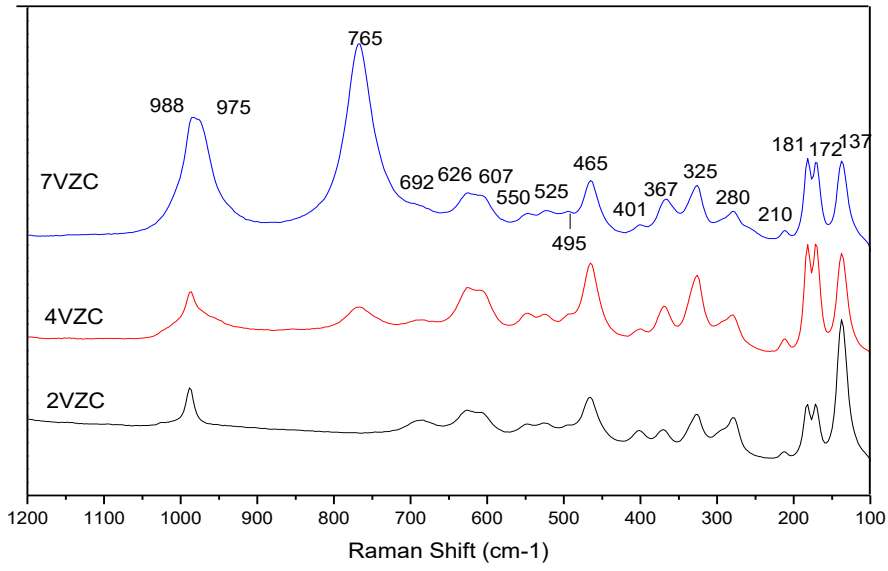

Figure 33. Raman spectra of catalyst with different V_2O_5 content supported over commercial zirconia. See text for attribution of bands.

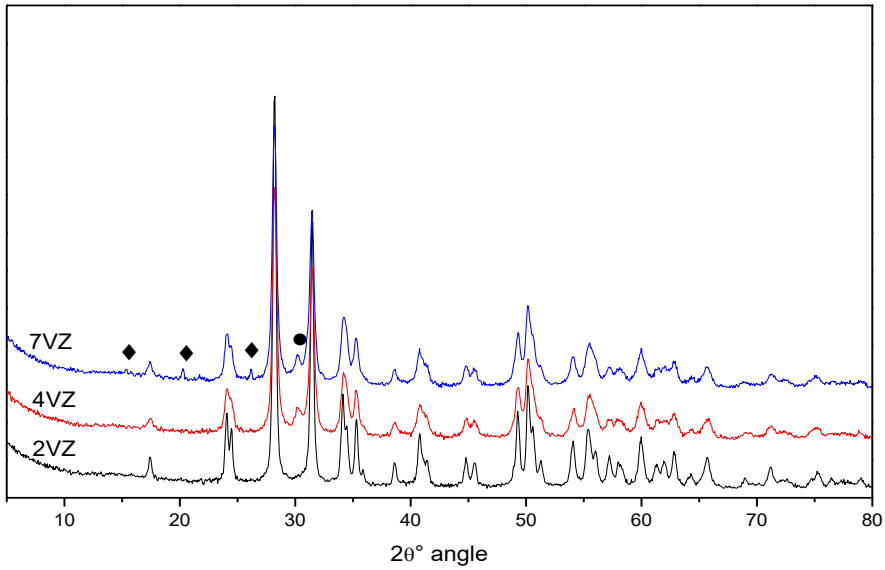

Figure 34. XRD pattern of catalysts with different V_2O_5 content supported over UniBO zirconia (indexed with ◆ are reflections of crystalline V_2O_5, with ● of tetragonal zirconia).

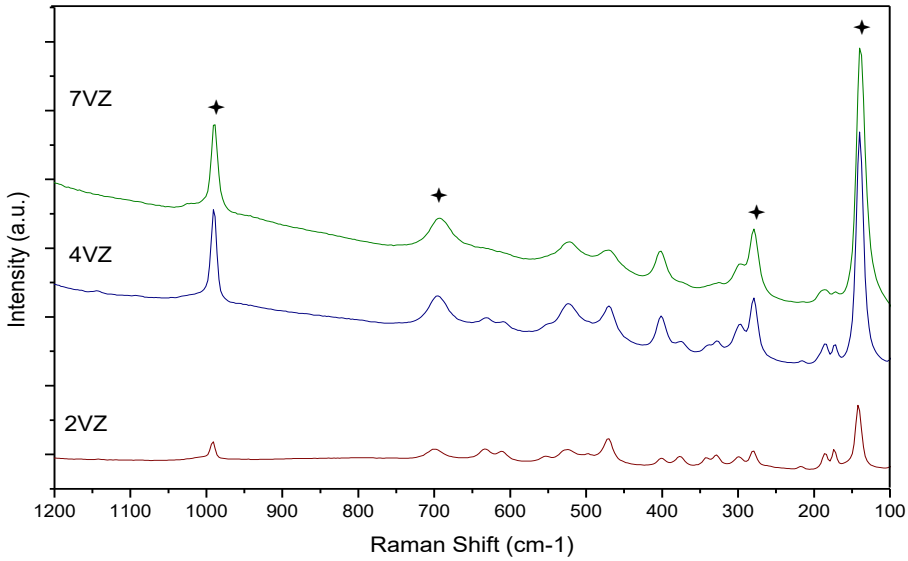

Figure 35. Raman spectra of catalysts with different V_2O_5 content supported over UniBO zirconia (indexed with ✦ bands attributable to V_2O_5, all the other bands are attributable to zirconia).

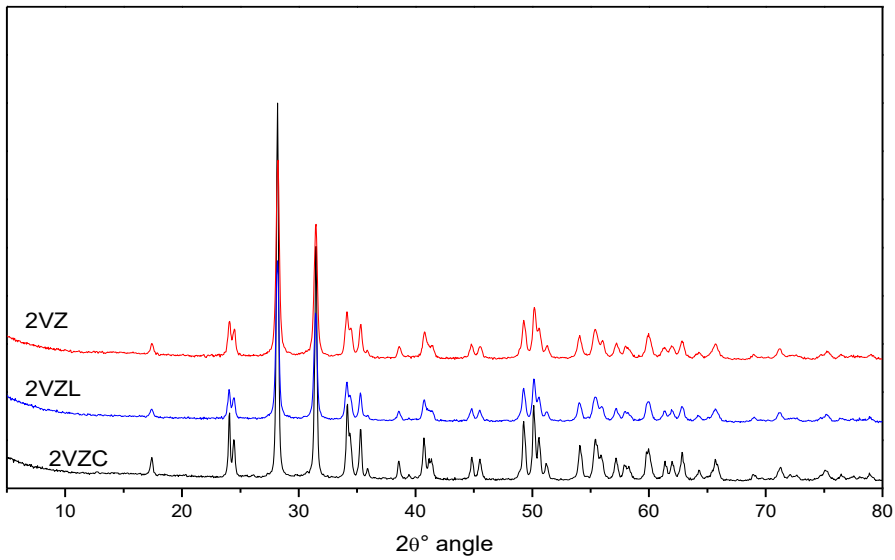

Figure 36. XRD pattern of catalysts with different Ss_A, and 2% V_2O_5 content.

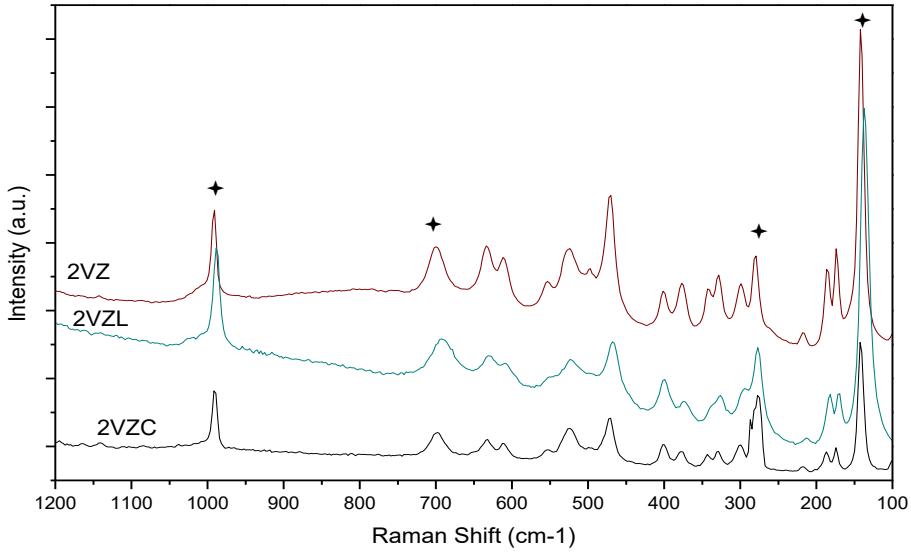

Figure 37. Raman spectra of catalysts with different Ss_A, 2% V_2O_5 content (indexed with ✦ are bands attributable to bulk V_2O_5, all the other bands attributable to zirconia).

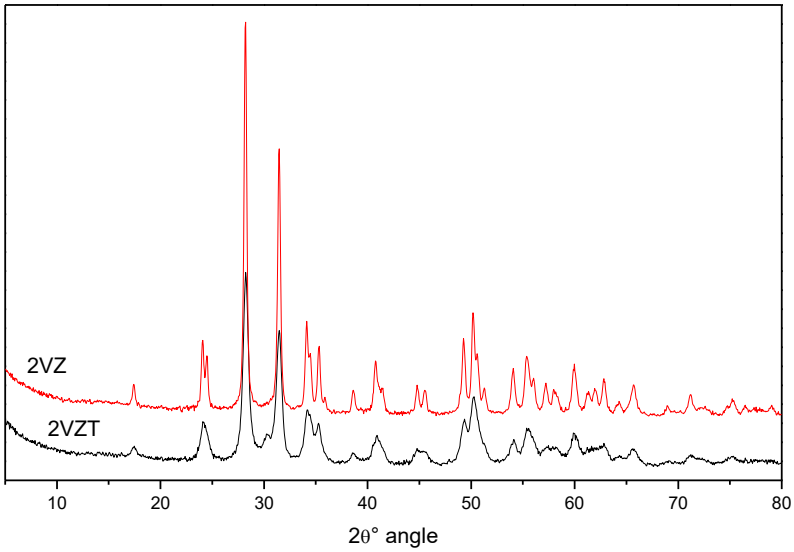

Figure 38. XRD pattern of 2VZ and 2VZT catalysts.

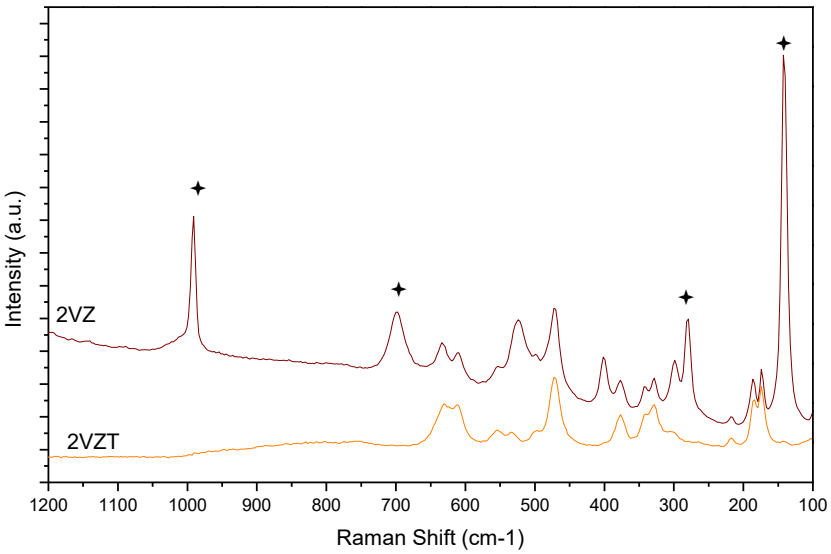

Figure 39. Raman spectra of 2VZ and 2VZT catalysts (indexed with ✦ are bands attributable to bulk V_2O_5, all the other bands attributable to zirconia).

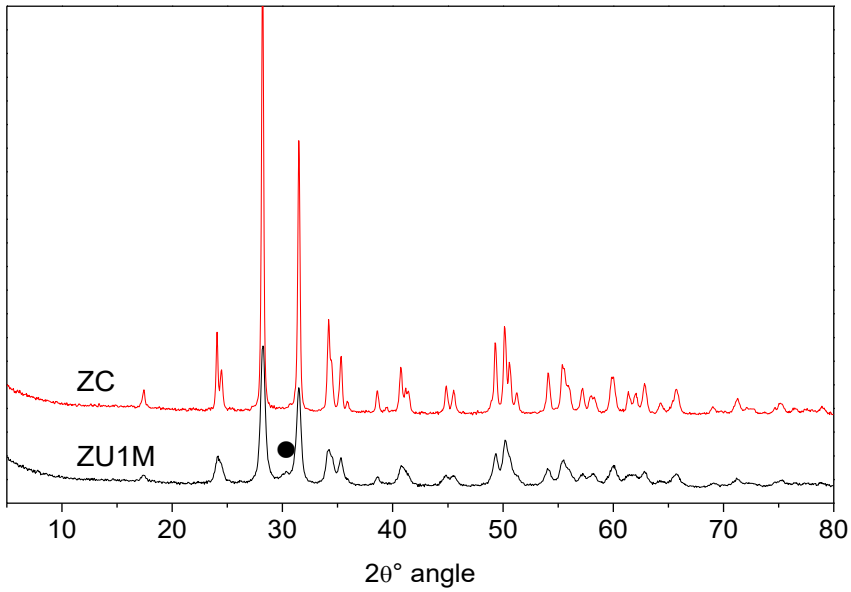

Figure 40. XRD patterns of commercial zirconia and UniBO zirconia supports. Reflection indexed with (●) is attributable to tetragonal ZrO_2.

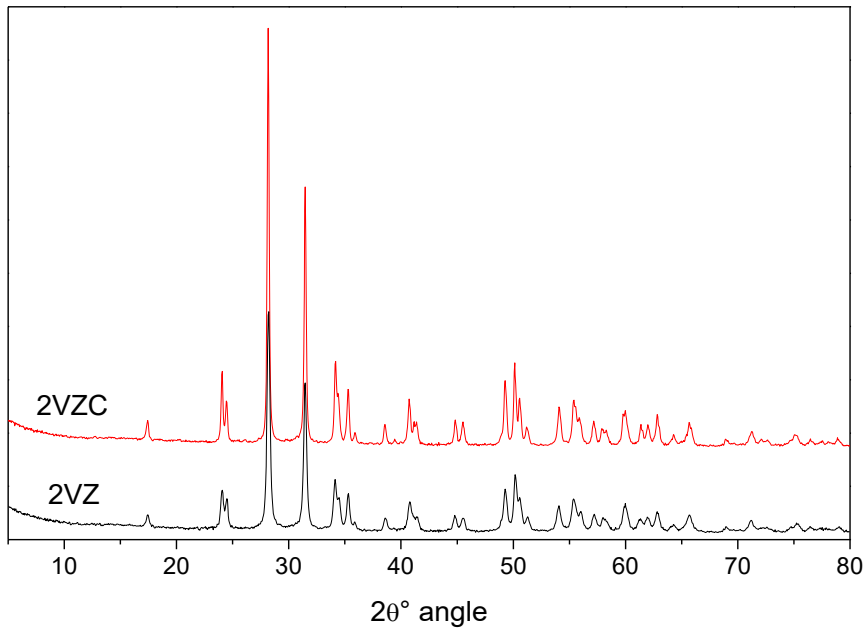

Figure 41. XRD patterns of catalysts containing 2% of V_2O_5 supported over commercial zirconia (2VZC) and UniBO zirconia (2VZ). All reflections are attributable to monoclinic zirconia.

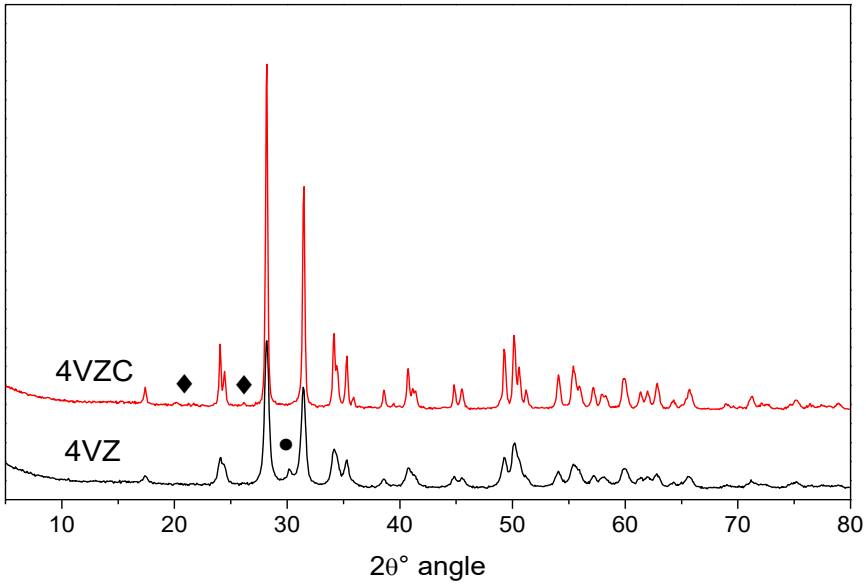

Figure 42. XRD patterns of catalysts containing 4% of V_2O_5 supported over commercial zirconia (4VZC) and UniBO zirconia (4VZ) supports. Reflections indexed with (◆) are attributable to V_2O_5, those indexed with (●)to tetragonal ZrO_2.

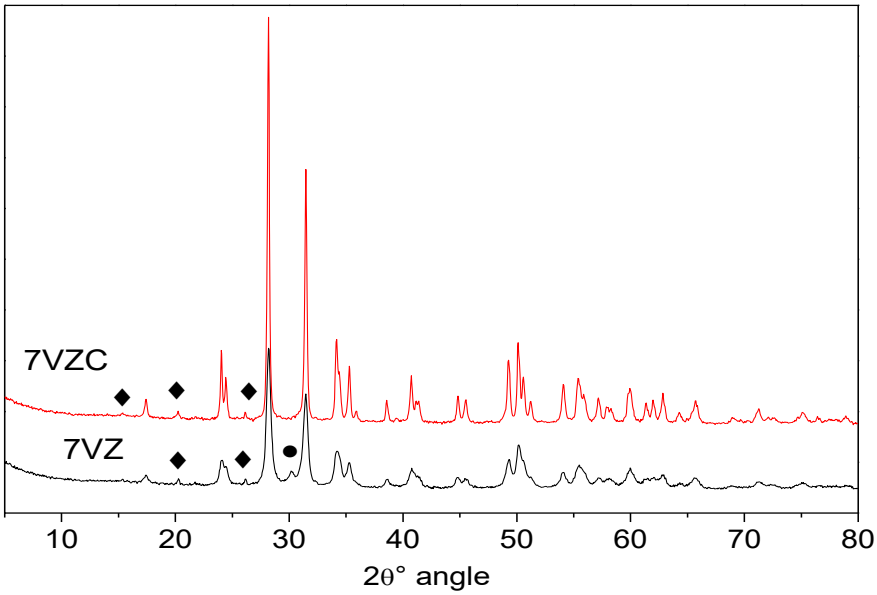

Figure 43. XRD patterns of catalysts containing 7% of V_2O_5 supported over commercial zirconia (7VZC) and UniBO zirconia (7VZ) supports. Reflections indexed with (◆) are attributable to V_2O_5, those indexed with (●)to tetragonal ZrO_2.

Figure 32 shows that that catalysts with higher Vanadium oxide content, namely 4% and 7%, supported over commercial zirconia, showed the presence of bulk crystalline V_2O_5, as evident from reflections at 16°,20° and 27° 2θ angle. Figure 34 reports the same comparison for catalysts with higher specific area. In this case, crystalline V_2O_5 formed only in the sample containing 7% V_2O_5, and in a lower amount than for the corresponding catalyst reported in figure 32. This can be attributed either to the fact that in catalysts having low Vanadium oxide content (regardless of the surface area), Vanadium ions are dispersed over the zirconia surface, with formation of isolated species, bi-dimensional structures or amorphous bulk aggregates, or to the presence of a low amount of crystalline V_2O_5, below the detection limit for the instrument.

By comparing figure 32 and figure 34, it is also possible to see that catalysts prepared with the support ZU1M present a small amount of the tetragonal zirconia phase (reflection at 30° 2θ, highlighted with *), while catalyst prepared with ZC (commercial zirconia) and ZU3M show only reflections attributable to the monoclinic form.

Raman spectra of all fresh catalysts (figure 33 and figure 35), show bands attributable to V_2O_5, at Raman shift 988cm^{-1}, 692cm^{-1} and 137cm^{-1}. In the case of samples 4VZC and 7VZC, strong bands at 975 cm^{-1} and 765cm^{-1} were also shown (figure 33), attributable to the formation of ZrV_2O_7 (zirconium pyrovanadate). However, when we focussed the laser beam over selected individual catalyst particles, some of them showed bands attributable to Zr pyrovanadate, but others did not; thus, the sample was not homogeneous. Therefore, we can hypothesize that Zr pyrovanadate formed because of either local surface overheating due to the laser beam, or a non-homogeneous Vanadium oxide distribution, with some particles which contained a greater amount of Vanadium oxide, those which gave rise to the formation of the pyrovanadate. These aspects will be discussed more in detail in the Section dedicated to in-situ Raman experiments. Evidence for the presence of bulk V_2O_5

occurred already with 2VZC, whereas vanadia was not seen from XRD pattern, probably because of its low amount. The intensity of Raman bands attributable to bulk Vanadium oxide increased along with the increase of active phase loading.

Figure 36 reports the XRD patterns of catalysts containing 2% V_2O_5 supported over zirconia with different surface area (supports ZC, ZU3L and ZU3M). All catalysts showed the same crystalline structure; however, differences were observed in crystallinity; ZC showed a better crystallinity, whereas ZU3L and ZU3M showed broader and less defined reflections. These differences are in line with the surface area values.

The comparison of Raman spectra for the same catalysts is reported in figure 37; the relative intensity of bands attributable to V_2O_5 and to zirconia followed the expected trend; in the sample with the higher surface area, Vanadium ions were more dispersed, and therefore the intensity of bands attributable to bulk Vanadium oxide decreased compared to the intensity of those attributable to zirconia.

Figure 38 and figure 39 compare features of two catalysts: one prepared by deposition of Vanadium oxide over a zirconia support of 25m^2/g (ZU1M; catalyst code 2VZ), and one prepared by deposition of Vanadium oxide over a high-surface-area zirconia (ZU1H, with 68m^2/g), but then calcined at 700°C in order to decrease its surface area (catalyst code 2VZT). It is evident from the XRD pattern that sample 2VZT showed a lower degree of crystallinity. Raman spectra were also very different; in the case of 2VZT, all the bands attributable to V_2O_5 species disappeared, namely those at 988cm^{-1}, 692cm^{-1}, 525 cm^{-1}, 280 cm^{-1} and 137cm^{-1}. A broad band appeared between 950cm^{-1} and 700cm^{-1}; bands in this region are attributed in literature to V-O-Zr bonds. Thus, it may be hypothesized that at 700°C V ions migrated from the catalyst surface into the zirconia structure, with development of a solid solution of the type $Zr_{1-x}V_xO_2$.

Comparisons of XRD patterns of catalysts prepared using commercial zirconia with those of catalysts prepared using the home-made zirconia (UniBO zirconia) are presented in figures 40-43. In general, the latter samples were less crystalline, and moreover reflections attributable to crystalline V_2O_5 appeared in correspondence of a greater amount of Vanadium oxide loading; this was clearly due to the better dispersion of Vanadium species achieved with the home-made zirconia support.

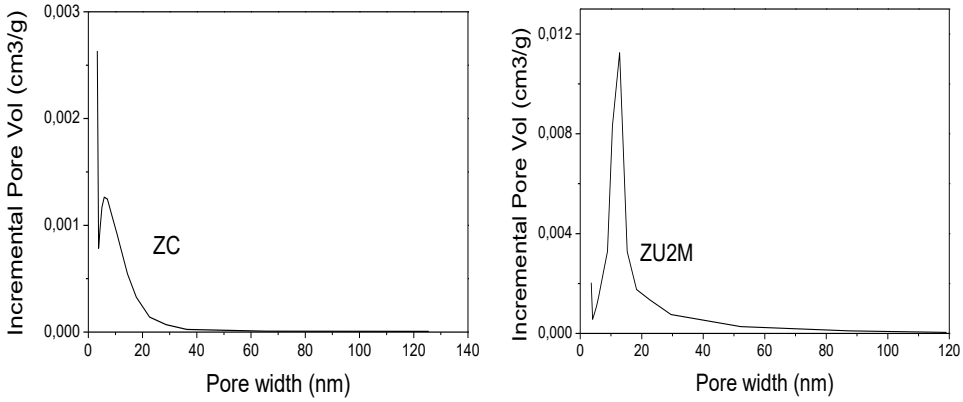

Figure 44. Pore size distribution of commercial zirconia and UniBO zirconia, 2nd stock.

Support	BET area (m^2/g)	Single pore V (cm^3/g)	BJH pore V (cm^3/g)
ZC	4.2	0.0176	0.0177
ZU3M	23.3	0.1072	0.1057
ZU3L	10.8	0.0859	0.0858

Table 3. comparison of specific surface area and pore volume for different supports

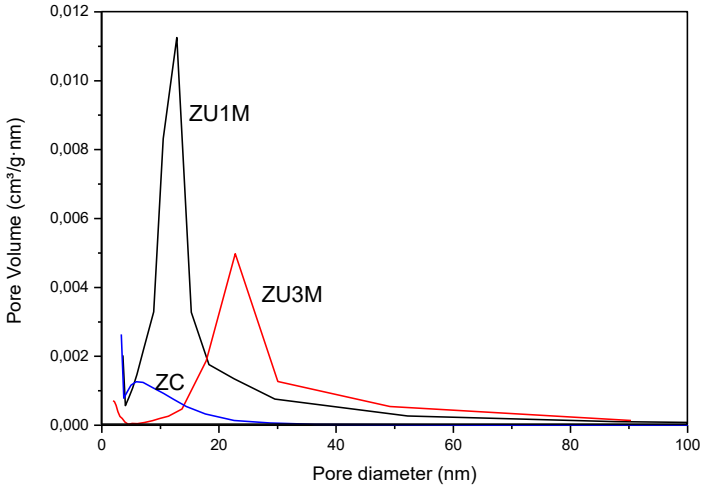

Figure 45. Pore size distribution of different supports.

Porosimetry analysis of supports gave us information about pore volume and size, along with a precise determination of the specific surface area. From figure 44, it is possible to see that pore size was different for ZC and ZU2M, shifting from an average size of 8nm for the former, to an average size of 12nm for the latter. The total pore volume was very different as well (see table3).

Figure shows that different calcination temperatures had important effects on porosity; higher temperatures led to the formation of pores with larger size, while their number and volume were reduced significantly.

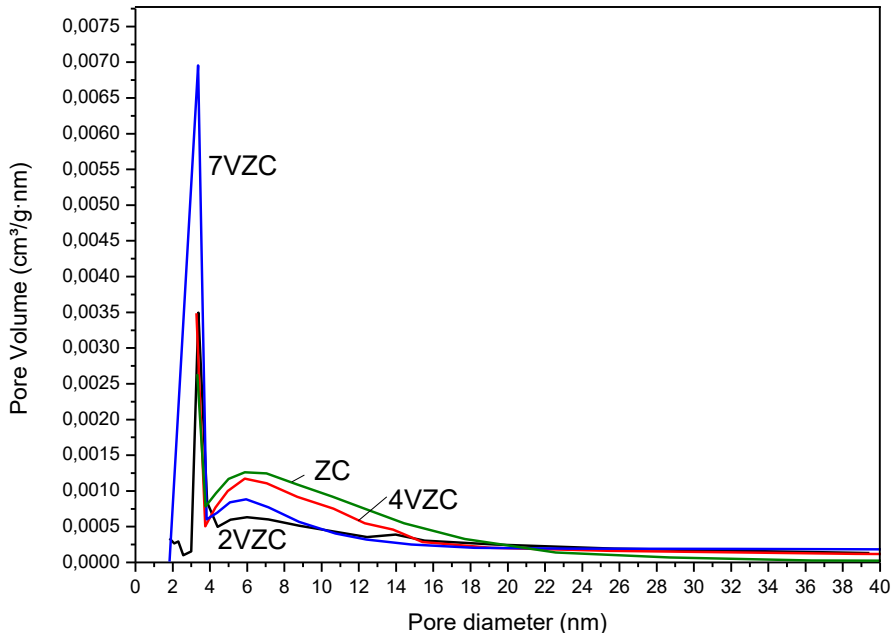

Figure 46. Pore size distribution of commercial zirconia (ZC) and of catalysts with different Vanadium oxide loading supported over commercial zirconia.

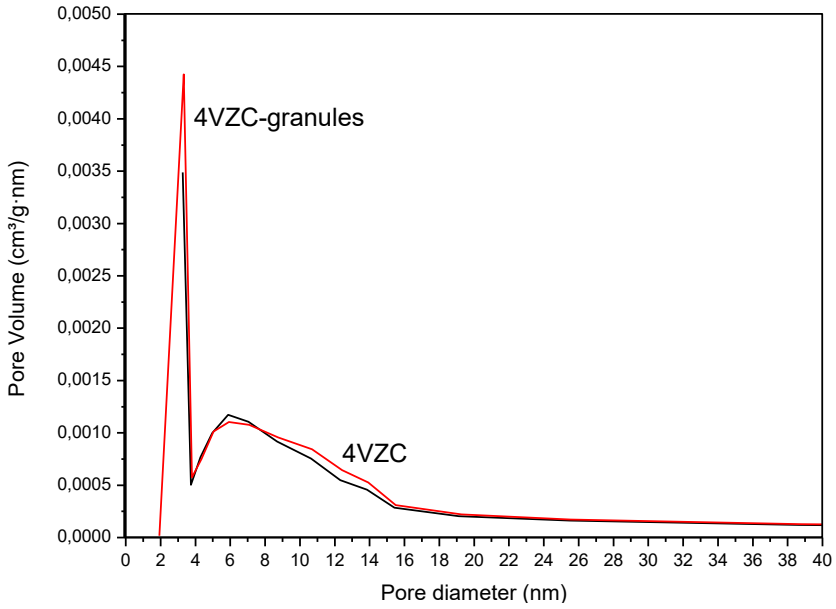

Figure 47. Pore size distribution of 4VZC catalyst powder and of the same catalyst after compression of the powder for the preparation of catalyst granules.

Catalyst	BET area (m^2/g)	Single pore V (cm^3/g)	BJH pore V (cm^3/g)
ZC	4.2	0.0176	0.0177
2VZC	4.8	0.0167	0.0166
4VZC	5.0	0.0236	0.0236
4VZC-granules	5.6	0.0243	0.0242
7VZC	5.4	0.0281	0.0282

Table 4. comparison of specific surface area and pore volume of commercial zirconia (ZC), and of catalysts with different Vanadium oxide loading over ZC. Sample 4VZC-granules has been prepared by first compressing 4VZC powder into tablets at 8-10 tons/cm^2, then crushing the tables into smaller particles and sieving the latter to prepare catalyst granules for reactivity experiments.

For what concerns the porosimetry of catalysts, we can see in Table 4 and figure 45 that deposition of Vanadium oxide on commercial zirconia (ZC) did not affect in a significant way surface area and pore volume. The slight increase of both surface area and pore volume observed for an increase of Vanadium oxide loading can be attributed to the porosity of the active phase itself. Vanadium oxide created new pores with an average size around 3nm, and the volume of pores of zirconia, with average size of 6nm, was decreased (figure 46).

We also compared the porosity of catalyst powder (4VZC) (i.e., after synthesis) and after preparation of catalyst granules, carried out by first pressing the powder at 8-10 tons/cm^2, to form big tablets, which were then broken into smaller particles (figure 47). It is shown that the procedure adopted did not affect powder morphology.

5.2 Reactivity experiments at picoline-rich and picoline-lean conditions

Preliminary experiments were carried out in order to check the presence of homogeneous gas-phase reactions. Some tests were carried out in the absence of catalyst, by co-feeding all reactants (3-picoline, O_2 and steam), while varying the temperature; feed composition was: 3-picoline 0.2%, O_2 2.8%, N_2 balance%, H_2O 66.6%. The mode of feeding was the same as that one conventionally adopted for the majority of catalytic experiments hereinafter described: 3-picoline and water were mixed to form a solution with the desired molar ratio, then the solution was fed by means of a syringe pump and vaporised inside an heated pipeline, where vapours were mixed with the O_2/N_2 gaseous stream. These experiments demonstrated that at 310°C 3-picoline conversion was 8%, and at 370°C it was ca 15%; traces of unknown compounds were found, which were not the same as those obtained during catalytic experiments.

Reference experiments were also carried out by using bare zirconia (surface area 25 m^2/g; sample ZU2M); in this case, conditions used were: feed composition (mol %) 3-picoline/oxygen/steam/inert 1.0/16.6/20/remainder; contact time was 2.0 s. Results were very similar to those obtained without any catalyst: conversion at 350°C was close to 11%, with unidentified products and only traces of nicotinic aldehyde.

Therefore, from these experiments it can be concluded that the contribution of the bare support to reactant conversion was negligible, and not much different from that one due to homogeneous, thermal reactions occurring in the gas phase.

Figure 48 shows the conversion of 3-picoline and yields to products in function of temperature, at the following conditions: picoline 1.0 mol%, H_2O 20 mol%, O_2 16.6 mol%, N_2 62.4 mol%, and contact time 2.0 s. The catalyst is 4VZ. These

conditions were chosen because in literature it is reported that catalysts made of Vanadium oxide supported over titania need the presence of co-fed steam; however, the role of steam will be discussed more in detail in another chapter of this thesis.

The reactant was completely converted at ca 290-300°C. Main products of the reaction were nicotinic acid (NAc), nicotinic aldehyde (3-pyridinecarbaldehyde, NAl), pyridine (PY), cyanopyridine (CP), CO and CO_2; traces of nicotinamide and bipyridine were also found, with selectivity which however was far less than 0.2%. NAl is the intermediate of partial oxidation, PY forms by decarboxylation of NAc, CO and CO_2 form by combustion of reactant and products, and CP forms by ammoxidation of picoline, where the N atom derives from the oxidative degradation of either picoline or products (NAc or NAl).

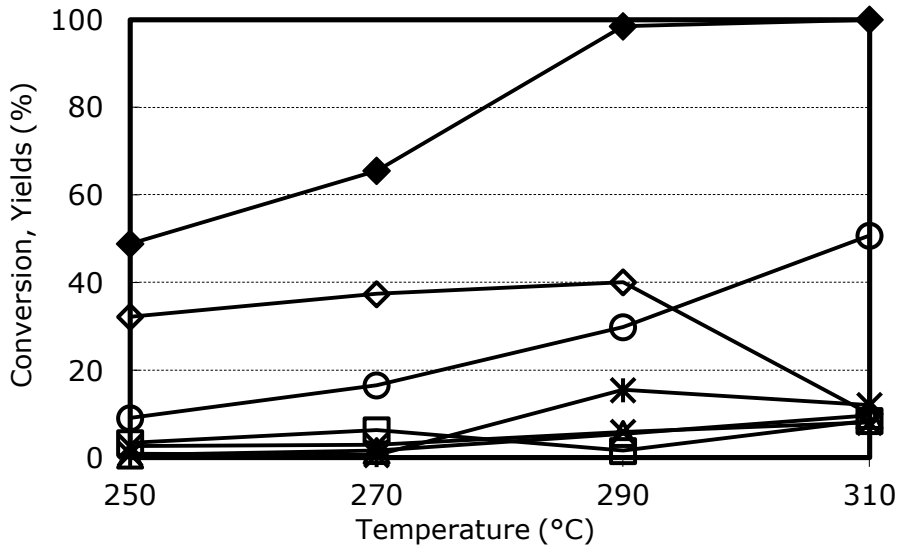

Figure 48. Effect of temperature on 3-picoline conversion and on yield to products. Reaction conditions: feed composition (molar %): picoline/oxygen/steam/inert 1.0/16.6/20/remainder; contact time 2.0 s. Symbols: picoline conversion (◆), yield to: nicotinic acid NAc (◇), nicotinic aldehyde NAl (✳), pyridine PY (△), cyanopyridine CP (□), CO (✕), and CO2 (○). Catalyst 4VZ.

At low temperature, the main product was NAc, with minor formation of by-products. However, an increase of temperature led to a decline of yield to NAc, and an increase of yield to all by-products; surprisingly, also the selectivity

to NAl increased, an event which cannot be attributed to oxygen starvation, because oxygen was always present in a large excess.

In general, however, the yield to NAl was very low throughout the entire range of temperature investigated, a clear indication that the catalyst used is efficient in the consecutive transformation of the aldehyde into NAc and CO_x. The best yield to NAc recorded was 40%.

Under the conditions used, the catalyst showed a poor performance; indeed, the literature on 3-picoline oxidation (see the chapter on literature analysis) with Vanadium oxide-based catalysts suggests that due to the strong interaction which develops between the products and the catalyst surface, it is necessary to use very low concentration of 3-picoline, and a large excess of steam, which helps the desorption of products and thus also facilitates the adsorption of the reactant, avoiding surface-saturation effects which may have several detrimental effects: scarce availability of oxidising sites, and formation of heavy compounds by consecutive reactions.

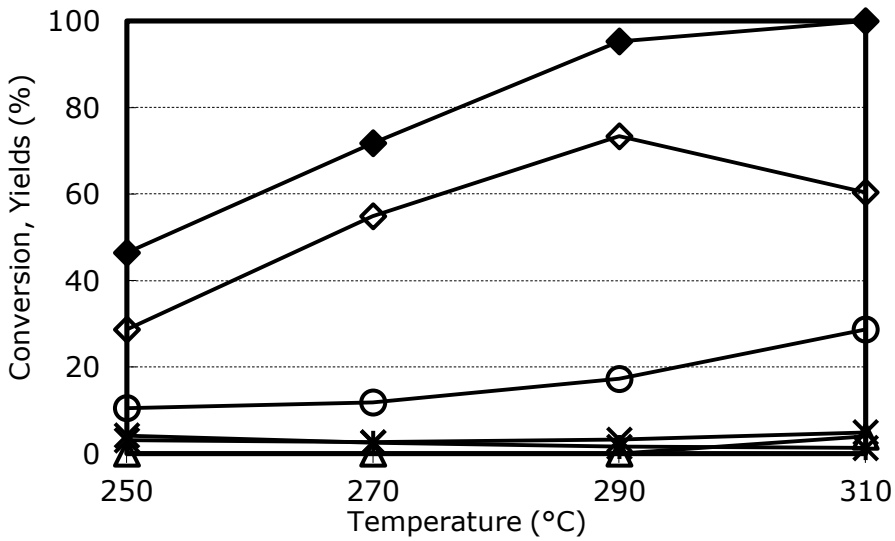

Figure 49. Effect of temperature on 3-picoline conversion and on yield to products. Reaction conditions: feed composition (molar %): picoline/oxygen/steam/inert 0.24/4.2/79.2/remainder; WHSV 0.02 h-1 (referred to picoline), contact time 1.2 s. Symbols: picoline conversion (◆), yield to: nicotinic acid NAc (◇), nicotinic aldehyde NAl (✳), pyridine PY (△), cyanopyridine CP (□), CO (✕), and CO2 (○). Catalyst 4VZ.

Therefore, we decided to use reactant-lean conditions; specifically, we chose the conditions similar to those reported in ref [40], for a catalyst based on silica-supported Vanadium oxide: 3-picoline 0.24%, O_2 4.2%, H_2O 79.2%, contact time 1.2 s. Figure 49 summarizes the results obtained. Under these conditions, hereinafter called “picoline-lean conditions”, the best yield to NAc was much greater (73.4%) than under picoline-rich conditions, with a corresponding lower formation of by-products.

We then tested catalyst 4VZC, under the same conditions as for tests in figure 48 (picoline-rich conditions, results reported in figure 50), and in figure 49 (picoline-lean conditions, results reported in figure 51). As shown in Table 2, 4VZ and 4VZC had the same loading of Vanadium oxide, but very different surface area. Also in this case, the better performance was obtained when the catalyst was used under picoline-lean conditions. The catalyst was less active than 4VZ (conversion at 310°C was close to 60-70% under both conditions with 4VZC, whereas with 4VZ conversion was total at both picoline-lean and picoline-rich conditions), as expected because of the lower surface area, which may make Vanadium oxide less dispersed and thus less available for the catalytic action. However, despite this, it is important to notice the excellent NAc yield registered with this catalyst; in fact, if compared to 4VZ, 4VZC displayed a better yield to NAc (79%) at picoline-lean conditions, and a much lower formation of by-products, especially CO_2.

Reasons for the better yield and selectivity to NAc of 4VZC compared to 4VZ can be different: (a) the lower surface area may allow to limit the consecutive oxidation of NAc to CO_2, because the intraparticle residence time of products inside particles pores is lower than for a larger surface area catalyst; (b) moreover, because of the lower surface area and the lower catalyst activity, it may be expected that the local (surface) temperature rise due to the exothermal reaction is lower; once again, this may disfavour parallel and consecutive oxidative degradation reactions; (c) a lower surface temperature

may also derive from a more efficient interparticle heat- (and mass-) transfer. In fact, diffusional limitations may occur when very fast and exothermal reactions occur, under laminar flow conditions; (d) the nature of the active sites in the two catalysts may be different; with 4VZ, a higher dispersion of Vanadium oxide is expected, and also a stronger interaction between V sites and zirconia surface, whereas in the case of 4VZC bulkier aggregates of Vanadium oxide form, because of the lower zirconia surface area. Catalysts characterisation (reported in the previous Chapter) suggests that indeed that this difference may play an important role.

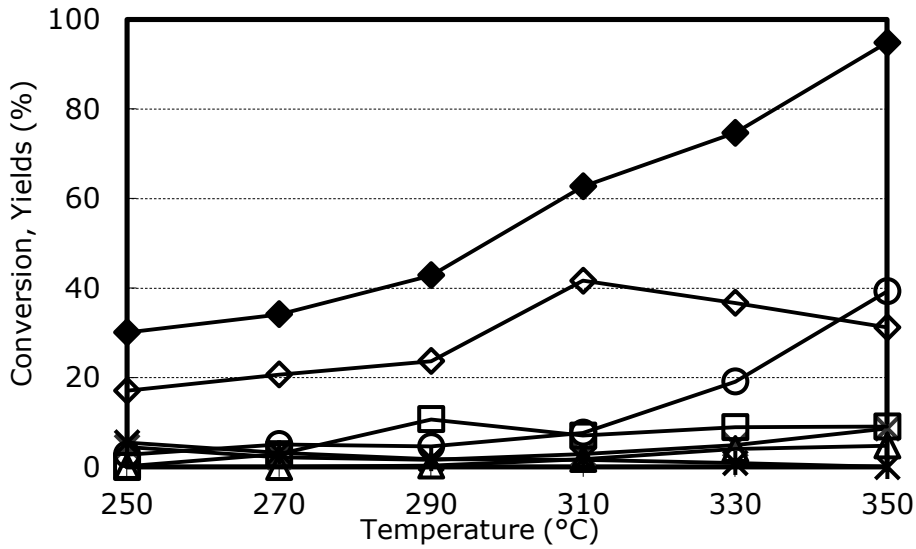

Figure 50. Effect of temperature on 3-picoline conversion and on yield to products. Reaction conditions: feed composition (molar %): picoline/oxygen/steam/inert 1.0/16.6/20/remainder; contact time 2.0 s. Symbols: picoline conversion (◆), yield to: nicotinic acid NAc (◇), nicotinic aldehyde NAl (✳), pyridine PY (△), cyanopyridine CP (□), CO (✕), and CO_2 (○). Catalyst 4VZC.

It should be also reminded that differences in catalytic performance may derive from a different particle efficiency; diffusion of reactants from particle external surface toward the active sites inside pores, or, vice versa, counter-diffusion of products from the inner part of catalyst particles to the external surface, may affect reaction rate with a consequent decrease of particle efficiency, finally causing the development of temperature and concentrations gradients across

the particle, which may finally affect the catalytic performance. Clearly, intraparticle mass- and heat-transfer limitations are affected by both porosity morphology and thermal conductivity of the catalyst, which in turn strongly depends on support properties.

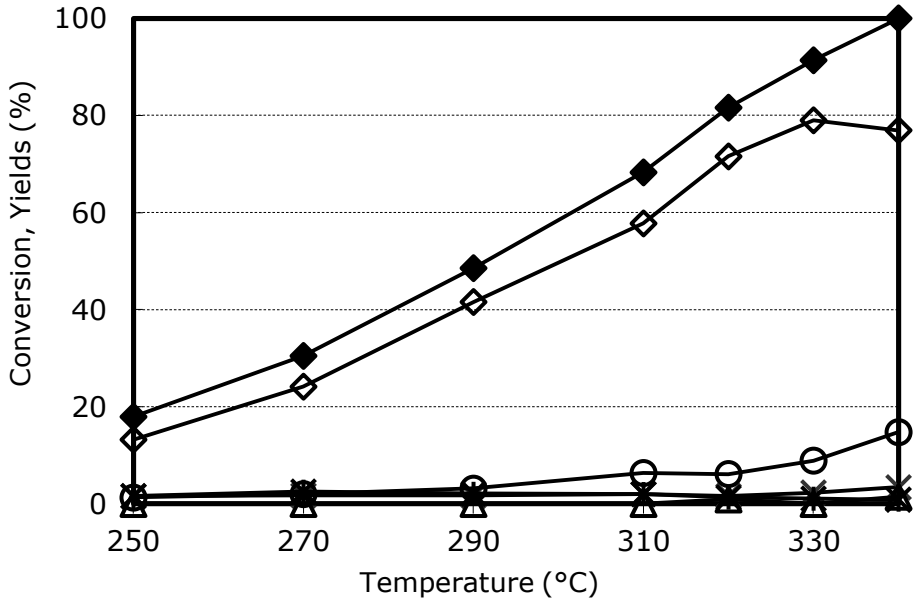

Figure 51. Effect of temperature on 3-picoline conversion and on yield to products. Reaction conditions: feed composition (molar %): picoline/oxygen/steam/inert 0.24/4.2/79.2/remainder; WHSV 0.02 h^{-1} (referred to picoline), contact time 1.2 s. Symbols: picoline conversion (◆), yield to: nicotinic acid NAc (◇), nicotinic aldehyde NAl (✳), pyridine PY (△), cyanopyridine CP (□), CO (✕), and CO_2 (○). Catalyst 4VZC.

These results suggest that this reaction needs catalysts with low surface area and relatively low Vanadium oxide content; moreover, for the same reason, the reaction has to be carried out with a low picoline concentration in feed. On the other hand, we cannot exclude that these peculiarities derive from the characteristics of the support used.

Because of the excellent results obtained with catalyst 4VZC, we carried some short-lifetime experiments, under picoline-lean conditions; results are plotted in figure 52.

During 11 h time-on-stream at 330°C, the catalyst showed a slight decline of NAc yield, from 79% to 75%, with a concomitant increase of yield to CO and CO_2; however, conversion remained close to 90% throughout the entire experiment. The slight decline of selectivity may be attributed to various factors, e.g., a progressive deposition of carbonaceous residues, or a modification of the redox properties of V sites.

Results reported so far suggest that the amount of V_2O_5 may be a key factor for catalytic performance. Therefore, we decided to investigate the behaviour of catalysts having either lower or higher Vanadium oxide loading. Figures 53-60 show results obtained with 2VZ, 2VZC, 7VZ and 7VZC, respectively, each one under both picoline-rich and picoline-lean conditions. Figures 61 and 62 summarise the results obtained; the maximum yield to NAc and the temperature at which 80% picoline conversion was achieved are plotted in function of Vanadium oxide loading, for the six catalysts investigated, under the two different reaction conditions used.

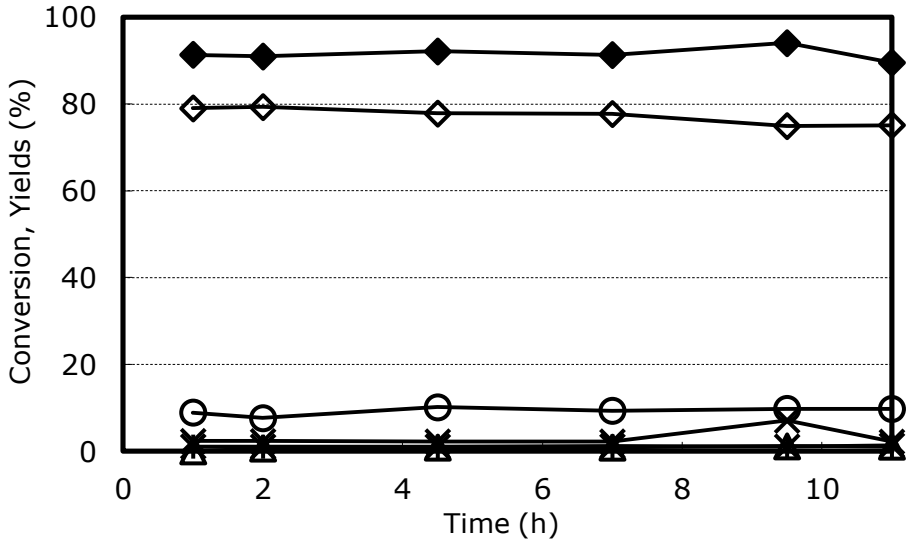

Figure 52. Effect of reaction time on 3-picoline conversion and on yield to products. Reaction conditions: feed composition (molar %): picoline/oxygen/steam/inert 0.24/4.2/79.2/remainder; WHSV 0.02 h^{-1} (referred to picoline), contact time 1.2 s, temperature 330°C. Symbols: picoline conversion (◆), yield to: nicotinic acid NAc (◇), nicotinic aldehyde NAl (✳), pyridine PY (△), cyanopyridine CP (□), CO (✕), and CO_2 (○). Catalyst 4VZC.

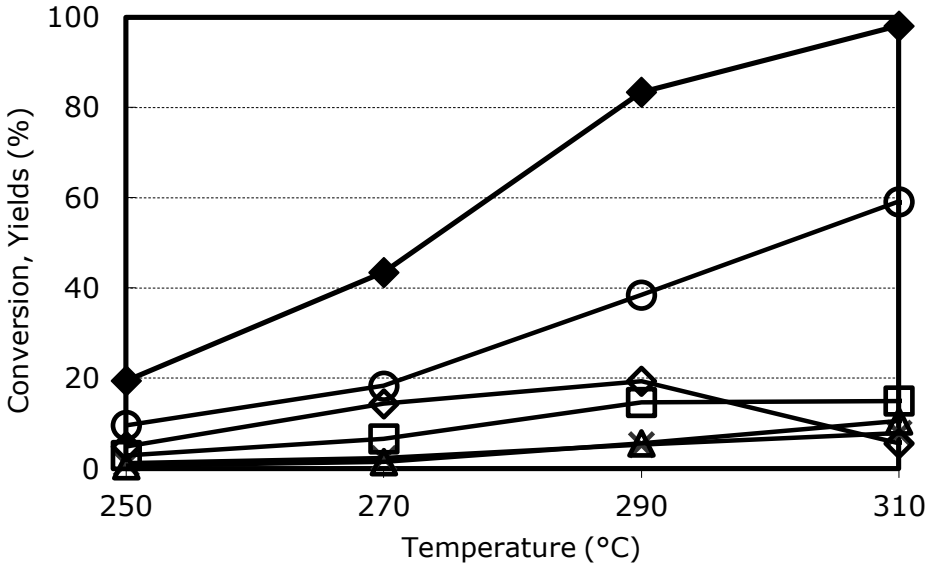

Figure 53. Effect of temperature on 3-picoline conversion and on yield to products. Reaction conditions: feed composition (molar %): picoline/oxygen/steam/inert 1.0/16.6/20/remainder; contact time 2.0 s. Symbols: picoline conversion (◆), yield to: nicotinic acid NAc (◇), nicotinic aldehyde NAl (✳), pyridine PY (△), cyanopyridine CP (□), CO (✕), and CO_2 (○). Catalyst 2VZ.

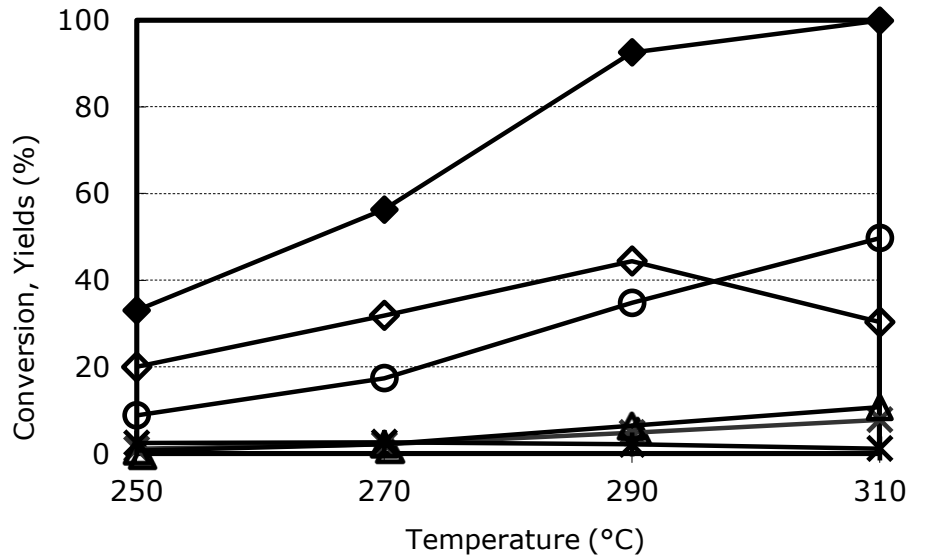

Figure 54. Effect of temperature on 3-picoline conversion and on yield to products. Reaction conditions: feed composition (molar %): picoline/oxygen/steam/inert 0.24/4.2/79.2/remainder; Symbols: picoline conversion (◆), yield to: nicotinic acid NAc (◇), nicotinic aldehyde NAl (✳), pyridine PY (△), cyanopyridine CP (□), CO (✕), and CO2 (○). Catalyst 2VZ.

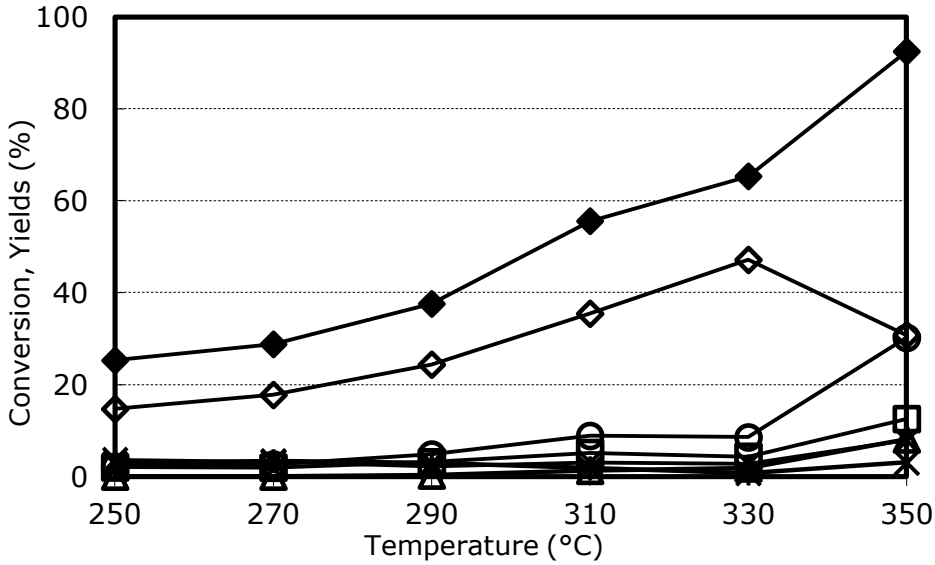

Figure 55. Effect of temperature on 3-picoline conversion and on yield to products. Reaction conditions: feed composition (molar %): picoline/oxygen/steam/inert 1.0/16.6/20/remainder; contact time 2.0 s. Symbols: picoline conversion (◆), yield to: nicotinic acid NAc (◇), nicotinic aldehyde NAl (✳), pyridine PY (△), cyanopyridine CP (□), CO (×), and CO_2 (○). Catalyst 2VZC.

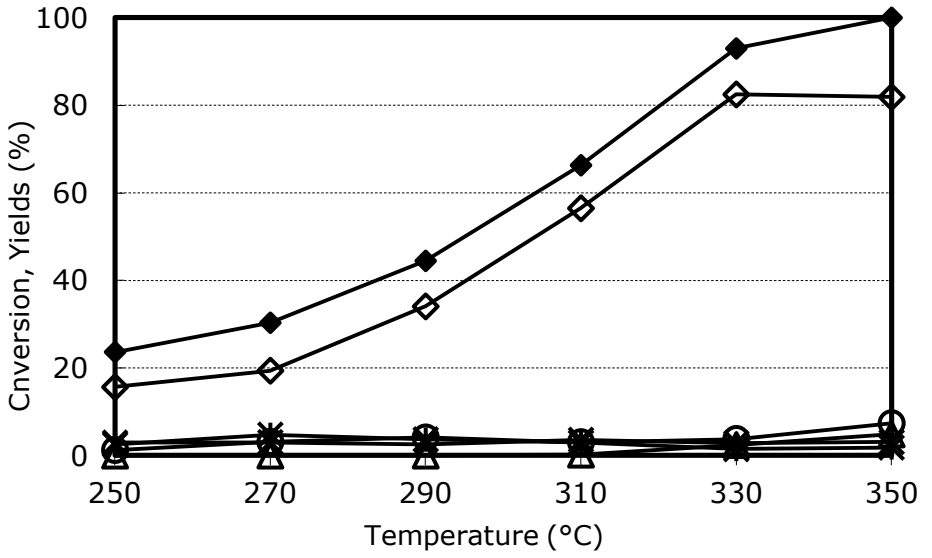

Figure 56. Effect of temperature on 3-picoline conversion and on yield to products. Reaction conditions: feed composition (molar %): picoline/oxygen/steam/inert 0.24/4.2/79.2/remainder; contact time 1.2 s. Symbols: picoline conversion (◆), yield to: nicotinic acid NAc (◇), nicotinic aldehyde NAl (✳), pyridine PY (△), cyanopyridine CP (□), CO (×), and CO_2 (○). Catalyst 2VZC.

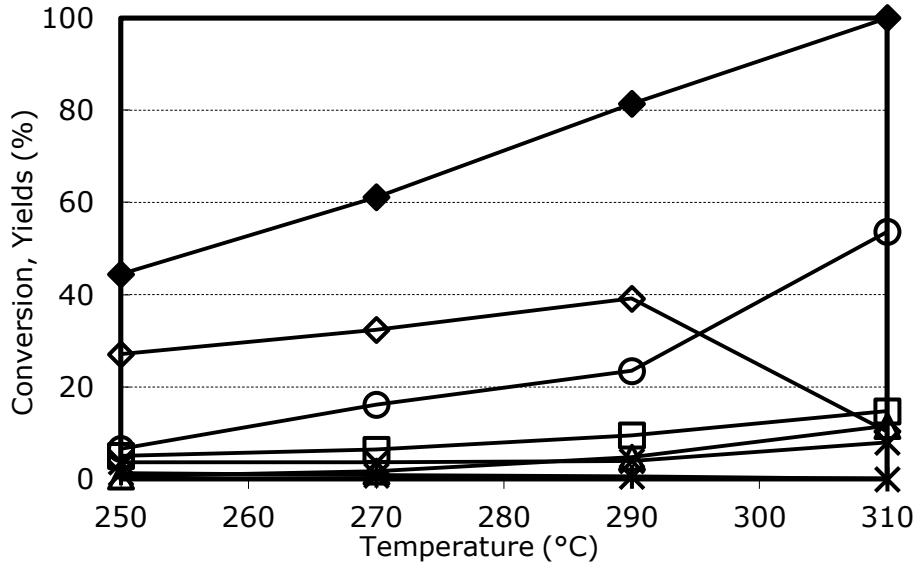

Figure 57. Effect of temperature on 3-picoline conversion and on yield to products. Reaction conditions: feed composition (molar %): picoline/oxygen/steam/inert 1.0/16.6/20/remainder; contact time 2.0 s. Symbols: picoline conversion (◆), yield to: nicotinic acid NAc (◇), nicotinic aldehyde NAl (✳), pyridine PY (△), cyanopyridine CP (□), CO (✕), and CO2 (○). Catalyst 7VZ.

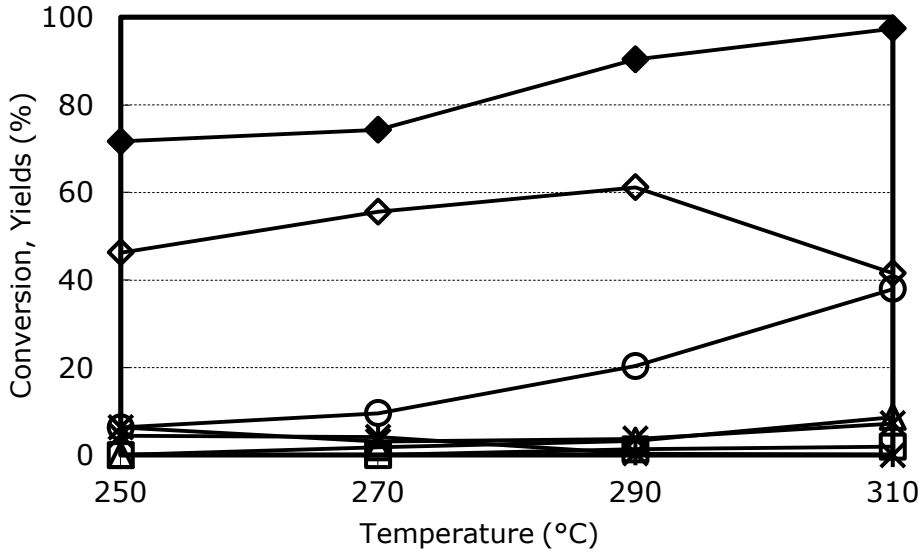

Figure 58. Effect of temperature on 3-picoline conversion and on yield to products. Reaction conditions: feed composition (molar %): picoline/oxygen/steam/inert 0.24/4.2/79.2/remainder; WHSV 0.02 h^{-1} (referred to picoline), contact time 1.2 s. Symbols: picoline conversion (◆), yield to: nicotinic acid NAc (◇), nicotinic aldehyde NAl (✳), pyridine PY (△), cyanopyridine CP (□), CO (✕), and CO_2 (○). Catalyst 7VZ.

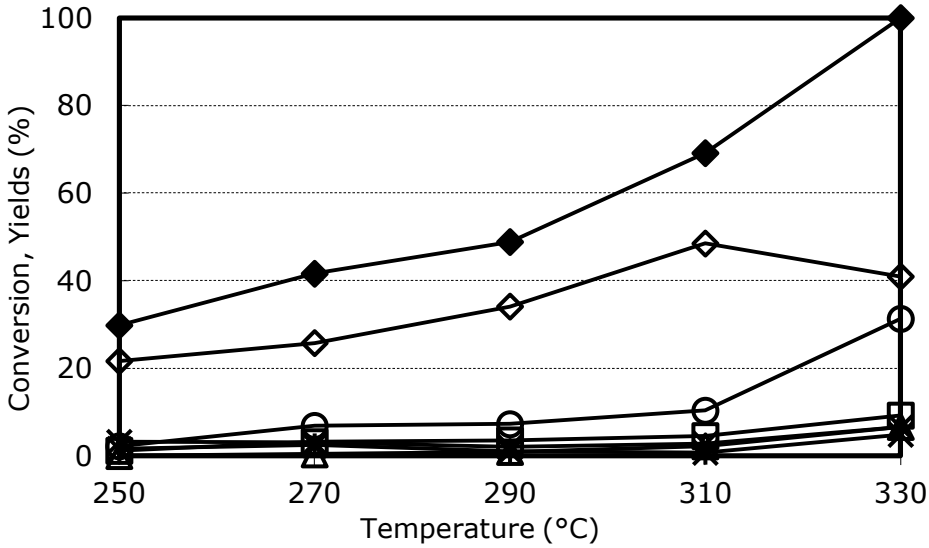

Figure 59. Effect of temperature on 3-picoline conversion and on yield to products. Reaction conditions: feed composition (molar %): picoline/oxygen/steam/inert 1.0/16.6/20/remainder; contact time 2.0 s. Symbols: picoline conversion (◆), yield to: nicotinic acid NAc (◇), nicotinic aldehyde NAl (✳), pyridine PY (△), cyanopyridine CP (□), CO (✕), and CO_2 (○). Catalyst 7VZC.

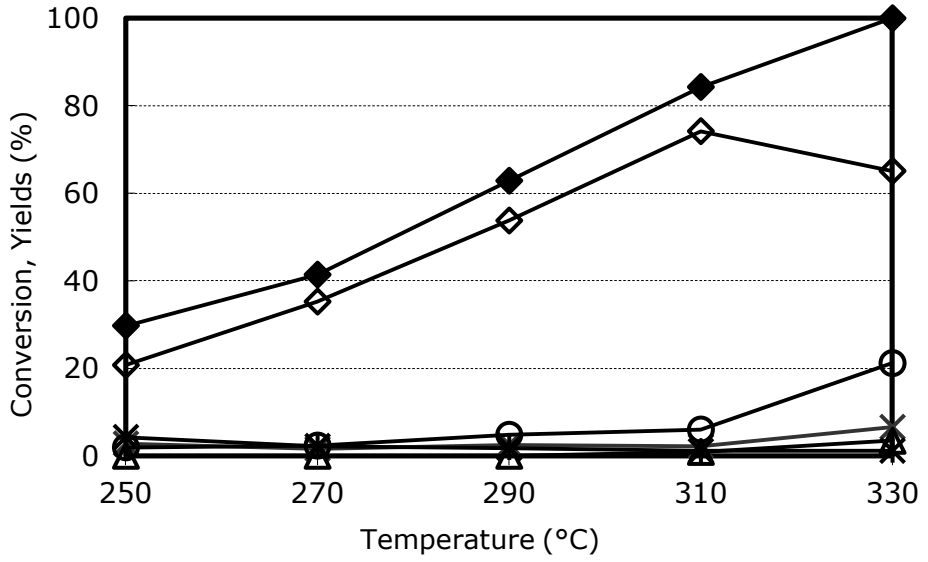

Figure 60. Effect of temperature on 3-picoline conversion and on yield to products. Reaction conditions: feed composition (molar %): picoline/oxygen/steam/inert 0.24/4.2/79.2/remainder; WHSV 0.02 h^{-1} (referred to picoline), contact time 1.2 s. Symbols: picoline conversion (◆), yield to: nicotinic acid NAc (◇), nicotinic aldehyde NAl (✳), pyridine PY (△), cyanopyridine CP (□), CO (✕), and CO_2 (○). Catalyst 7VZC.

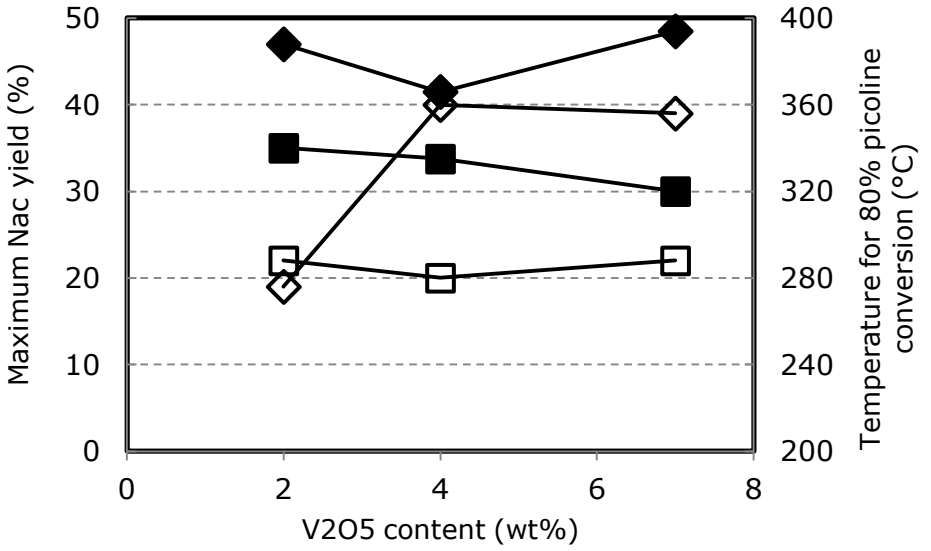

Figure 61. Effect of Vanadium oxide loading in catalysts prepared using commercial zirconia (full symbols ◆■, catalysts 2VZC, 4VZC, 7VZC), and catalysts prepared with the zirconia prepared at UniBO (open symbols ◇□, catalysts 2VZ, 4VZ, 7VZ) on best NAc yield (◆◇), and temperature for 80% picoline conversion (■□). Feed composition (mol%): picoline/oxygen/steam/inert 1.0/16.6/20/remainder.

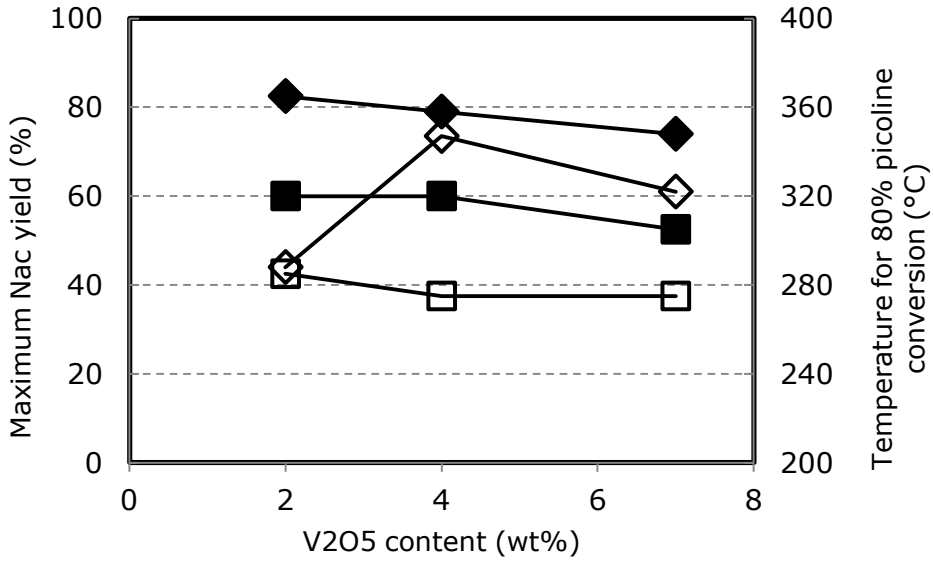

Figure 62. Effect of Vanadium oxide loading in catalysts prepared using commercial zirconia (full symbols ◆■), and catalysts prepared by zirconia prepared at UniBO (open symbols ◇□) on best NAc yield (◆◇), and temperature for 80% picoline conversion (■□). Feed composition (molar %): picoline/oxygen/steam/inert 0.24/4.2/79.2/remainder. Catalysts as in Figure 60.

Under picoline-rich conditions (figure 61), catalysts prepared using the commercial zirconia support (ZC) were less active than those prepared with the home-made zirconia (ca 25 m^2/g surface area), since the 80% conversion was achieved at higher temperature. However, the former samples gave a higher maximum yield to NAc. It is also interesting to notice that with both catalyst series, the activity was only marginally affected by Vanadium oxide loading; in fact, the temperature at which 80% conversion was achieved decreased by 20°C only, from 340 to 320°C (the decreasing trend was obviously expected, because of the higher loading of active phase), for catalysts prepared with commercial zirconia. In the case of samples prepared with the 25 m^2/g area zirconia, instead, the temperature for 80% conversion was practically unaffected by the Vanadium oxide loading, being always close to 280-290°C. This demonstrates that diffusional limitations may indeed affect the catalytic performance, especially with the catalyst series characterised by a higher surface area. In other words, conversion was not much affected by the amount of active phase, because when reactants reach the catalyst surface after diffusing across the boundary layer, react with a limited number of active sites, and also diffusion inside pores, where the largest fraction of active sites is located, only marginally contributes to catalytic performance. Another experimental result which supports the hypothesis of intraparticle transfer limitations is the evidence that with catalysts made by supporting Vanadium oxide over the home-made zirconia, picoline conversion was less affected by temperature than in the case of catalysts prepared with commercial zirconia, which is a phenomenon typically encountered when the apparent activation energy is relatively low. It is well known that under conditions of intraparticle diffusional limitations, the apparent activation energy becomes lower than for a reaction where the chemical reaction fully controls the kinetics. In case of interparticle diffusion limitation, activation energy may become very low, equal to a few kcal/mole.

For what concerns the best NAc yield, trends were different depending on catalyst support. In the case of catalysts prepared with commercial zirconia, best yield was comprised between 40 and 50%, regardless of Vanadium oxide loading. In the case of catalysts prepared with the ≈25 m^2/g, home-made zirconia, similar yields (close to 40%) were shown for catalysts having 4 and 7 wt% V_2O_5, whereas a much lower yield (20%) was obtained with the catalyst having 2% Vanadium oxide only. This may be attributed either to the exposed (i.e., not covered by Vanadium oxide) zirconia surface, which might play a direct role in the reaction, or to the fact that at low active phase loading the prevailing species is made of highly dispersed, isolated, Vanadium species (which instead are formed in minor amount with the low-surface-area commercial zirconia support), covalently bound to zirconia surface via V-O-Zr moieties. These active species might play a negative role on catalytic activity. When Vanadium oxide loading is increased, other active species become the prevailing ones, such as polymeric V-O-V species, still anchored to the surface, or Vanadium oxide bulk aggregates. However, the former hypothesis (a direct contribution of zirconia surface on reactivity) can be discharged, based on preliminary catalytic results obtained with bare zirconia.

Under picoline-lean conditions (figure 62), trends were similar to those obtained under picoline-rich conditions. Also in this case, catalysts prepared with commercial zirconia were less active but more selective to NAc than those prepared with the ≈ 25 m^2/g home-made support. In this case, a clear decreasing trend for the best yield to NAc in function of Vanadium oxide loading was shown with catalysts prepared using commercial zirconia. With catalysts having higher surface area, a low best yield to NAc (40%) was again observed with 2VZ; the increase of Vanadium oxide loading led to a remarkable increase of best yield, i.e., from 40% (2VZ), to 73% with 4VZ and 61% with 7VZ. The expected decreasing trend for the temperature of 80% picoline conversion

was shown for both catalyst series, but also in this case the activity was only marginally affected by Vanadium oxide loading.

Data reported clearly highlight the importance of the support morphology. Therefore, we decided to investigate more in detail the role of surface area on catalytic performance; we prepared and tested samples containing 2 wt% V_2O_5, deposited over home-made zirconia with different surface area: 2VZL and 2VZH (see Table 2 for catalyst codes), in order to compare them with 2VZ and 2VZC, whose reactivity was already reported in previous figures.

Results obtained with catalyst 2VZL are shown in Figures 63 and 64(at picoline-lean and picoline-rich conditions, respectively), whereas performance of 2VZH at picoline-lean conditions is shown in figure 65. Figure 66 summarizes results at picoline-lean conditions, for catalysts having 2 wt% V_2O_5, deposited over zirconia with different surface area. It is shown that an increase of the surface area led to higher conversion rates, but 2VZ and 2VZH showed similar activity. The trend experimentally observed may be attributed to the fact that a better dispersion of Vanadium species on a medium-high surface area renders more V sites available for the reaction. An alternative hypothesis is that under conditions of heat- (and mass-) transfer limitations in high-surface-area catalysts, the true temperature at the catalyst surface is higher than with low-surface-area zirconia, which finally leads to a higher conversion rate. Similar explanations can also be given for the decrease of NAc yield observed at increasing Vanadium oxide loading; either the Vanadium active sites which form with highly dispersed systems are intrinsically less selective to NAc (and more active for combustion), or again the higher combustion rate might be due to the higher local temperature. It is also possible that both picoline and products undergo consecutive combustion within the pores present in catalysts with higher surface area, because of the greater intraparticle residence time of molecules diffusing and counter-diffusing in pores.

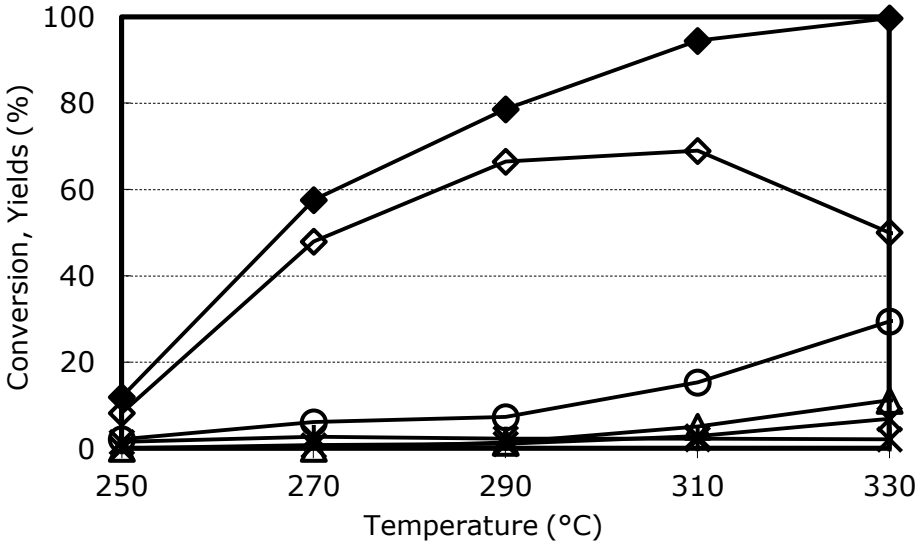

Figure 63. Effect of temperature on 3-picoline conversion and on yield to products. Reaction conditions: feed composition (molar %): picoline/oxygen/steam/inert 0.24/4.2/79.2/remainder; contact time 1.2 s. Symbols: picoline conversion (◆), yield to: nicotinic acid NAc (◇), nicotinic aldehyde NAl (✳), pyridine PY (△), cyanopyridine CP (□), CO (✕), and CO_2 (○). Catalyst 2VZL.

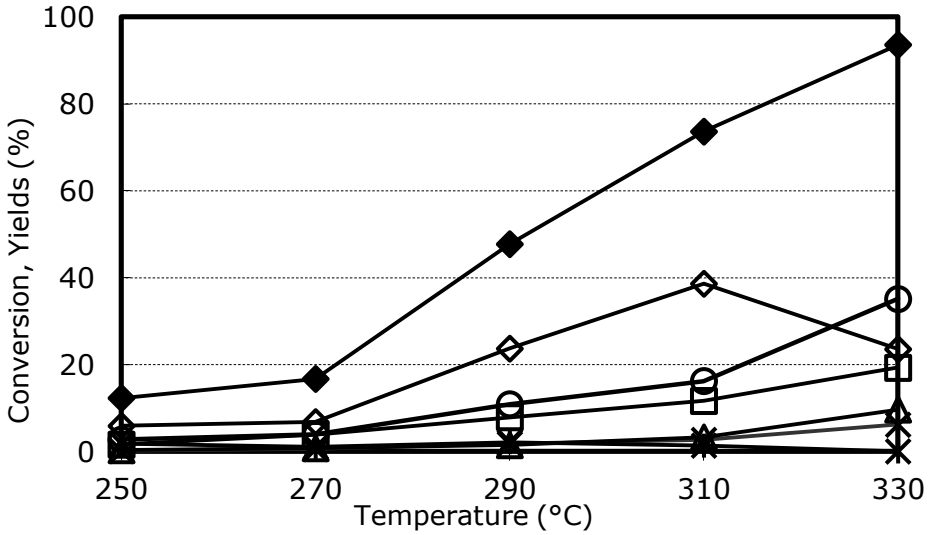

Figure 64. Effect of temperature on 3-picoline conversion and on yield to products. Reaction conditions: feed composition (molar %): picoline/oxygen/steam/inert 1.0/16.6/20/remainder; contact time 2.0 s. Symbols: picoline conversion (◆), yield to: nicotinic acid NAc (◇), nicotinic aldehyde NAl (✳), pyridine PY (△), cyanopyridine CP (□), CO (✕), and CO_2 (○). Catalyst 2VZL.

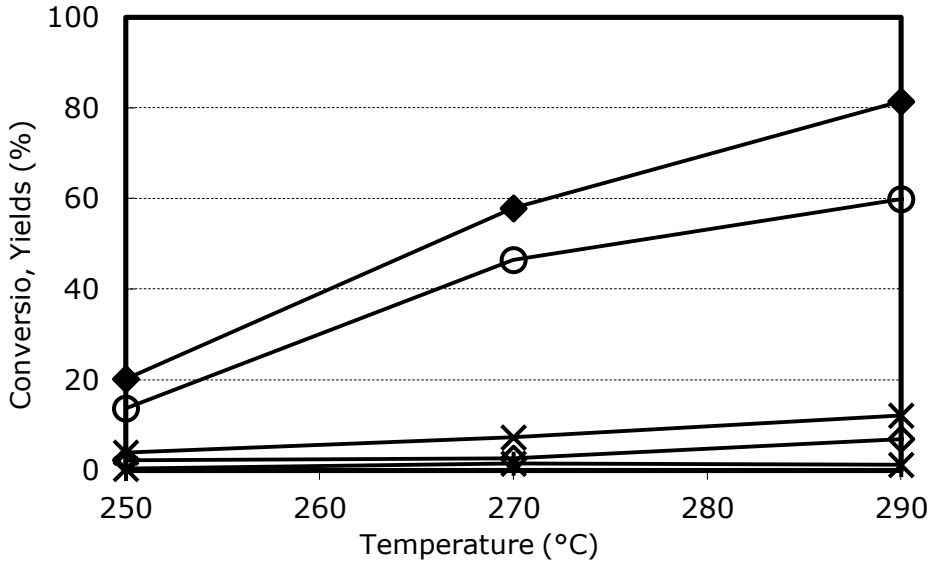

Figure 65. Effect of temperature on 3-picoline conversion and on yield to products. Reaction conditions: feed composition (molar %): picoline/oxygen/steam/inert 0.24/4.2/79.2/remainder; contact time 1.2 s. Symbols: picoline conversion (◆), yield to: nicotinic acid NAc (◇), nicotinic aldehyde NAl (✳), pyridine PY (△), cyanopyridine CP (□), CO (✕), and CO_2 (○). Catalyst 2VZH.

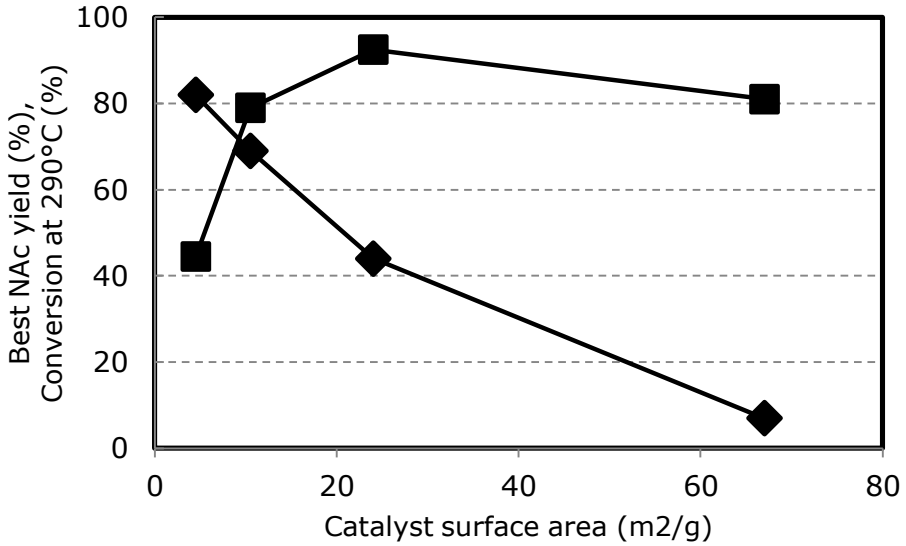

Figure 66. Summary of the effect of zirconia surface area on catalytic performance: best NAc yield (◆) and conversion at 290°C (■). Vanadium oxide for all catalysts: 2 wt% V_2O_5. Reactivity at picoline-lean conditions.

Finally, we tested the catalytic performance of sample 2VZT (see Table 2 for catalyst code), which was prepared by high-temperature calcination of a

precursor made of 2 % Vanadium oxide deposited over a high-surface area support. The peculiarity of this catalyst is that despite the similar surface area as for 2VZ, its chemical-physical features were completely different from those shown by this latter catalyst (see figures 37 and 38). This was probably due to the fact that at high temperature V oxide reacted with the support, forming either an amorphous V/Zr mixed oxide, or a solid solution of V ions inside the zirconia structure. The results of catalytic tests under the two different conditions are displayed in Figures 67 and 68. The comparison of catalytic performance of 2VZT and 2VZ (the latter is reported in figure 53 and figure 54, under picoline-rich and picoline-lean conditions, respectively) shows that despite the very different chemical-physical features of the two catalysts, the performance of 2VZT was not much different from that one of 2VZ.

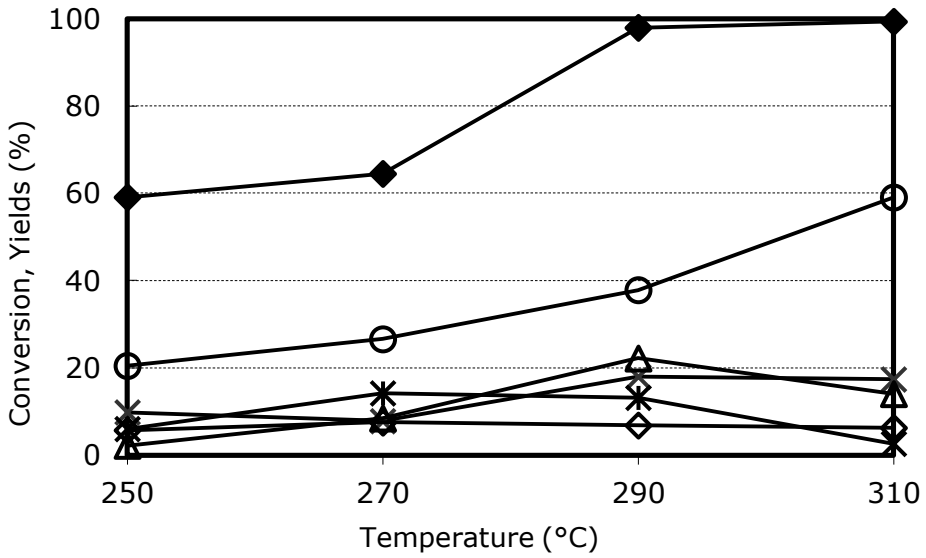

Figure 67. Effect of temperature on 3-picoline conversion and on yield to products. Reaction conditions: feed composition (mol %): picoline/oxygen/steam/inert 1.0/16.6/20/remainder; contact time 2.0 s. Symbols: picoline conversion (◆), yield to: nicotinic acid NAc (◇), nicotinic aldehyde NAl (✳), pyridine PY (△), cyanopyridine CP (□), CO (✕), and CO_2 (○). Catalyst 2VZT.

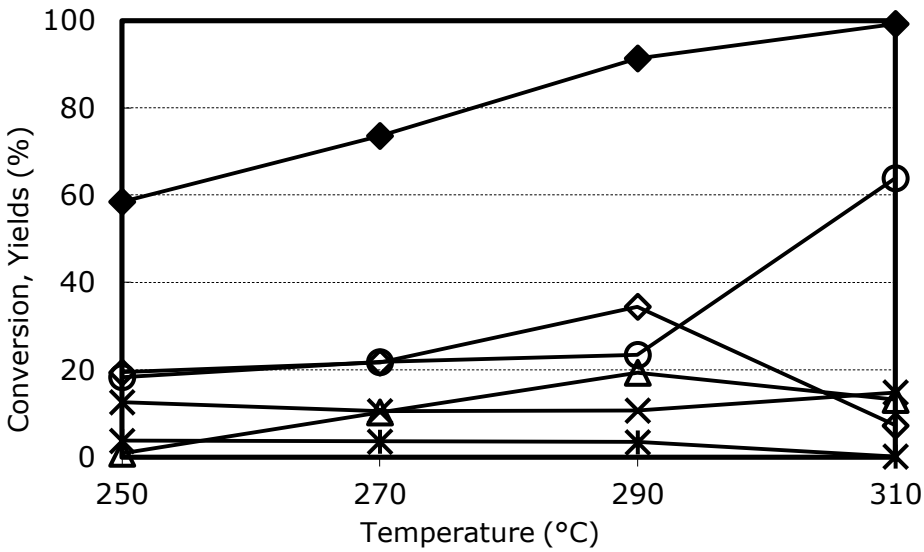

Figure 68. Effect of temperature on 3-picoline conversion and on yield to products. Reaction conditions: feed composition (molar %): picoline/oxygen/steam/inert 0.24/4.2/79.2/remainder; WHSV 0.02 h-1 (referred to picoline), contact time 1.2 s. Symbols: picoline conversion (◆), yield to: nicotinic acid NAc (◇), nicotinic aldehyde NAl (✳), pyridine PY (△), cyanopyridine CP (□), CO (✕), and CO2 (○). Catalyst 2VZT.

Indeed, best NAc yield was the higher with 2VZ at both reaction conditions, but one might have expected a much greater difference, because of the huge difference of chemical-physical features. This suggests that under reaction conditions a metastable phase may form, which acts as true active compound for the reaction, and whose features are closer to those obtained by the high-temperature treatment of 2VZ, rather than to those of the original 2VZ. This point will be discussed in the Chapter dedicated to in-situ Raman experiments.

5.3 A detailed study of the effect of reaction parameters

Results of catalytic experiments clearly highlight the importance of reaction parameters on catalytic behaviour. Therefore, we decided to carry out a more detailed study of the effect of some parameters. We first investigated the effect of the O_2-to-3-picoline molar ratio in feed. Indeed, reactivity experiments demonstrate that the best performance is observed at picoline-lean conditions, despite the O_2-to-3-picoline molar ratio used in this case (equal to 17,5) was higher than both the stoichiometric one for NAc synthesis (1.5) and even of that one used under picoline-rich conditions (16.6). This suggests that the use of a large excess of O_2 is not detrimental for catalytic performance. This phenomenon, which is quite unexpected for selective oxidation reactions, is attributable to the fact that because of the strong interaction between the reactant (3-picoline) and the active site, surface saturation may easily occur, and the rate-limiting step of the reaction becomes the reoxidation of reduced V sites. In other words, excess O_2 is needed to increase the turnover frequency and keep V sites more oxidised; in this aim, steam also contributes in facilitating the desorption of adsorbed products and keep a "clean" and oxidised surface. On the other hand, it may also be expected that selectivity to NAc and CO_2 are affected by the molar feed ratio.

Therefore, we carried out experiments using different O_2 molar fractions, with a twofold aim: to confirm the hypothesis about the role of O_2, and to increase the selectivity to NAc; figure 69 plots conversion and yields in function of the feed ratio, at the temperature of 330°C, with 0.2 mol% picoline and 66.6% water in feed, at the contact time of 1.4 s; the catalyst used was 2VZC. Concentration of picoline and water in the feed were slightly reduced from those used in previous tests in order to make experiments over a wider range of O_2-to-3-picoline molar ratio while keeping the ratio H_2O-to-3-picoline unchanged and avoiding the use of pure oxygen. Nitrogen was used as the ballast component to achieve the desired O_2-to-3-picoline ratio. Figure 70

shows the details of catalytic performance for 2VZC under the above cited conditions, with variation of temperature.

Results in figure 69 show that a decrease of the feed ratio from 35 down to 7 (which corresponds to 1.4 mol% O_2 in feed) led to a non-negligible decline of conversion, from 98% down to 93%; this supports the hypothesis of the presence of surface saturation effects. At the same time, however, an increase of yield to NAc was shown, which also corresponds to a relevant increase of selectivity.

However, in order to infer a more clear effect of feed ratio on selectivity to NAc, we carried out some experiments at the feed ratio equal to 7 while increasing contact time; the aim of this experiment was that one of achieving picoline conversion closer to 98%, in order to allow a fair comparison with results reported in figure 69. The results of these experiments are shown in figure 71. An increase of contact time from 1.2s until 1.62s led to an increase of picoline conversion (from 93% to 96%), and a corresponding increase of yield to NAc.

Now it is possible to compare the NAc selectivity at isoconversion (96-98%) in function of the O_2-to-3-picoline molar feed ratio (results taken from figures 69 and 71); at the feed molar ratio of 35, selectivity to NAc was 75 %, whereas at the feed ratio of 14, it was equal to 83%, and the same value was also obtained at the feed ratio of 7.

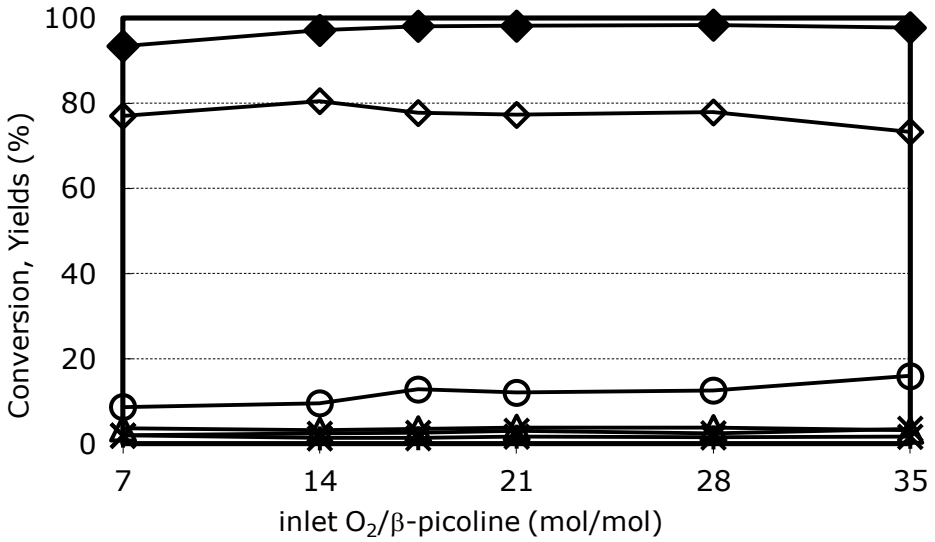

Figure 69. Effect of the O_2-to-3-picoline inlet molar ratio on conversion, and yield to products. Reaction conditions: feed composition (molar %):picoline/oxygen/steam/inert 0.2/varied/66.6/remainder; contact time 1.4 s; temperature 330°C. Symbols: picoline conversion (◆), yield to: nicotinic acid NAc (◇), nicotinic aldehyde NAl (✳), pyridine PY (△), cyanopyridine CP (□), CO (✕), and CO_2 (○). Catalyst 2VZC.

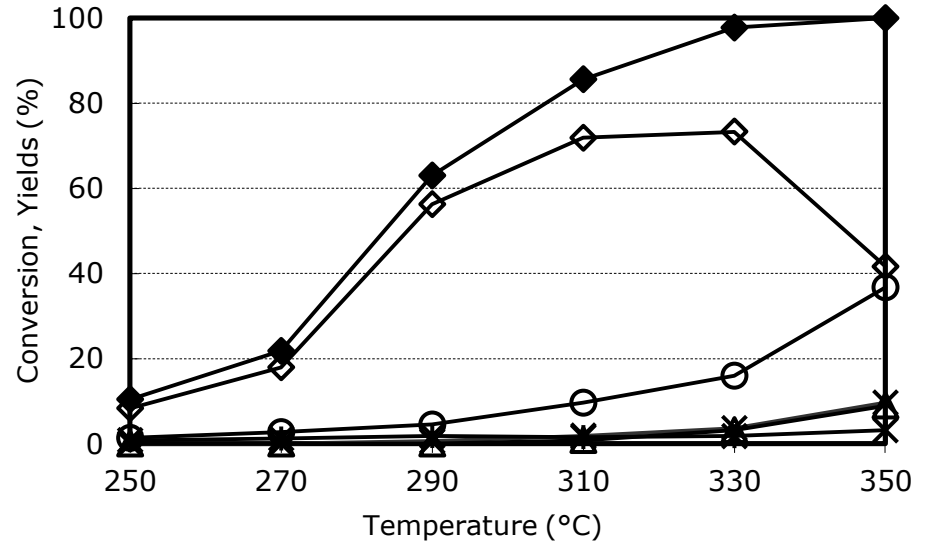

Figure 70. Effect of temperature on conversion and yield to products. Reaction conditions: feed composition (molar %): picoline/oxygen/steam/inert 0.2/7/66.6/remainder; contact time 1.4 s. Symbols: picoline conversion (◆), yield to: nicotinic acid NAc (◇), nicotinic aldehyde NAl (✳), pyridine PY (△), cyanopyridine CP (□), CO (✕), and CO_2 (○). Catalyst 2VZC.

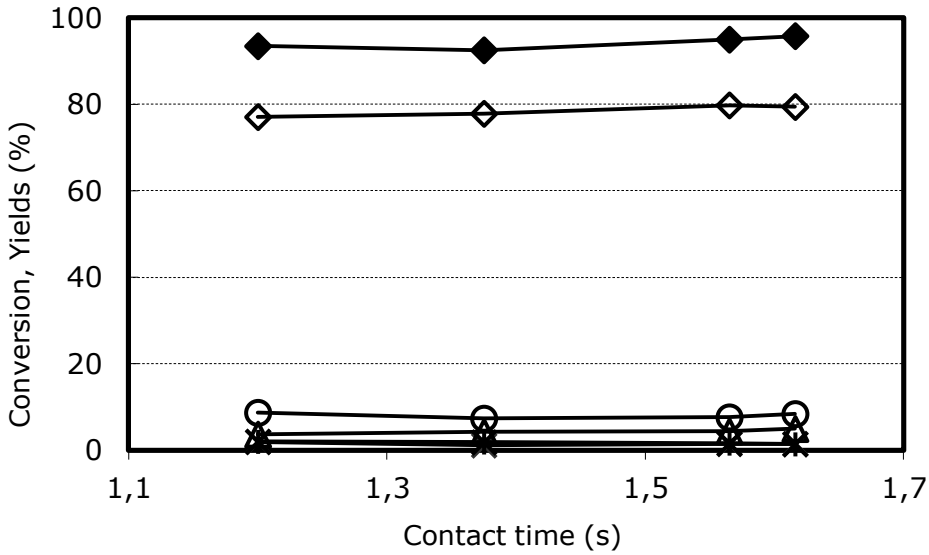

Figure 71. Effect of contact time on conversion and yield to products. Reaction conditions: feed composition (molar %): picoline/oxygen/steam/inert 0.2/1.4/66.5/remainder; temperature 330°C. Symbols: picoline conversion (◆), yield to: nicotinic acid NAc (◇), nicotinic aldehyde NAl (✳), pyridine PY (△), cyanopyridine CP (□), CO (✕), and CO2 (○). Catalyst 2VZC.

Concluding, excess O_2 in feed is needed in order to push picoline conversion until values close to 98%; however, a feed ratio lower than 20 led to a better NAc selectivity. A compromise of a molar ratio between 12 and 18 might be the best option.

The best yield to NAc was equal to 82.5% (figure 56), at picoline conversion 93% (which corresponds to an excellent NAc selectivity of 88.7%) achieved using 0.24 mol% of picoline and 4.2 mol% O_2 in feed (which corresponds to a molar ratio of 17.5), and 66.6 mol% of steam, at 330°C.

All the results clearly indicate that one of the most important parameters is the inlet molar fraction of β-picoline; indeed, when the reaction was carried at the so-called picoline-rich conditions, the best yield to NAc registered was definitely lower than that observed at picoline-lean conditions. However, one obvious disadvantage is that with 0.2 mol% picoline only, and despite the better yield and selectivity to NAc, the productivity is low, much lower than that one obtained using a greater concentration of picoline in feed. Therefore,

in order to check whether we could keep a good NAc yield, while increasing productivity, we carried out experiments with increased picoline molar fraction, while keeping constant the O_2-to-picoline molar ratio (equal to 14, in the optimal range as inferred from previous experiments), steam molar fraction, temperature and contact time. Results are shown in figure 72; catalyst used was 2VZC. It is shown that an increase of picoline molar fraction led to a non-negligible decline of conversion (an event which confirms the presence of surface saturation effects, as hypothesized), with a corresponding decline of NAc yield, too. However, selectivity to NAc was not so much affected, and even increased from 83 to 86%.

We also tried to push picoline conversion at 0.5 mol% picoline in feed, using contact time of 1.7 s (instead of 1.2), and O_2-to-picoline ratio equal to 14; this allowed us to reach a conversion as high as 88% (instead of 80% at 1.2 s contact time), with 72.2 % yield to NAc (instead of 69.2%), but with a lower selectivity to NAc, equal to 82% (instead of 86%). This definitely confirms the importance of having low picoline molar fraction in feed, in order to avoid the saturation of catalyst surface; in fact, even though higher picoline molar fractions allowed us to maintain good NAc selectivity at moderate conversion, any attempt to increase conversion finally led to a decreased selectivity, with a marginal increase of NAc yield.

We finally investigated the role of steam; indeed, under picoline-lean conditions, we typically employed large amounts of steam. The effect of steam is shown in figure 73, for an interval of steam molar fraction between 36 and 87 mol%.

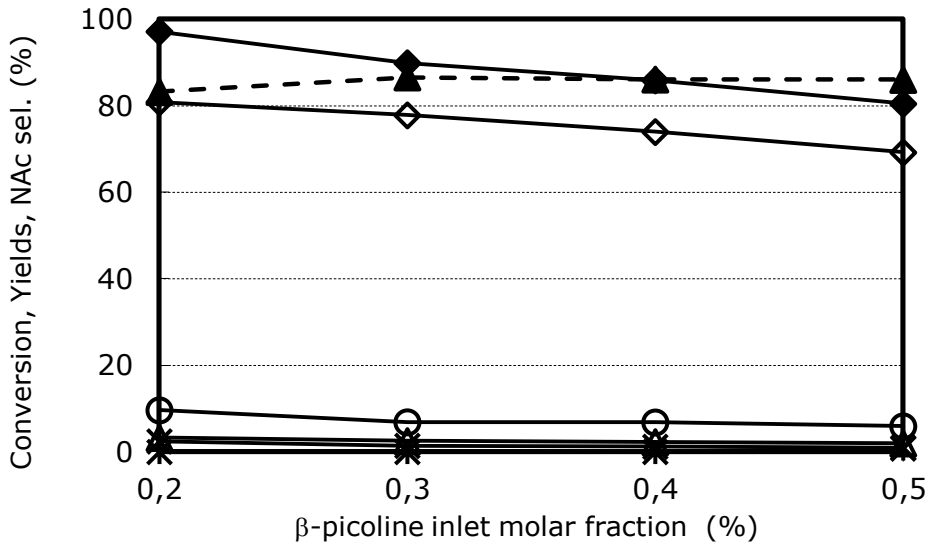

Figure 72. Effect of 3-picoline inlet molar fraction on conversion, yield to products and selectivity to NAc. Reaction conditions: feed composition (molar %): picoline/oxygen/steam/inert varied/varied/66.5/remainder; contact time 1.4 s. Oxygen/picoline mol ratio = 14; temperature 330°C. Symbols: picoline conversion (◆), yield to: nicotinic acid NAc (◇), nicotinic aldehyde NAl (✳), pyridine PY (△), cyanopyridine CP (□), CO (✕), and CO_2 (○); selectivity to NAc (dotted line) (▲) Catalyst 2VZC.

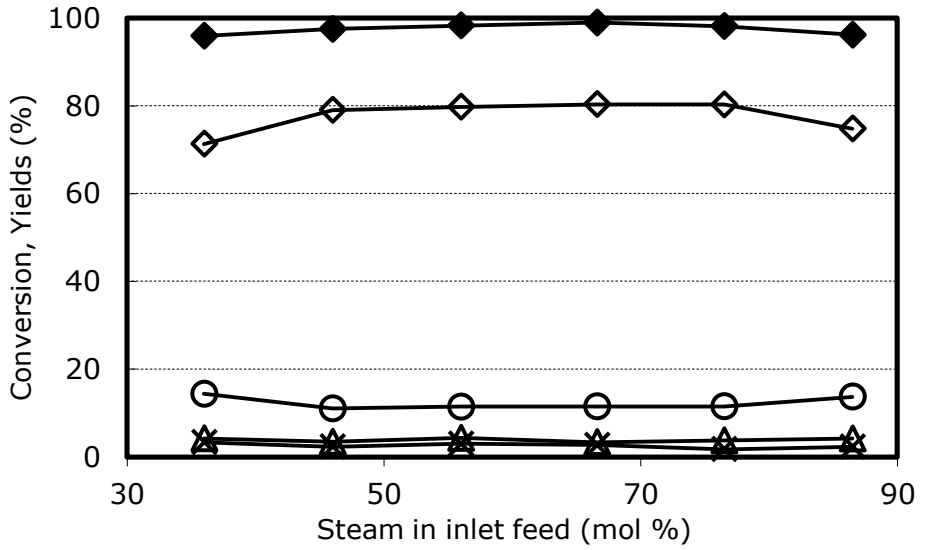

Figure 73. Effect of water inlet molar fraction on conversion and yield to products. Reaction conditions: feed composition (molar %): picoline/oxygen/steam/inert 0.2/2.8/varied/remainder; contact time 1.2 s; temperature 330°C. Symbols: picoline conversion (◆), yield to: nicotinic acid NAc (◇), nicotinic aldehyde NAl (✳), pyridine PY (△), cyanopyridine CP (□), CO (✕), and CO2 (○).Catalyst 2VZC.

Experiments highlight the need for a large amount of steam. There is an optimum amount of steam, in the range 45-to-85 mol %, which led to the highest conversion (97% and more), and to 80% yield to NAc. Lower molar fractions of steam not only caused a decline of conversion and NAc yield, but also a remarkable decrease of selectivity, from 81% down to 74%, the latter at 36 mol% steam in feed. Surprisingly, lower NAc selectivity (78%) was also observed with 86 mol% steam in feed.

Finally, we carried out some experiments by modifying the method of reactants feeding; in fact, in literature it is claimed that a separate feeding of steam and picoline allows to minimise the thermal decomposition of picoline occurring in the gas phase before the catalytic bed [38]. In our “separate-feeding” mode, water was pumped with a dedicated pipeline directly on the top of the catalytic bed, whereas picoline was fed in the usual way, through the heated pipeline entering the top of the reactor. A third experiment was carried out by feeding both liquid streams of water and picoline directly over the catalytic bed. Table 5 compares the catalytic performance obtained. It is shown that the conventional feeding mode (Test 1, data from figure 72) led to better conversion and NAc yield compared to the alternative feeding modes. On one hand, this demonstrates that the co-feeding mode used by us is the most proper method, at least with our experimental apparatus; on the other hand, it also shows that the vaporisation of reactants is a key issue, which may considerably affect the output of experiments. This has to be attributed to the decomposition of picoline in the gas phase, the extent of which is probably greatly affected by conditions used for its vaporisation and feed to the catalyst bed. This is also demonstrated by results of experiments reported in Table 6; in the Table, Tests 1 and 2 were taken from figures 56 and 69, respectively (catalyst 2VZC). When we slightly declined contact time (Test 3), we obtained a decrease of conversion, as expected, but also a remarkable increase of selectivity to NAc. The final experiment (Test 4), was carried out exactly in the same conditions as

for Test 3, but decreasing the temperature of the heated line used for the vaporisation of reactants in the conventional co-feeding mode. Again, an increase of selectivity was shown, with final NAc yield and selectivity very similar to those of Test 1 (figure 56).

Test	PY Yield (%)	NAl Yield (%)	CP Yield (%)	NAc Yield (%)	CO Yield (%)	CO_2 Yield (%)	Picoline Conv (%)	NAc Sel. (%)
1	3.3	0.0	1.0	80.9	2.4	9.6	97.2	83.2
2	2.5	0.6	1.0	72.2	1.0	6.4	83.6	86.4
3	2.2	0.3	0.8	78.8	1.1	5.9	89.1	88.4

Table 5 Comparison of conventional and alternative mode for feeding reactants to the reactor.
1) Reaction condition: picoline 0.2%, O_2/picoline 14, H_2O 66.6%, contact time 1.4s, T 330°C
2) Reaction conditions: picoline 0.2%, O_2/picoline 14, H_2O 66.6%, contact time 1.4s, T 330°C. Water fed directly over the catalyst bed.
3) Reaction conditions: picoline 0.2%, O_2/picoline 14, H_2O 66.6%, contact time 1.4s, T 330°C. Mixture Water+picoline fed directly over the catalyst bed.

Test	% Picoline	% H_2O	τ (s), T (°C)	T inlet heating (°C)	Picoline Conv (%)	NAc Select. (%)
1	0.24	79.8	1.2 , 330	200	93.0	88.5
2	0.2	66.6	1.4 , 330	220	98.2	79.2
3	0.2	66.6	1.2 , 330	220	96.3	83.7
4	0.2	66.6	1.2 , 330	200	94.6	86.9

Table 6. Optimisation of catalytic performance with 2VZC. For all experiments: T 330°C, O2/picoline molar feed ratio 17.5.

Overall, the reactivity experiments carried out with the V_2O_5/ZrO_2 catalysts allowed us to draw some important conclusions:

1. The oxidation of 3-picoline to nicotinic acid is remarkably affected by catalyst composition. In general, low surface area and low Vanadium oxide loading lead to better yield and selectivity, at least with our V_2O_5/ZrO_2 catalysts. This probably derives from a combination of various factors, amongst which the presence of mass- and heat-transfer

limitations seem to play an important role. The nature of V species, which is known to be affected by V dispersion, is also an important parameter. However, it cannot be excluded that the V species identified in catalysts at room temperature do not correspond to those which form in the reaction environment; this will be discussed later, in the section dedicated to the in-situ characterisation of catalysts.

2. In order to achieve good yield and selectivity to nicotinic acid it is necessary to feed very diluted streams, containing low molar fraction of picoline (lower than 0.5%), an excess of O_2 (with an optimal O_2-to-picoline feed ratio between, say, 10 and 20), and a large amount of steam as the ballast component. This is due to the strong interaction of picoline with active sites, which leads to surface saturation effects. Steam plays the role of facilitating the desorption of products, while excess O_2 is needed in order to accelerate V reoxidation.
3. A crucial point is the mode used for reactants feed; by the way, the need for steam makes the reaction not so easy to manage from an experimental viewpoint in lab-scale apparatus. An optimisation of the apparatus and of the plant section dedicated to liquid reactants vaporisation, mixing with O_2/N_2 and feeding, is evidently necessary; during my PhD, I could dedicate only a limited time to this problem, which instead necessitates a more detailed investigation. Despite these uncertainties, we could obtain and replicate a best nicotinic acid yield over 80%.

5.4 V_2O_5/ZrO_2 catalysts: characterisation of used samples

After catalytic tests, catalysts were characterized in order to check whether any modification had occurred under reaction conditions. Raman spectroscopy and X-ray diffraction were used as tools to monitor catalysts characteristics.

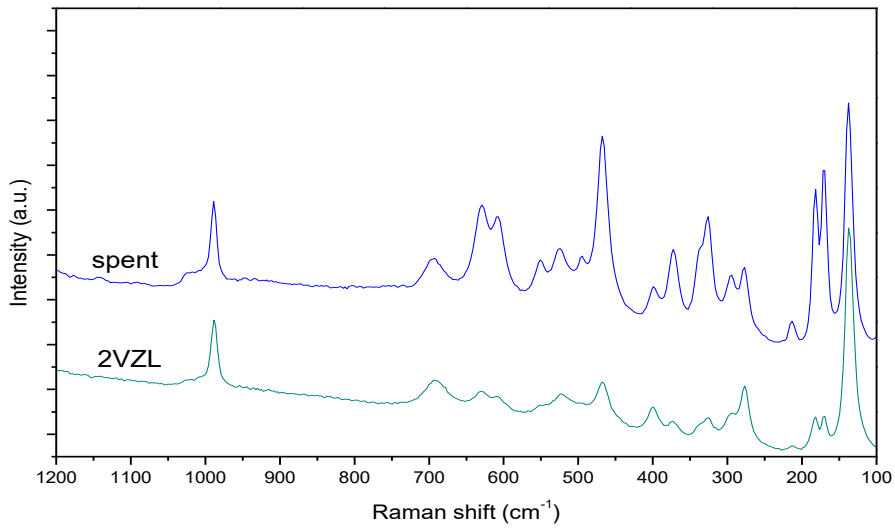

Figure 74. Raman spectra of catalyst before and after reaction, at picoline-lean conditions,9h on stream, temperature from 250°C to 330°C, catalyst 2VZL.

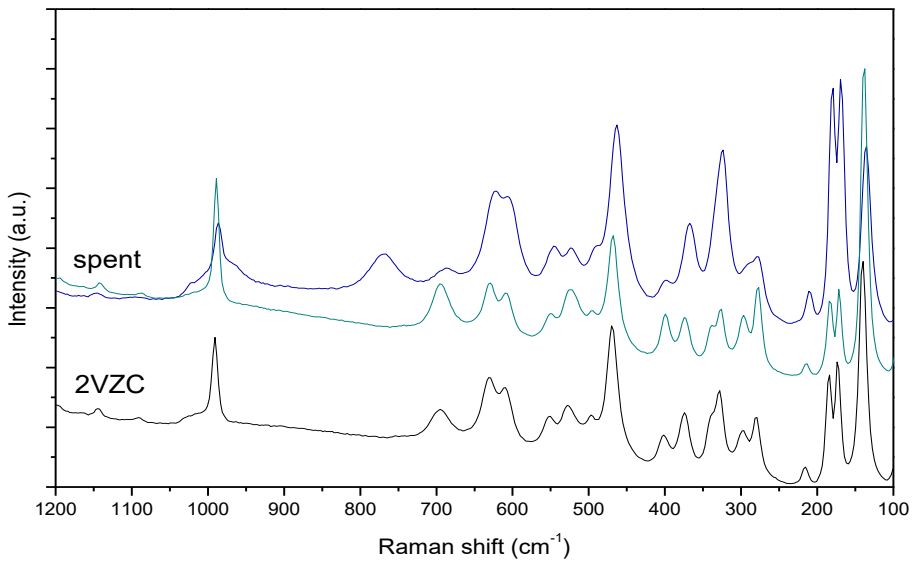

Figure 75. Raman spectra of catalyst before and after reaction (in the latter case, two different spectra were taken by focusing the laser beam on two different particles), at picoline-lean conditions, 9h on stream, temperature from 250°C to 330°C, catalyst 2VZC.

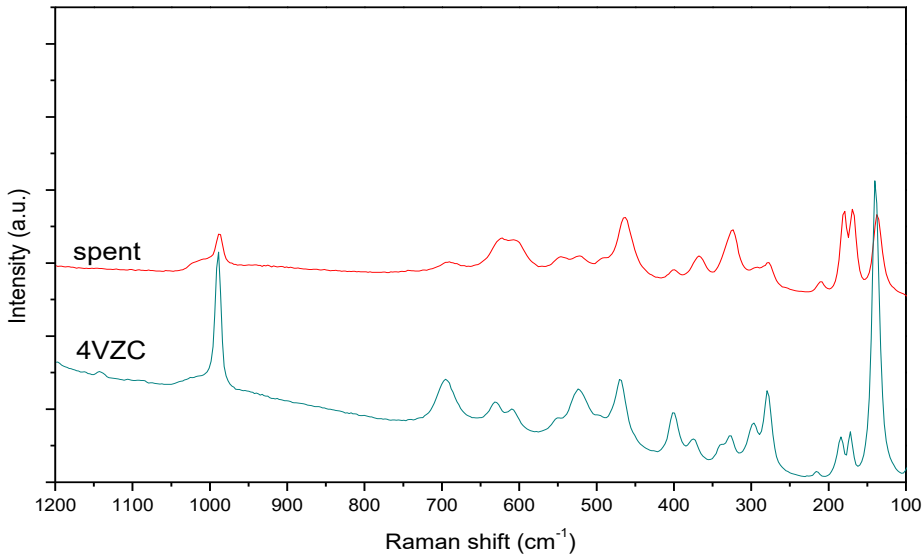

Figure 76. Raman spectra of catalyst before and after reaction, at picoline-lean conditions, 9h on stream, temperature from 250°C to 330°C, catalyst 4VZC.

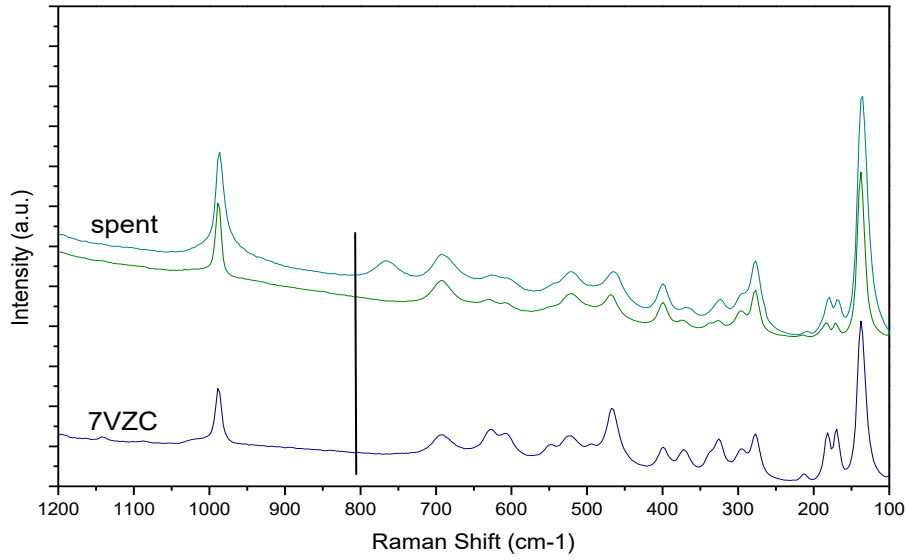

Figure 77. Raman spectra of catalyst before and after reaction, at picoline-lean conditions (in the latter case, two different spectra were taken by focusing the laser beam on two different particles), 9h on stream, temperature from 250°C to 330°C, catalyst 7VZC.

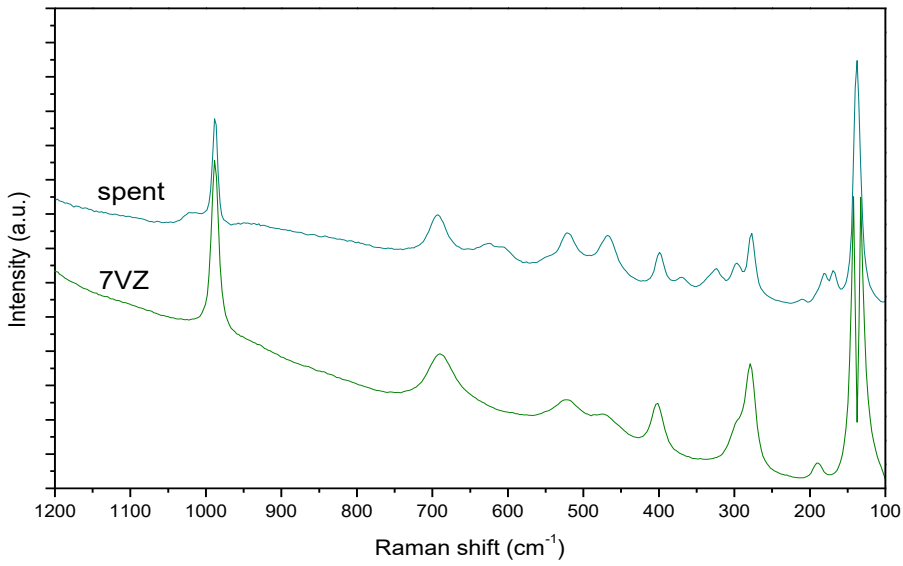

Figure 78. Raman spectra of catalyst before and after reaction, at picoline-lean conditions, 9h on stream, temperature from 250°C to 330°C, catalyst 7VZ.

Comparison of the Raman spectra for various catalysts are reported in figures 74-78. It is evident that all catalysts underwent some modification during reaction. In used catalysts, the intensity of all bands attributable to V_2O_5, at 988cm^{-1}, 692cm^{-1}, 525cm^{-1}, 280cm^{-1} and 137cm^{-1}, was reduced. The reduced intensity might be explained as being due either to the reduction of Vanadium oxide, or to its dispersion occurring under reaction conditions. A band at ca 760-770 cm^{-1} Raman shift appeared for 2VZC and 7VZC (figure 75 and figure 77), which can be tentatively attributed to ZrV_2O_7, zirconium pyrovanadate; another band belonging to Zr pyrovanadate is reported to fall at ca 980 cm^{-1} Raman shift, close to the stretching of the vanadyl bond in V_2O_5. However, it is also shown that not all spectra recorded by focusing the laser beam on different particles showed these features.

Indeed, Raman spectra of spent catalysts looked more similar to that one of fresh 2VZT catalyst reported in figure 39. During reaction, surface overheating probably occurred due to the exothermal nature of the reaction and the low

thermal conductivity of zirconia. High surface temperature might have favoured migration of V ions into the zirconia structure, with formation of an unstable amorphous-like intermediate compound that finally evolved into ZrV_2O_7. Thus, it may also be possible that depending on the temperature gradient used to cool the catalyst from the reaction temperature down to room temperature, or on the time length at which the catalyst was left in air at 330°C after reaction, the above cited phenomena might have occurred or not.

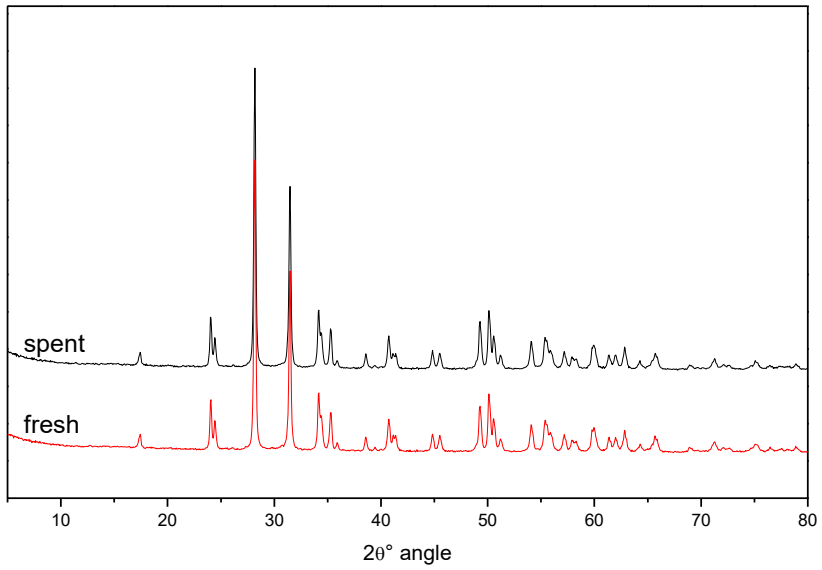

Figure 79. XRD pattern of spent (black), and fresh catalyst (red). Catalyst 2VZC.

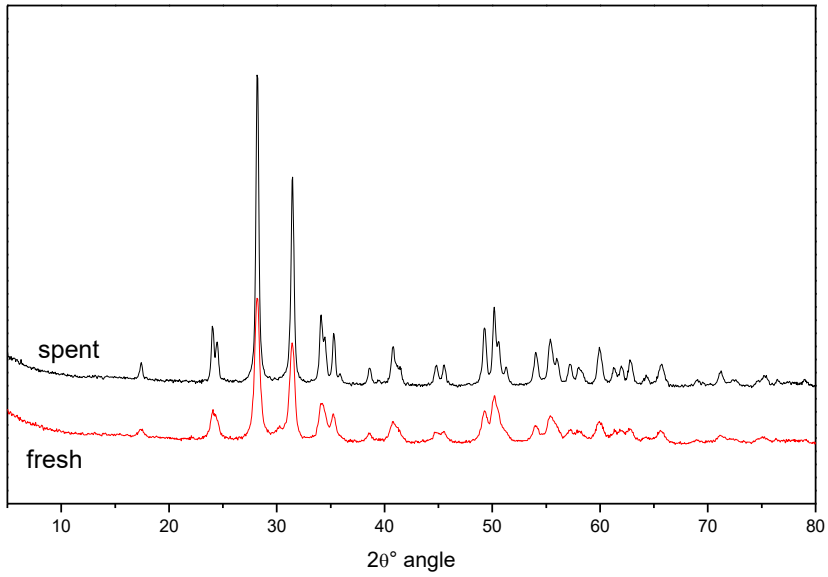

Figure 80. XRD pattern of spent (black), and fresh catalyst (red). Catalyst 2VZL.

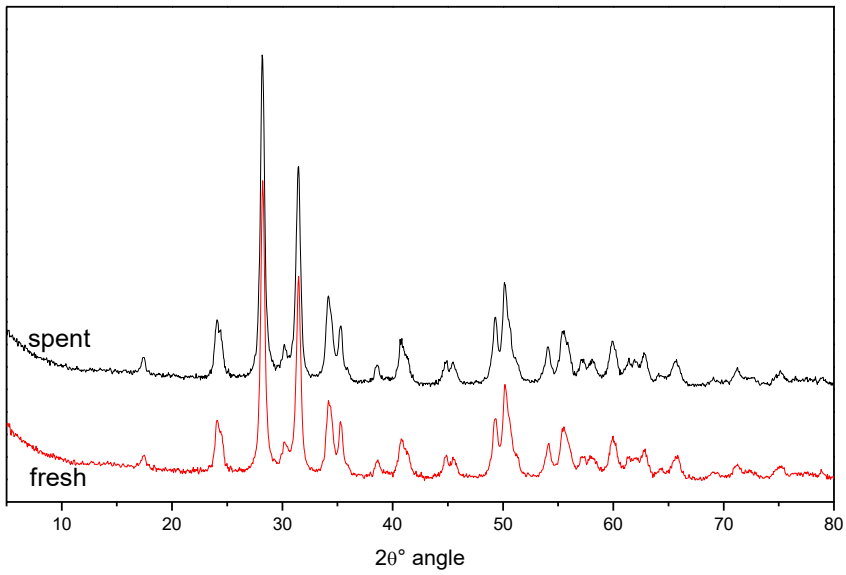

Figure 81. XRD pattern of spent (black), and fresh catalyst (red). Catalyst 4VZ.

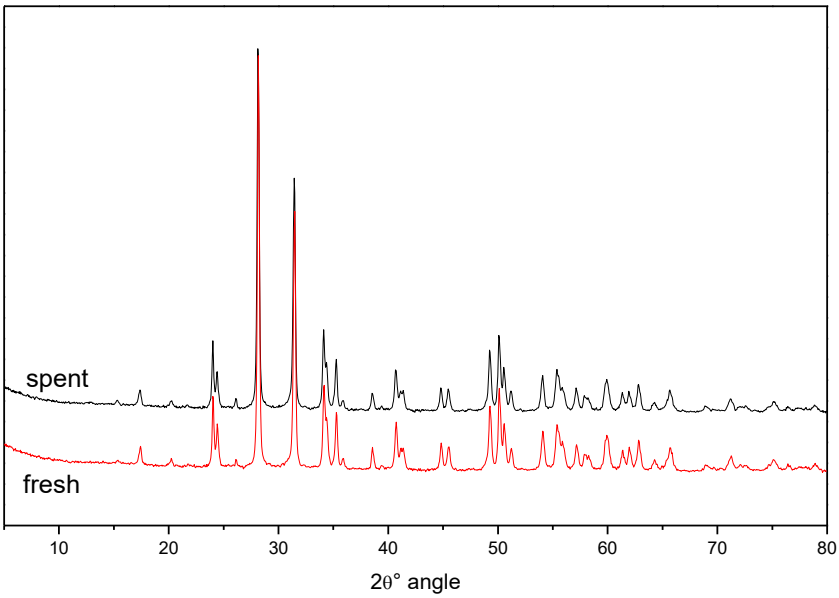

Figure 82. XRD pattern of spent (black), and fresh catalyst (red). Catalyst 7VZC.

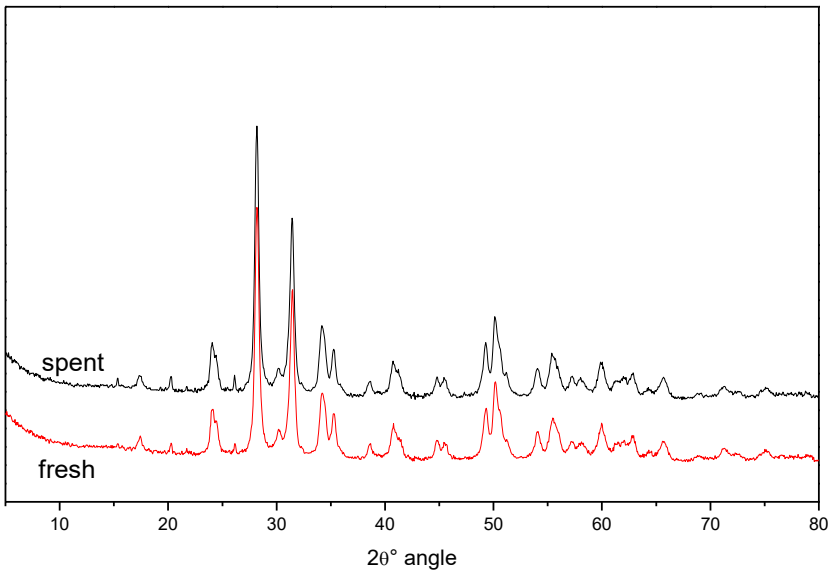

Figure 83. XRD pattern of spent (black), and fresh catalyst (red). Catalyst 7VZ.

Figures 79-83 report XRD patterns of spent catalysts, compared with the pattern of the corresponding fresh catalyst.

It is evident that in general catalysts maintained the same crystallinity features. However, in some cases an increase of crystallinity was observed, since reflections attributable to both zirconia and V_2O_5 appeared to be more sharp after reaction. This effect was emphasized with catalysts prepared using the home-made UniBO support, namely 4VZ and 7VZ, that were calcined at lower temperature, whereas for 2VZL, 2VZC and 7VZC this effect was less pronounced. Overheating of catalyst due to the exothermal nature of the reaction coupled with the intrinsic low thermal conductivity of zirconia are probably the cause of sintering of smaller crystallites that led to a higher crystallinity.

It is also known from ref [165] that Vanadium can induce a phase transformation of cubic and tetragonal zirconia into the monoclinic phase; however, this did not seem to be the case for our samples.

5.5 V_2O_5/ZrO_2 catalysts, in-situ Raman characterization

From Raman spectroscopy characterisation of used catalysts, we noticed that some modifications in catalyst structure had occurred during reaction. Therefore we carried out in-situ Raman experiments in order to draw a more complete picture on the nature of these transformations. Methods and thermal ramps used were described in paragraph 2.3.3.

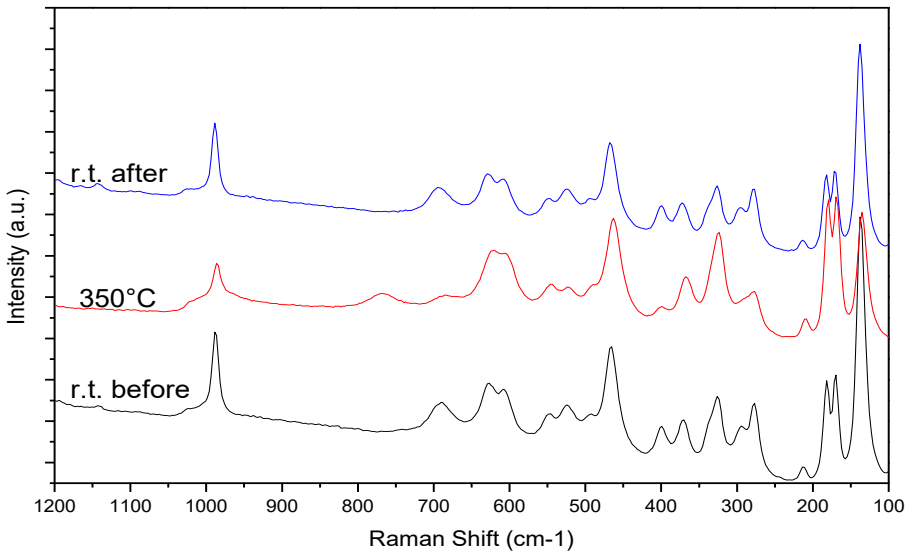

Figure 1. In-situ Raman spectra, Temperature ramp A (from bottom to top), catalyst 2VZC.

Figure 84 and figure 85 report Raman spectra recorded during the experiment carried out with ramp A, for catalysts with 2% and 4% Vanadium oxide supported over commercial zirconia (2VZC and 4VZC). In the case of 2VZC, at 350°C a new compound formed (band at 765cm^{-1}). From literature [166], this band is attributed to ZrV_2O_7. However, this band disappeared after cooling down the sample to r.t. In the case of 4VZC, the same phenomenon was seen, even though the band was present, albeit of very low intensity, also before the Raman experiment. At 350°C, the intensity increased, and when the sample was cooled down to r.t., the band disappeared.

These results demonstrate that upon heating, the formation of Zr pyrovanadate (or of a precursor for its formation) occurred, but this compound was not stable, and decomposed to yield back ZrO_2 and V_2O_5 when the sample was cooled.

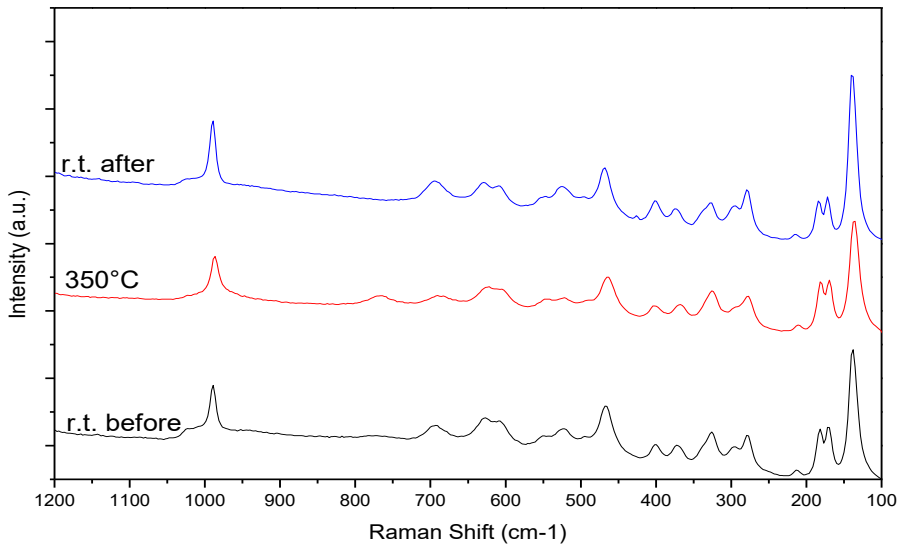

Figure 85. In-situ Raman spectra, Temperature ramp A (from bottom to top), catalyst 4VZC.

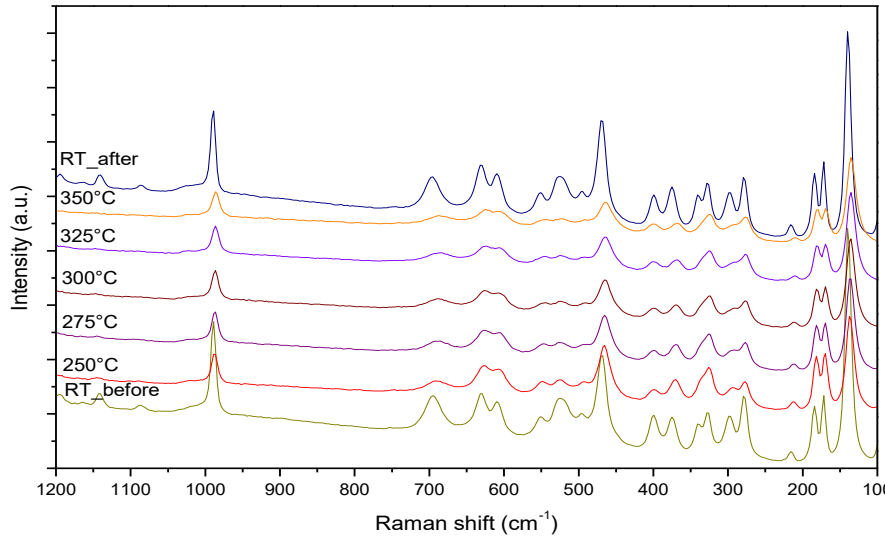

Figure 86. In-situ Raman spectra, Temperature ramp B (from bottom to top), catalyst 2VZ.

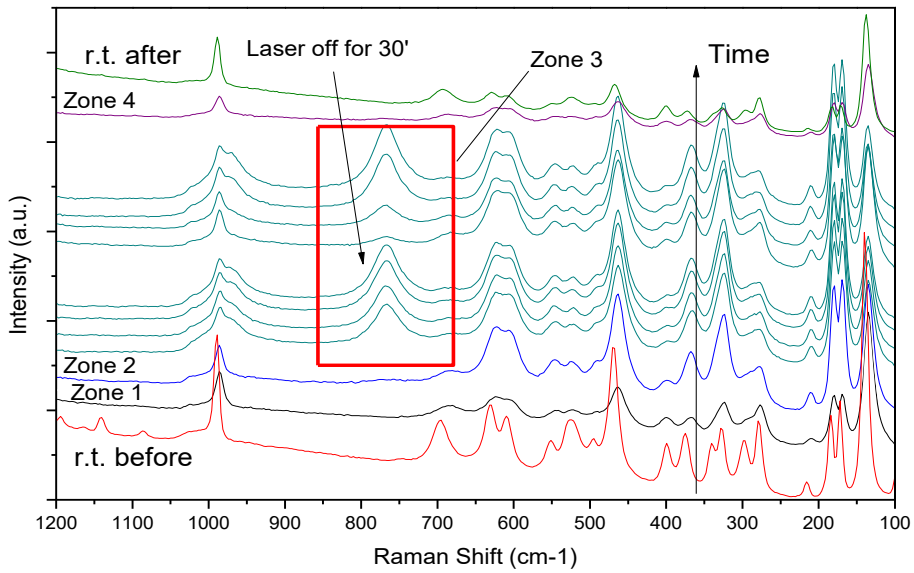

Figure 87. In-situ Raman spectra, Temperature ramp A (from bottom to top), catalyst 2VZ. The isothermal step starts at the second spectrum from the bottom. Different colours of spectra refer to different spots at which the laser beam was focused. During the isothermal step, in zone 3, the laser beam was turned off, and then turned on again.

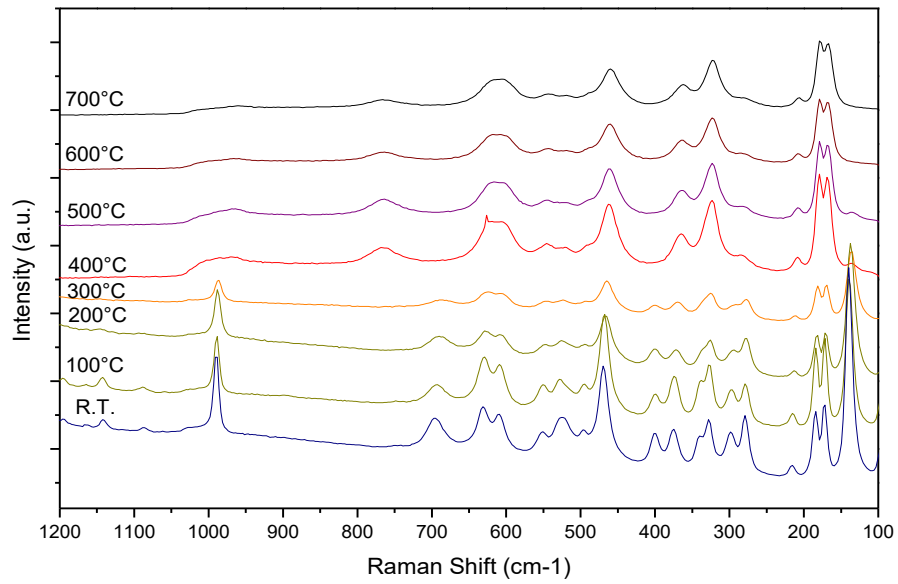

Figure 88. In-situ Raman spectra, Temperature ramp C (heating ramp, from bottom to top), catalyst 2VZ.

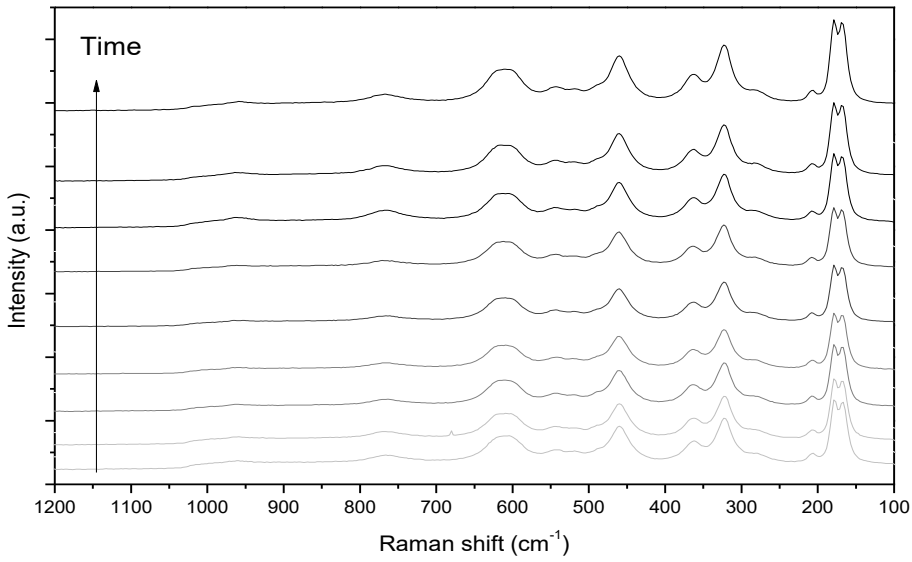

Figure 89. In-situ Raman spectra, Temperature ramp C (isotherm at 700°C, from bottom to top), catalyst 2VZ.

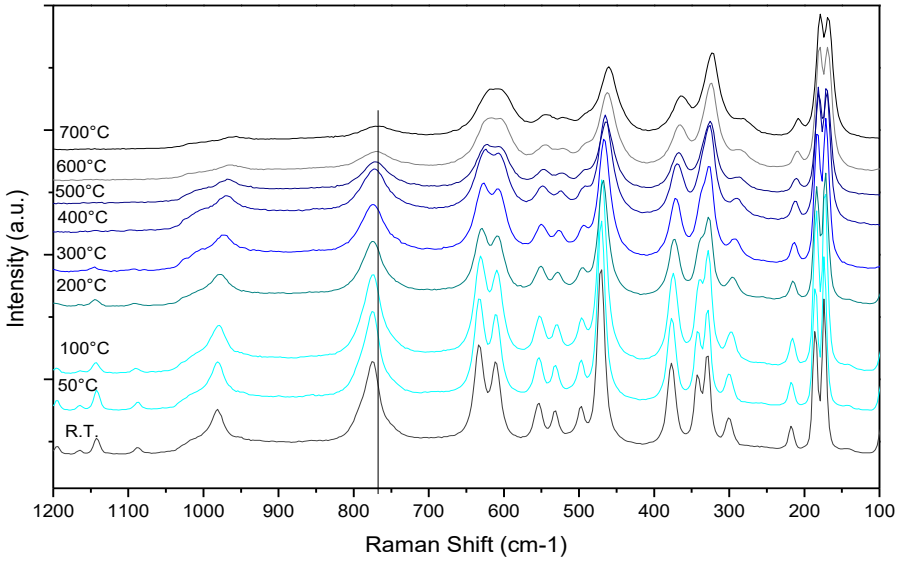

Figure 90. In-situ Raman spectra, Temperature ramp C (cooling ramp, from top to bottom); catalyst 2VZ.

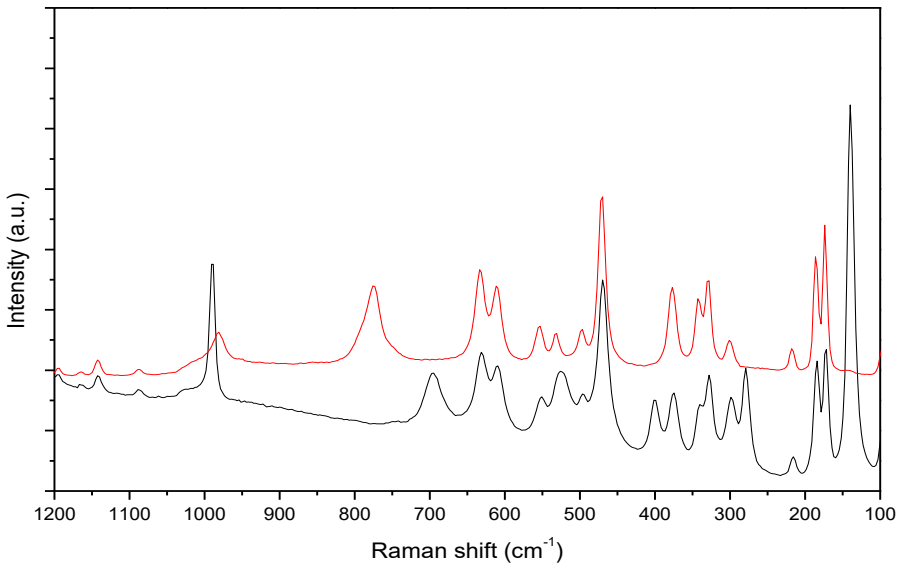

Figure 91. Raman spectra at r.t. before (black) and after (red) the in-situ experiment with ramp C; catalyst 2VZ.

Previous in-situ Raman experiments did not explain why sometimes ZrV_2O_7 was observed in spent catalysts, sometimes was not. Therefore, other experiments with different temperature ramps were carried out, in order to investigate more in depth on the catalyst behaviour at high temperature. Results for 2VZ are reported in figures 86-91.

Figure 86 shows that with a slow heating ramp (thermal ramp B), with intermediate steps for spectra recording, the band at 765cm^{-1} was never observed at any temperature. Conversely, when a direct heating ramp up to 350°C was used (figure 87, thermal ramp A), the formation of ZrV_2O_7 was observed for some of the particles where the laser beam was focused. However, in the same figure, it is possible to see that the formation of this compound was not seen for all catalysts particles, but only for a few of them. Moreover, when the laser beam was turned off, while keeping the sample at 350°C, the band at 765 cm^{-1} disappeared. When the laser was turned on again, bands attributable to ZrV_2O_7 appeared again, and their intensity increased

during time. After the cooling ramp (top spectrum), ZrV_2O_7 disappeared and V_2O_5 was formed again.

The spectrum was recorded even under more severe conditions; in experiment carried out with ramp C, temperature as high as 700°C was reached. Spectra recorded during the heating ramp (figure 88) show that the Zr pyrovanadate formed at temperature above 400°C in concomitance with V_2O_5 consumption. During the isothermal period, spectra were continuously recorded (figure 89), and ZrV_2O_7 was stable under these conditions.

Raman spectra were also recorded during the cooling ramp down to r.t.; these spectra, reported in figure 90, show that in this case the Zr pyrovanadate was maintained at room temperature, while no bands attributable to V_2O_5 were seen (988cm^{-1}, 692cm^{-1}, 525 cm^{-1}, 280 cm^{-1} and 137cm^{-1}). However, the band at 765 cm^{-1} shifted to 775 cm^{-1} upon cooling.

Figure 91 reports the spectra of fresh 2VZ and that one of 2VZ after ramp C, both recorded at r.t. Bands at 980 and 775 cm^{-1}, both attributable to ZrV_2O_7, are well evident.

In summary, the formation of the Zr pyrovanadate is greatly affected by the conditions used for thermal treatment. Either local overheating or an inefficient control of particle temperature, especially in V-richer samples, may lead to the formation of Zr pyrovanadate. However, the compound formed is not stable, and during the isothermal step at 350°C (during which the particle temperature may decrease because of heat dissipation) or during cooling, it reverses back to zirconia and vanadia. Conversely, when a slow heating ramp is used, and the maximum temperature is no higher than 350°C, the compound does not form; therefore, it seems that under thermodynamically-controlled conditions the formation of this compound is not possible at mild temperature.

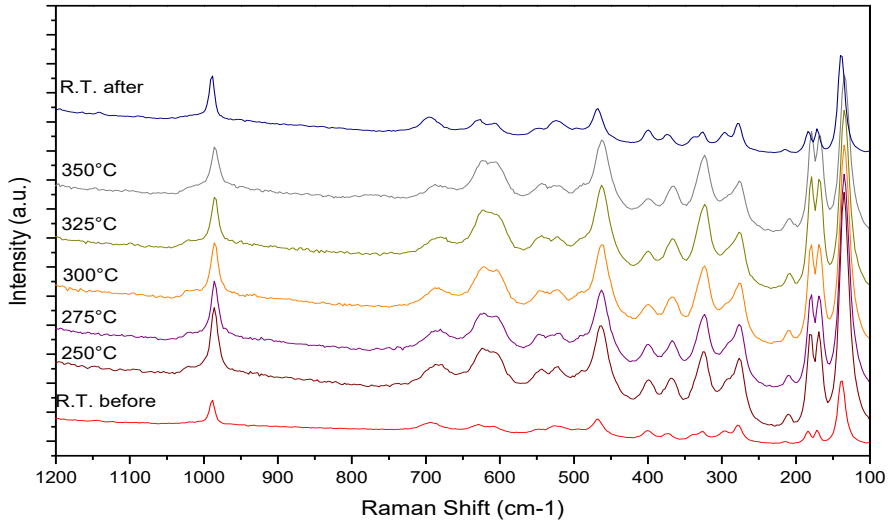

Figure 92. In-situ Raman spectra, Temperature ramp B (from bottom to top), catalyst 4VZ.

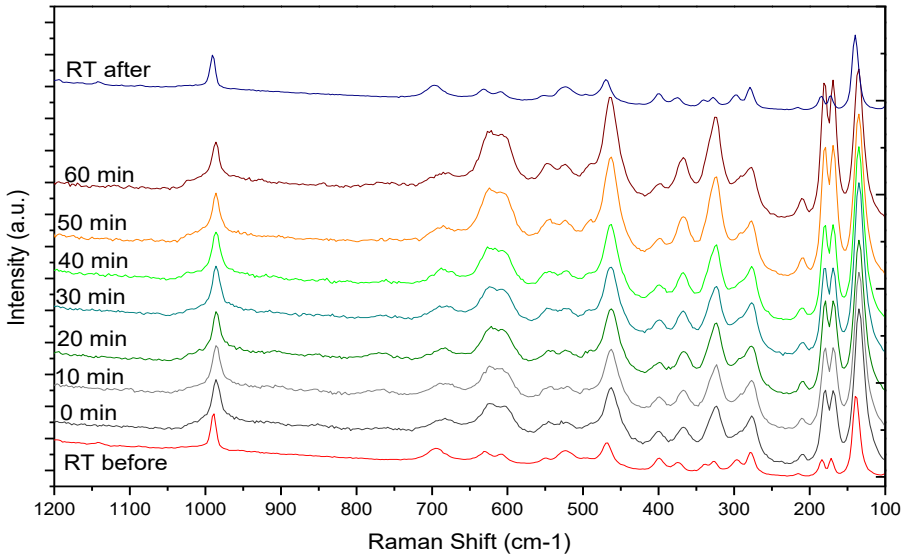

Figure 93. In In-situ Raman spectra, Temperature ramp A (isotherm at 350°C, from bottom to top), catalyst 4VZ.

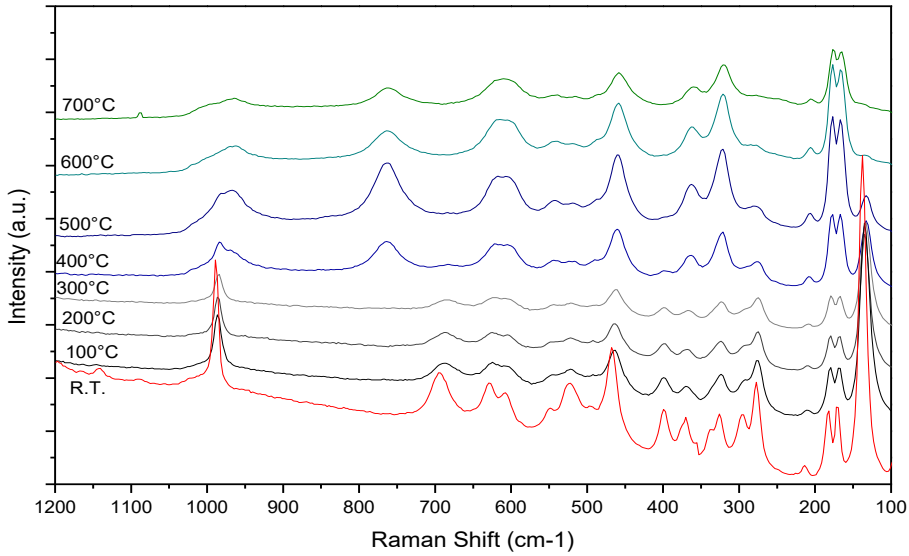

Figure 94. In-situ Raman spectra, Temperature ramp C (heating ramp, from bottom to top), catalyst 4VZ.

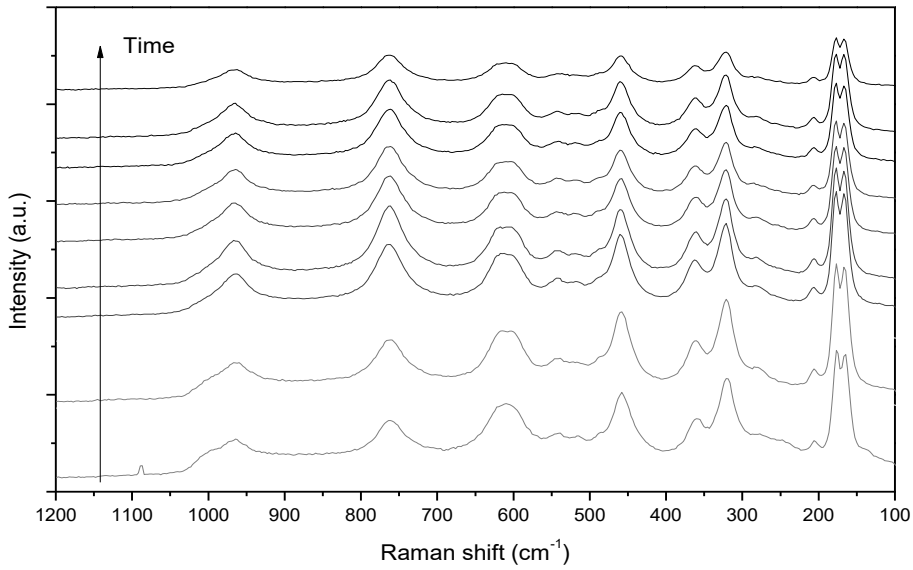

Figure 95. In-situ Raman spectra, Temperature ramp C (isotherm at 700°C, from bottom to top), catalyst 4VZ.

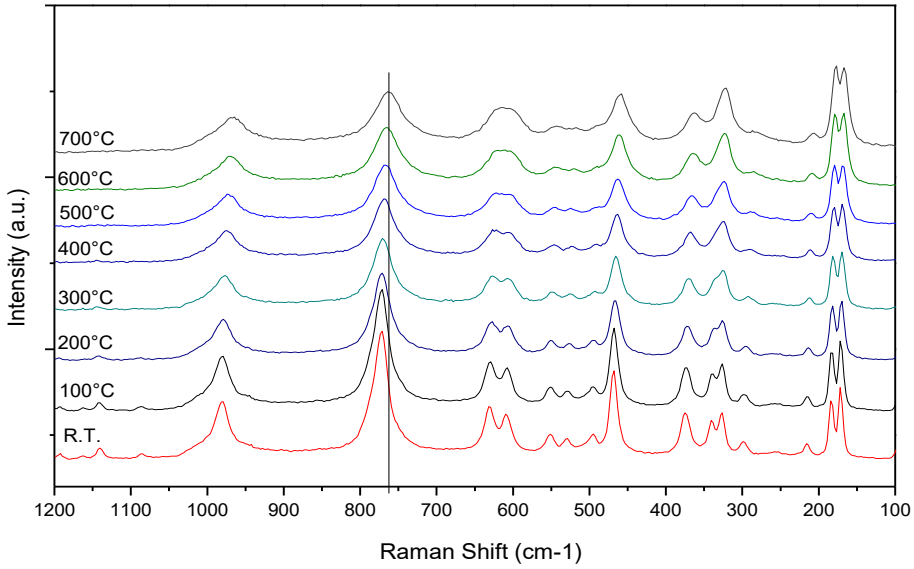

Figure 96. In-situ Raman spectra, Temperature ramp C (cooling ramp, from top to bottom), catalyst 4VZ.

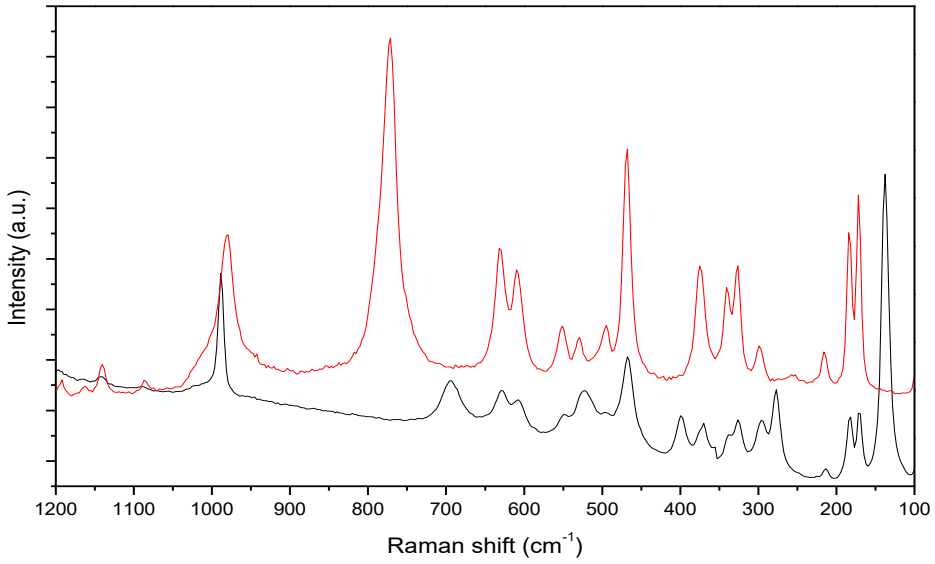

Figure 97. Raman spectra at r.t. before (black) and after (red) in-situ experiment with ramp C; catalyst 4VZ.

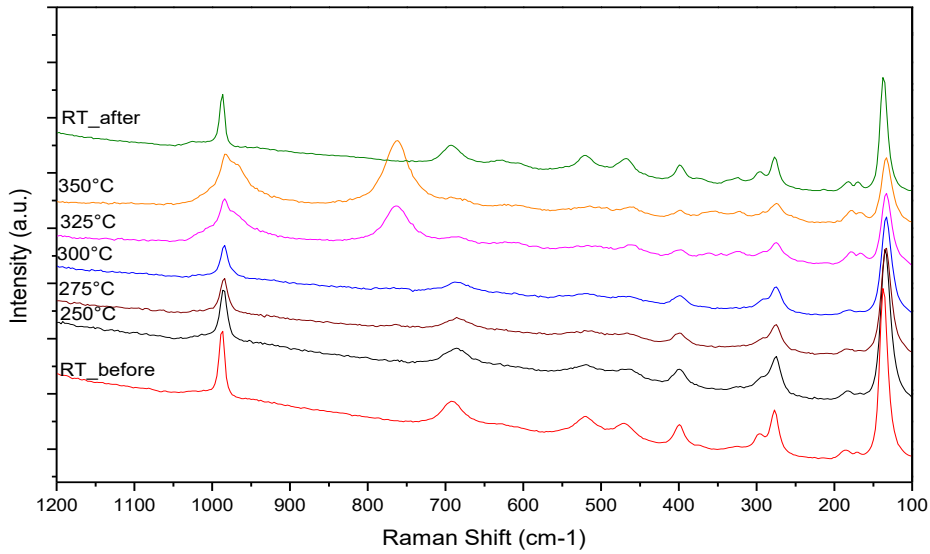

Figure 98. In-situ Raman spectra, Temperature ramp B (from bottom to top), catalyst 7VZ.

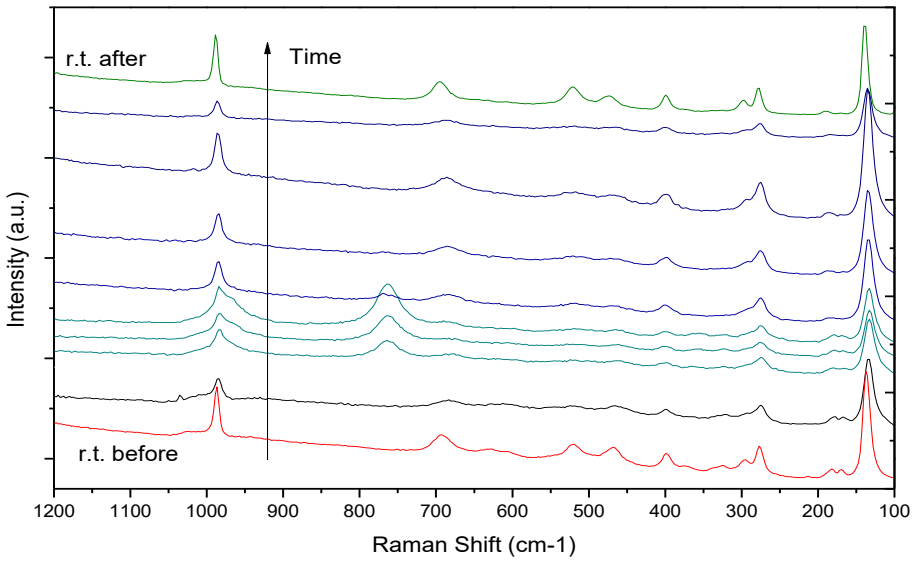

Figure 99. In-situ Raman spectra, Temperature ramp A (isothermal step, from bottom to top), catalyst 7VZ.

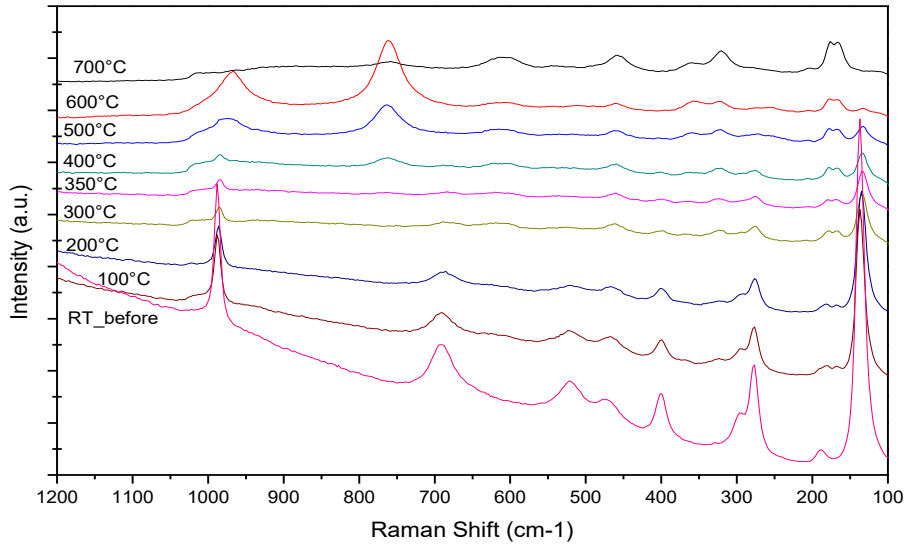

Figure 100. In-situ Raman spectra, Temperature ramp C (heating ramp, from bottom to top), catalyst 7VZ.

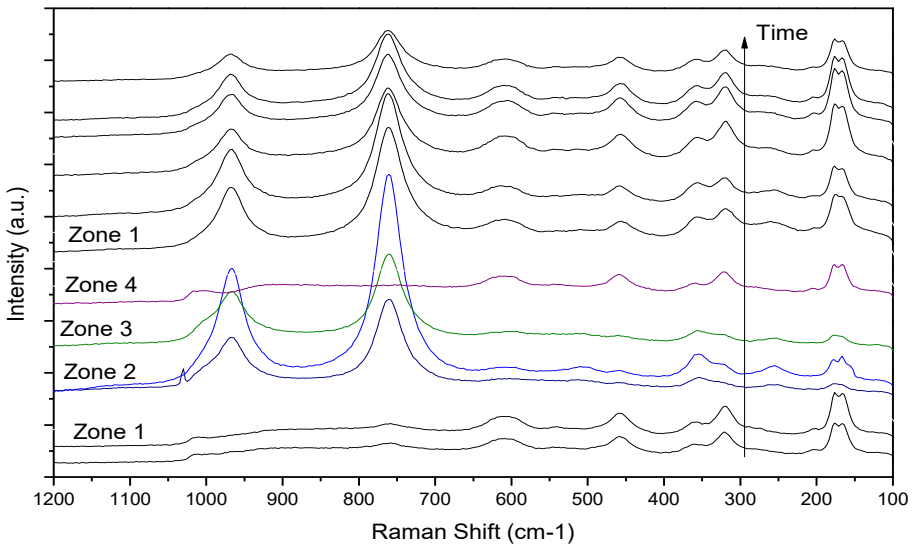

Figure 101. In-situ Raman spectra, Temperature ramp C (isotherm at 700°C, from bottom to top), different colours refer to different particles on which the laser beam was focused; catalyst 7VZ.

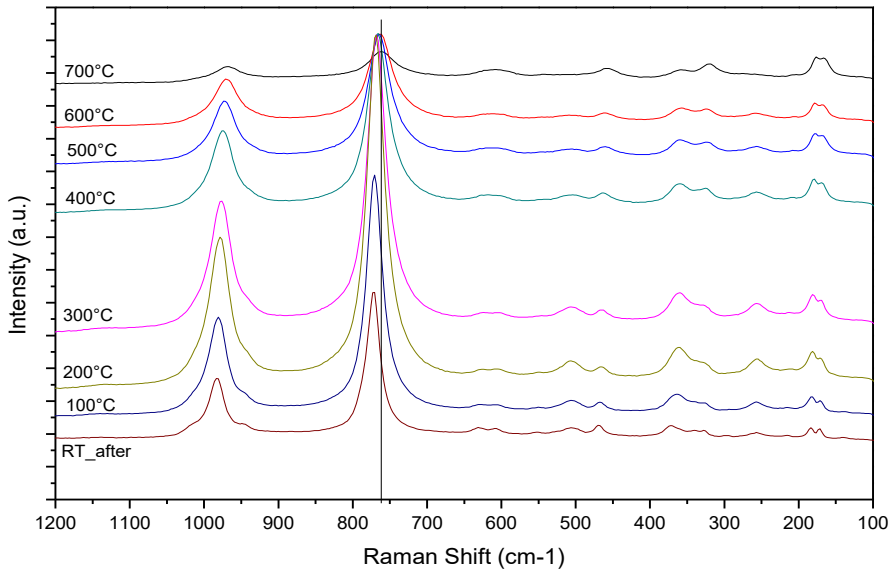

Figure 102. In-situ Raman spectra, Temperature ramp C (cooling ramp, from top to bottom), catalyst 7VZ.

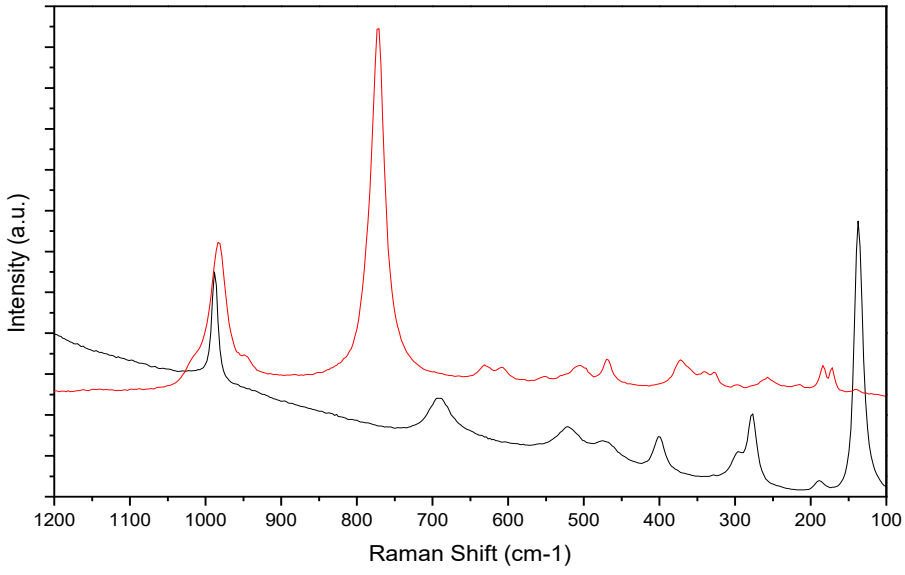

Figure 103. Raman spectra at r.t. before (black) and after (red) in-situ experiment with ramp C; catalyst 7VZ.

Catalysts containing different Vanadium oxide amount were treated using the same procedure described above; spectra are shown in figures 92-103.

The behaviour shown was similar for all catalysts, regardless of Vanadium oxide content; in all cases, the formation of ZrV_2O_7 was reversible until 350°C, and in experiment with ramp C, the formation of Zr pyrovanadate occurred at above 400°C. Differences were shown in regard to the disappearance of V_2O_5; for example, the band at 137cm^{-1} Raman shift disappeared at 400°C, 500°C and 600°C with 2VZ, 4VZ and 7VZ, respectively. The band at 765cm^{-1}, attributed to Zr pyrovanadate, became more intense along with the increase of Vanadium oxide content.

Spectra shown in figure 101 confirm that these transformations did not occur for all particles. In some cases, bands of Zr pyrovanadate were not shown, and the spectrum was more similar to that one previously observed with sample 2VZT (figure 39), with no bands attributable to either V_2O_5 or Zr pyrovanadate, and with a broad absorption covering the spectral range 700-900 cm^{-1}, an indication of the possible formation of $Zr_{1-x}V_xO_2$ solid solutions.

All these experiments suggest that during picoline oxidation the in-situ generation of compounds different from those formed during calcination of the fresh catalyst may occur. Indeed, even though we should take into account that in-situ Raman experiments are not really representative of the true situation during catalytic experiments, nevertheless we can hypothesize that local overheating due to the laser beam may somehow simulate the local temperature increase due to the reaction exothermicity, with also enhanced thermal effects due to the poor conductivity of zirconia. Results demonstrate that under specific conditions, the Zr pyrovanadate generated is stable, whereas there are conditions at which its formation may occur only temporarily, and when conditions which led to its generation cease, the compound is reversed back to ZrO_2 and V_2O_5. This might explain why with used

catalysts, ex-situ Raman characterisation revealed the formation of this compound only occasionally.

In order to check whether Zr pyrovanadate (eventually generated in-situ under reaction conditions) may be the true active phase in our catalysts, we deliberately treated at 700°C in the oven muffle sample 7VZC, in order to form a relevant quantity of stable ZrV_2O_7 (catalyst code 7VZC-TT). The ex-situ Raman spectrum (figure 104) recorded at r.t. for 7VZC-TT is compared with that one of the 7VZC after treatment in the Raman cell (ramp C). It is shown that the spectra were similar, thus ZrV_2O_7 formation took place in both cases, moreover the compound was stable.

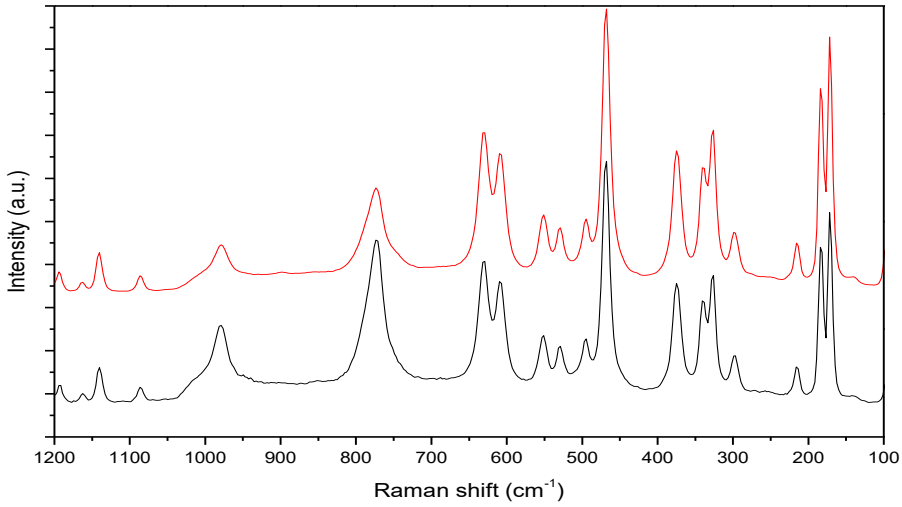

Figure 104. Comparison of Raman spectra of 7VZC calcined at 700°C in muffle oven (7VZC-TT, top), and in Raman cell (bottom).

Porosimetry analysis gave a specific surface area of 5.0 m^2/g, slightly lower than that one of the original 7VZC catalyst. This catalyst was tested under picoline-lean conditions; yields and conversion are plotted in function of temperature in figure 105.

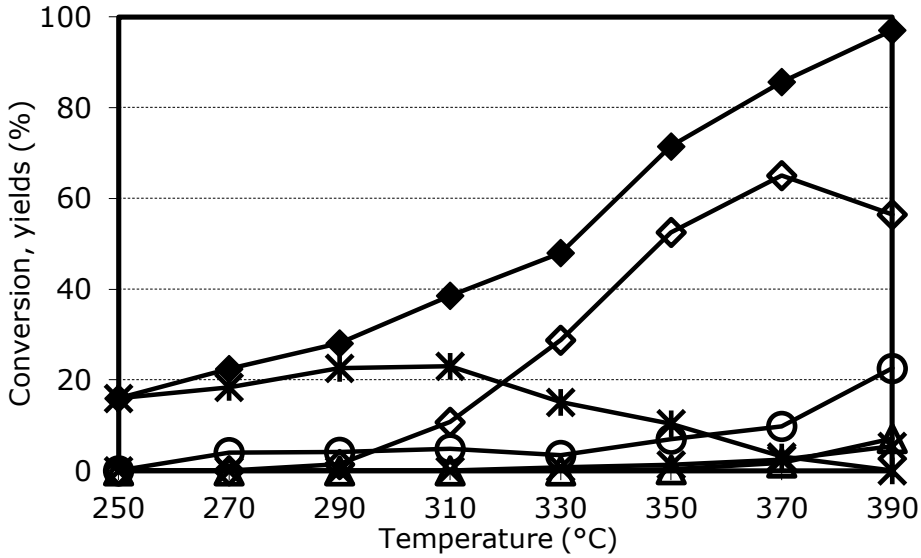

Figure 105. Effect of temperature on 3-picoline conversion and on yield to products. Reaction conditions: feed composition (molar %): picoline/oxygen/steam/inert 0.24/4.2/79.2/remainder; WHSV 0.02 h^{-1} (referred to picoline), contact time 1.2 s. Symbols: picoline conversion (◆), yield to: nicotinic acid NAc (◇), nicotinic aldehyde NAl (✳), pyridine PY (△), cyanopyridine CP (□), CO (✕), and CO_2 (○). Catalyst 7VZC-TT.

Comparing these results with those reported in figure 60, obtained using the same reaction conditions with 7VZC, it is clear that the zirconium pyrovanadate was less active than 7VZC, because conversion was lower in the whole range of temperature investigated. Below 310°C, 7VZC-TT was highly selective to NAl, which instead formed with low or nil selectivity with all zirconia-based catalysts, at least under picoline-lean conditions. Maximum yield to NAc was 65% achieved at 370°C, whereas it was 74% at 310°C with 7VZC.

High selectivity towards NAl can be due to two different factors, (a) a lower efficiency in NAl oxidation to NAc, or (b) a decreased acidity of the catalyst, that allows easy desorption of NAl formed. A study performed by Pieck et al. [165] on V_2O_5/ZrO_2 for *o*-xylene oxidation to phthalic anhydride, comparing the behaviour of supported vanadia species with ZrV_2O_7, clearly indicate that both effects are present. In fact, NH_3-TPD profile showed that Zr pyrovanate has a very low acidity compared to V_2O_5/ZrO_2. The comparison of catalytic performance at the same level of *o*-xylene conversion, demonstrated a reduced

selectivity to phthalic anhydride for the Zr pyrovanadate, and an enhanced *o*-tolualdehyde selectivity, while selectivity to deep oxidation products turned out to be unaffected.

However, in our case besides Zr pyrovanadate also ZrO_2 was present in 7VZC-TT catalyst; preparation of a stoichiometric Zr pyrovanadate by reacting Vanadium oxide and zirconia in the proper amount might help to elucidate on the catalytic behaviour of this compound in 3-picoline oxidation.

5.6 V_2O_5/ZrO_2-TiO_2 catalysts: preparation and characterisation

Results reported so far demonstrate that zirconia is a good support for Vanadium oxide, and that the optimal catalyst based on V_2O_5/ZrO_2 has to be characterised by a low surface area, and by a low loading of Vanadium oxide. It is worth noting that these features contrast with literature indications, where in general catalysts based on titania-supported Vanadium oxide are characterised by surface area values and Vanadium oxide contents which are both remarkably higher than those shown by our systems. Moreover, our data seem to indicate that with our zirconia-based catalysts, the need for such characteristics might be related to heat transfer limitations, which may affect the overall reaction rate especially with catalysts having both high surface area and high density of V active sites. Indeed, since no mention is made in the literature about these problems for reactions carried out in lab-scale reactors and with V_2O_5/TiO_2 catalysts shaped in particles similar to those of our catalysts, we were wondering whether the problem met might derive from the bad heat-conductive properties of zirconia.

In fact, it is reported that for zirconia ceramics (cubic phase) typical thermal conductivity values fall in the interval 1.8-2.2 W/(m K), which is considerably lower than typical values for titania (ranging between 4.8 and 11.8 W/(m K)), and even for alumina. In fact, cubic zirconia is used as a refractory and insulating material; moreover, also the bulk density of zirconia is higher than that of titania. We have not found in literature the value of thermal conductivity for monoclinic zirconia, to compare with that of anatase, but it can be expected that similar differences are also met with our oxides, albeit prepared at milder conditions (e.g., lower calcination temperature) than ceramic materials.

In order to check whether the characteristics of zirconia might affect negatively the catalytic performance, we decided to test a catalyst prepared using a mixed ZrO_2-TiO_2 support; if thermal conductivity of zirconia is the reason for the

drawbacks encountered, they should be partially overcome by using a mixed oxide support. We did not prepare a V_2O_5/TiO_2 catalyst, because there is already plenty of literature available on this class of catalysts for picoline oxidation.

However, it should be mentioned that the aim of this study was not so much finding a better catalyst, but to have a deeper insight on problems associated to the management of such an exothermal reaction. Indeed, a catalyst containing a smaller amount of active phase (in our case, only 2 wt% of V_2O_5 for 2VZC, much less than that reported in literature for V_2O_5/TiO_2 catalysts) is preferable from an industrial viewpoint compared to a catalyst having a greater amount of it.

The preparation of the support, made of 50 wt% TiO_2 (anatase) and 50% ZrO_2, was carried out with a similar procedure as for zirconia; the catalyst contained the 20 wt% of V_2O_5 (similar to the amount used in literature for titania-supported catalysts) and had a surface area of 21 m^2/g (catalyst code 20VTZ). It is worth noting that a catalyst having these features should offer a poor catalytic performance, based on results obtained with our zirconia-based systems.

Figure 106 shows the results obtained with 20VTZ under the optimised reaction conditions: feed composition (mol %) 3-picoline 0.24%, O_2 4.2%, H_2O 79.2%, N_2 balance, τ 1.2s. Results demonstrate that with this catalyst type it was possible to achieve 85% yield to NAc, with 98% conversion of picoline, at 270°C, thus at considerably lower temperature than with zirconia-based catalysts. Indeed, already at 250°C conversion of picoline was 87%. Therefore, it can be concluded that with V_2O_5/ZrO_2 catalysts, the characteristics of the support is the main reason for the need of both a low surface area and a low Vanadium oxide content.

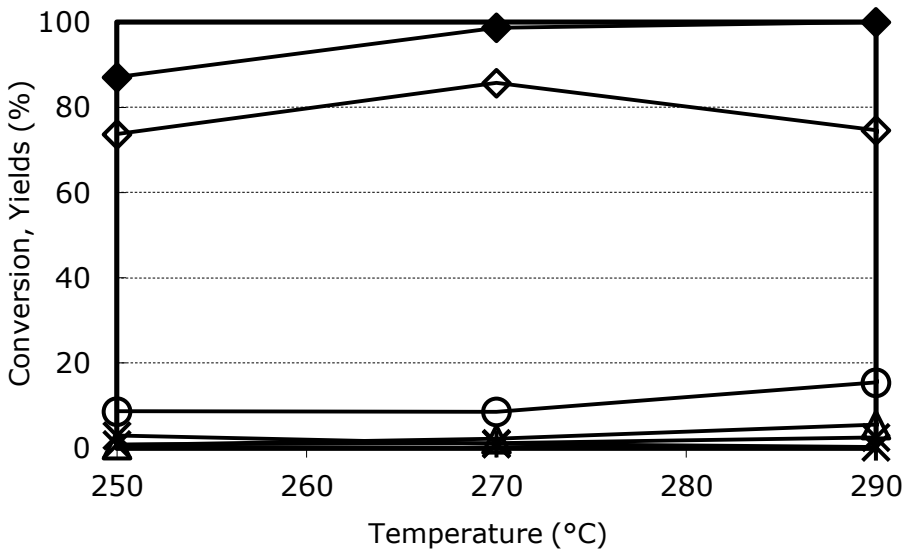

Figure 106. Effect of temperature on 3-picoline conversion and on yield to products. Reaction conditions: feed composition (molar %): picoline/oxygen/steam/inert 0.24/4.2/79.2/remainder; WHSV 0.02 h^{-1} (referred to picoline), contact time 1.2 s. Symbols: picoline conversion (◆), yield to: nicotinic acid NAc (◇), nicotinic aldehyde NAl (✳), pyridine PY (△), cyanopyridine CP (□), CO (✕), and CO_2 (○). Catalyst 20VTZ.

At similar picoline-lean conditions (figure 107), but with a slightly different ratio between reactants, again a very good 78% NAc yield was obtained.

In view of this excellent result, we decided to investigate further the reactivity of this catalyst. We first hoped that with such catalyst type it were possible to operate even at picoline-rich conditions, in order to achieve a much higher NAc productivity compared to picoline-lean conditions. Results of experiments carried out using picoline-rich conditions at three different values of contact time are shown in figures 108-110. We also tested the reactivity in the absence of steam (figures 111-113), again at three different contact time values), in order to check whether the presence of steam is anyway needed for the reaction, as it was for V_2O_5/ZrO_2 catalysts.

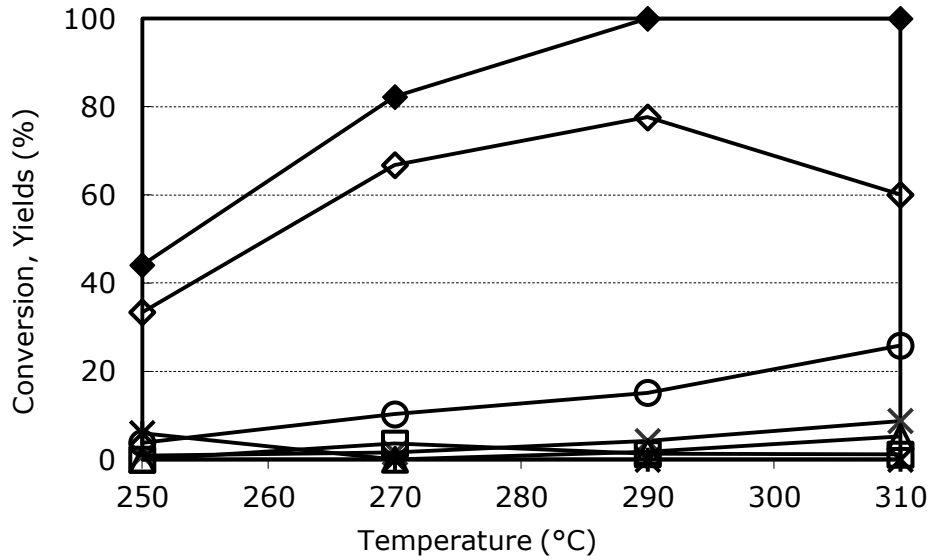

Figure 107. Effect of temperature on 3-picoline conversion and on yield to products. Reaction conditions: feed composition (molar %): picoline/oxygen/steam/inert 0.2/7.0/66.5/remainder; contact time 1.4 s. Symbols: picoline conversion (◆), yield to: nicotinic acid NAc (◇), nicotinic aldehyde NAl (✳), pyridine PY (△), cyanopyridine CP (□), CO (×), and CO_2 (○). Catalyst 20VTZ.

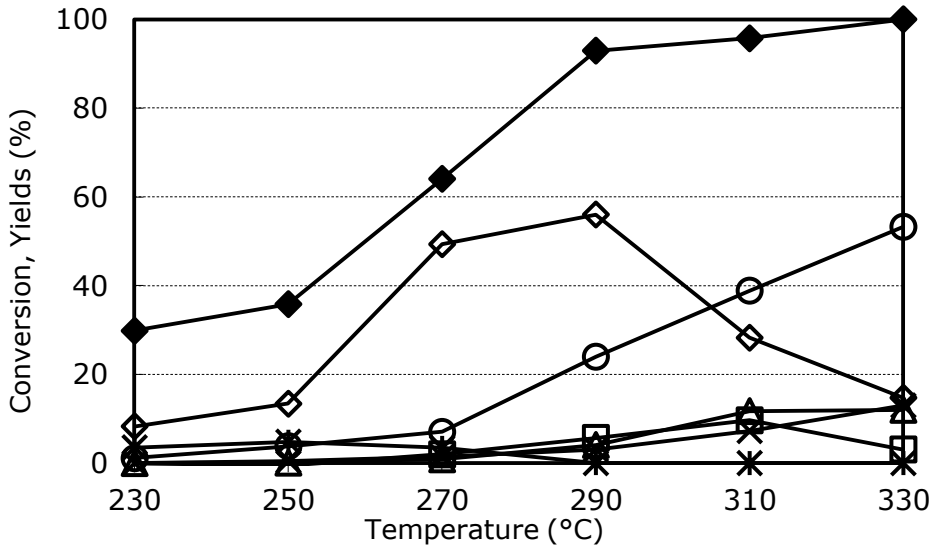

Figure 108. Effect of temperature on 3-picoline conversion and on yield to products. Reaction conditions: feed composition (molar %): picoline/oxygen/steam/inert 1.0/16.6/20.0/remainder; contact time 1.0 s. Symbols: picoline conversion (◆), yield to: nicotinic acid NAc (◇), nicotinic aldehyde NAl (✳), pyridine PY (△), cyanopyridine CP (□), CO (×), and CO_2 (○). Catalyst 20VTZ.

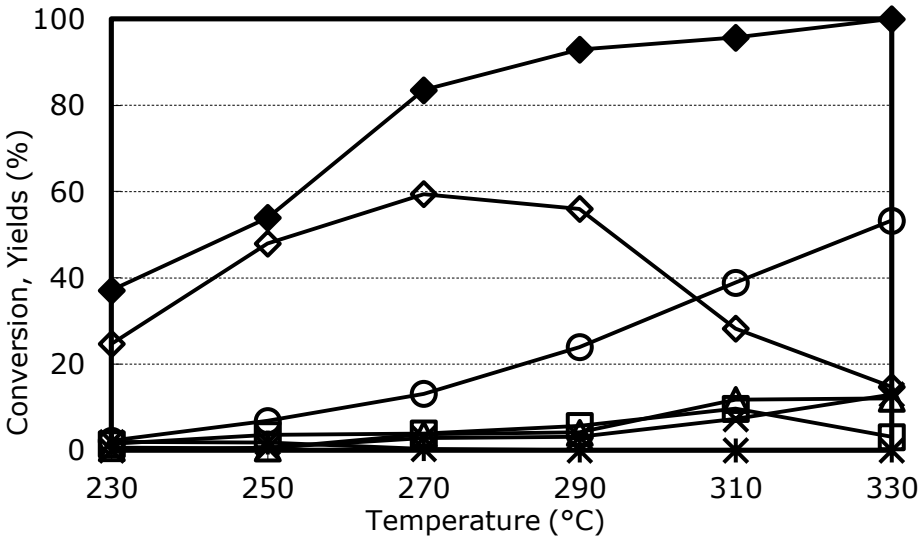

Figure 109. Effect of temperature on 3-picoline conversion and on yield to products. Reaction conditions: feed composition (molar %): picoline/oxygen/steam/inert 1.0/16.6/20.0/remainder; contact time 2.0 s. Symbols: picoline conversion (◆), yield to: nicotinic acid NAc (◇), nicotinic aldehyde NAl (✳), pyridine PY (△), cyanopyridine CP (□), CO (✕), and CO_2 (○). Catalyst 20VTZ.

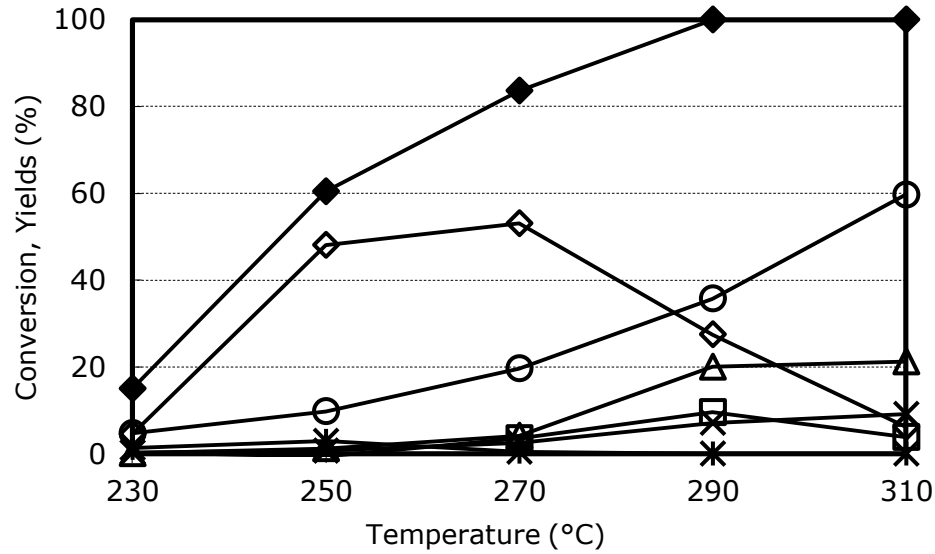

Figure 110. Effect of temperature on 3-picoline conversion and on yield to products. Reaction conditions: feed composition (molar %): picoline/oxygen/steam/inert 1.0/16.6/20.0/remainder; contact time 3.0 s. Symbols: picoline conversion (◆), yield to: nicotinic acid NAc (◇), nicotinic aldehyde NAl (✳), pyridine PY (△), cyanopyridine CP (□), CO (✕), and CO_2 (○). Catalyst 20VTZ.

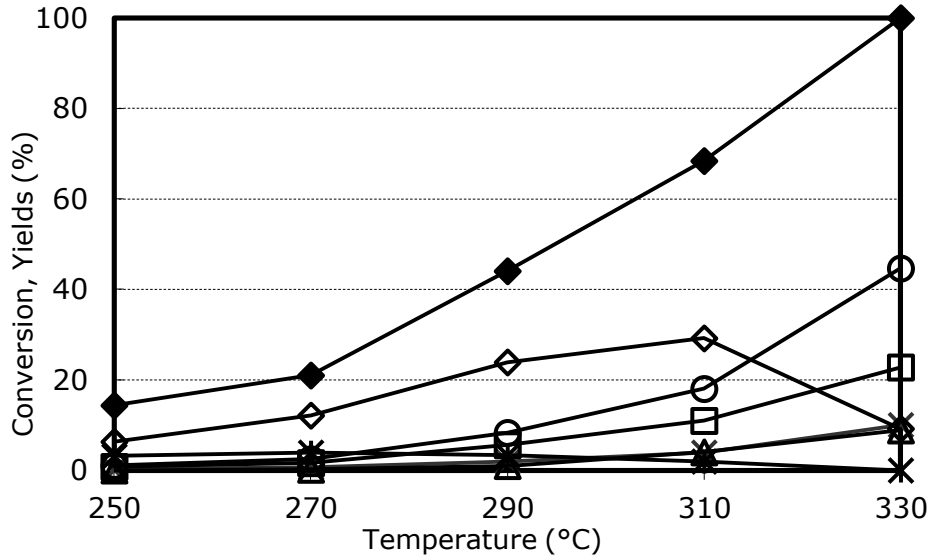

Figure 111. Effect of temperature on 3-picoline conversion and on yield to products. Reaction conditions: feed composition (molar %): picoline/oxygen/steam/inert 1.0/20.8/0/remainder; contact time 1.0 s. Symbols: picoline conversion (◆), yield to: nicotinic acid NAc (◇), nicotinic aldehyde NAl (✳), pyridine PY (△), cyanopyridine CP (□), CO (✕), and CO_2 (○). Catalyst 20VTZ.

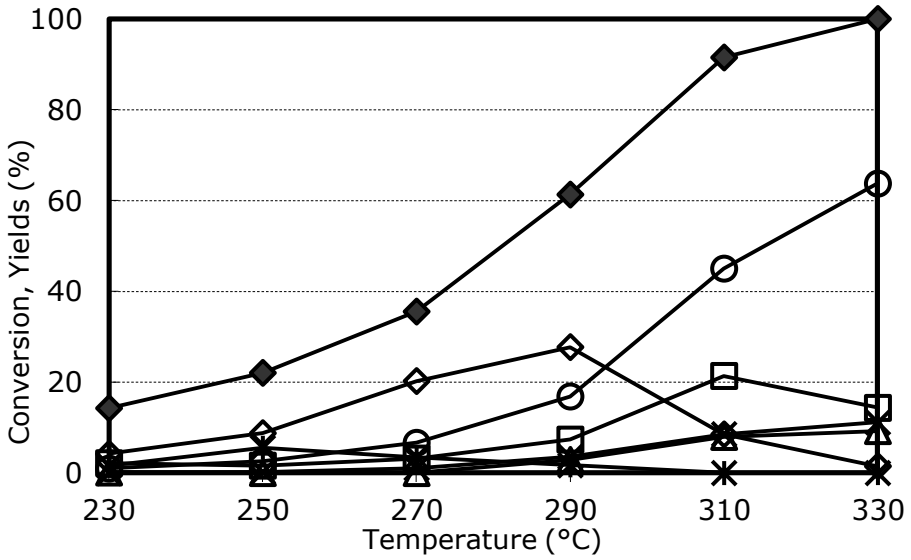

Figure 112. Effect of temperature on 3-picoline conversion and on yield to products. Reaction conditions: feed composition (molar %): picoline/oxygen/steam/inert 1.0/20.8/0/remainder; contact time 2.0 s. Symbols: picoline conversion (◆), yield to: nicotinic acid NAc (◇), nicotinic aldehyde NAl (✳), pyridine PY (△), cyanopyridine CP (□), CO (✕), and CO_2 (○). Catalyst 20VTZ.

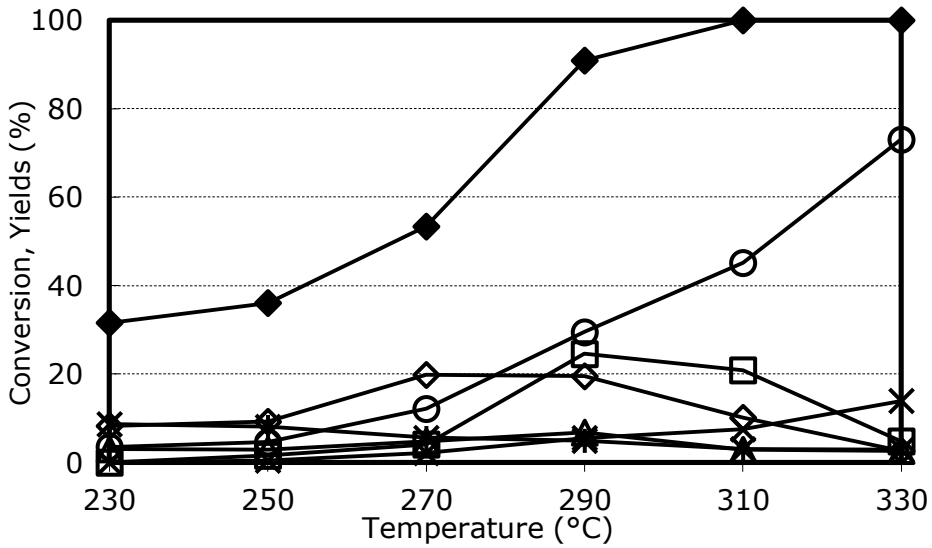

Figure 113. Effect of temperature on 3-picoline conversion and on yield to products. Reaction conditions: feed composition (molar %): picoline/oxygen/steam/inert 1.0/20.8/0/remainder; contact time 3.0 s. Symbols: picoline conversion (◆), yield to: nicotinic acid NAc (◇), nicotinic aldehyde NAl (✳), pyridine PY (△), cyanopyridine CP (□), CO (✕), and CO_2 (○). Catalyst 20VTZ.

In fact, these experiments might permit to distinguish if steam plays a "chemical" role, for instance by assisting products desorption and contributing in maintaining a more "clean" surface (in this case, water would play a positive role on performance regardless of heat-transfer limitations), or if instead its role is mainly that one of favouring heat dissipation. In the latter case, in fact, with a catalyst type for which heat transfer is no longer crucial as it was for V_2O_5/ZrO_2, we should not observe an important effect of steam.

Results clearly indicate the following:

1. Unfortunately, under picoline-rich conditions the performance was not so good as it was at picoline-lean conditions. Best yield to NAc was no higher than 60%. We can hypothesize that heat-transfer problems, albeit less crucial than with V_2O_5/ZrO_2 catalysts, still may play a role and affect catalytic behaviour.
2. The increase of contact time led to an increase of conversion, both with and without steam, but had a limited (negative) effect on the maximum

NAc yield. The formation of cyanopyridine increased, but also this by-product underwent combustion, with a decline of yield which started at a defined temperature; the latter was a function of contact time.

3. Steam still played an important role in the reaction; both picoline conversion and NAc yield were considerably enhanced in the presence of steam. This is also shown by comparing results reported in figure 109 (20% steam) and figure 112 (0% steam), with those in figures 114 and 115, which report results achieved with 10% and 66.6% steam in feed, respectively. The greatest improvement of performance was shown passing from 0 to 10% steam in feed; afterwards (20% and 66.6% steam), a smaller improvement of both conversion and maximum yield was shown.

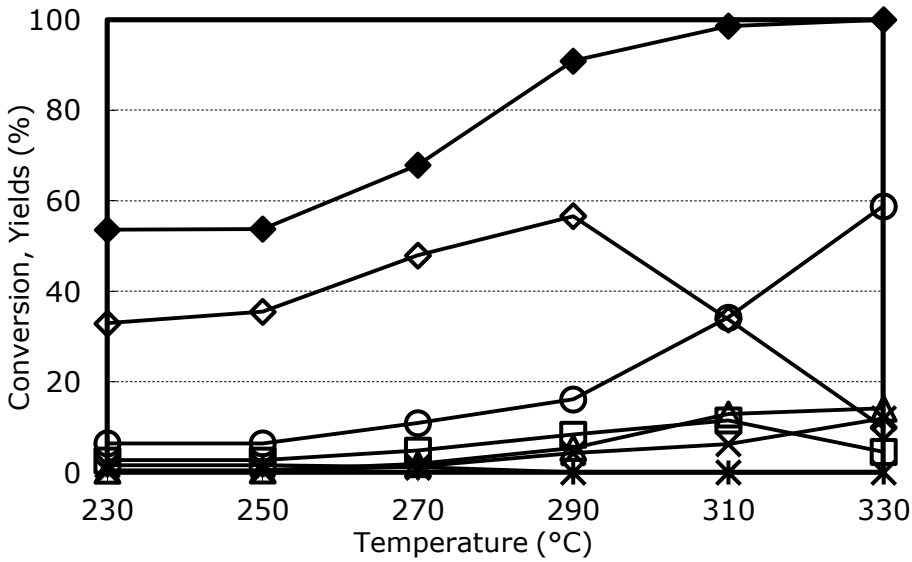

Figure 114. Effect of temperature on 3-picoline conversion and on yield to products. Reaction conditions: feed composition (molar %): picoline/oxygen/steam/inert 1.0/18.7/10.0/remainder; contact time 2.0 s. Symbols: picoline conversion (◆), yield to: nicotinic acid NAc (◇), nicotinic aldehyde NAl (✳), pyridine PY (△), cyanopyridine CP (□), CO (✕), and CO_2 (○). Catalyst 20VTZ.

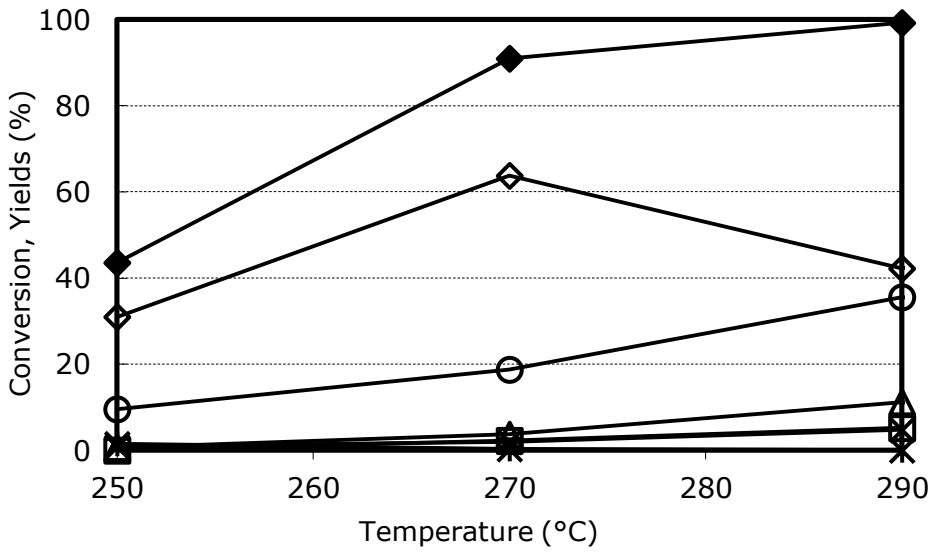

Figure 115. Effect of temperature on 3-picoline conversion and on yield to products. Reaction conditions: feed composition (molar %): picoline/oxygen/steam/inert 1.0/15.0/66.6/remainder; contact time 2.0 s. Symbols: picoline conversion (◆), yield to: nicotinic acid NAc (◇), nicotinic aldehyde NAl (✳), pyridine PY (△), cyanopyridine CP (□), CO (✕), and CO_2 (○). Catalyst 20VTZ.

For what concerns the role of picoline and oxygen partial pressure, previously reported experiments already highlighted the fact that the best performance is achieved at low reactant concentration in feed, and that a high O_2/picoline ratio is necessary with zirconia-based catalysts. A more systematic comparison of performance in function of these parameters is illustrated in the following section. We varied picoline partial pressure (while keeping a large excess of O_2, equal to ca 16.6 mol%), and a moderate amount of steam (20%). It is worth noting that results in figures 106 and 107 already demonstrated the optimal performance of this catalyst at picoline-lean conditions, but those experiments were carried out with a much greater partial pressure of steam and a lower one of oxygen.

Figure 116 summarizes the results obtained. It is shown that indeed at these conditions an increase of picoline partial pressure led to a better maximum NAc yield, even though conversion was remarkably decreased. This indicates that the rate determining step of the process was V reduction by picoline, and that

in the presence of steam (which limits or avoids surface saturation) a higher picoline/O_2 had a positive effect on the highest yield to NAc. This is because V oxidation state under working conditions was, in average, close to 5+, and therefore a greater number of oxidising sites was available; under these conditions, combustion greatly contributed to the decrease of NAc yield and selectivity. Conversely, a better selectivity and maximum NAc yield was achieved under conditions at which the gas-phase was less oxidizing, i.e., with a higher picoline/O_2 feed ratio. It should be mentioned now that most likely this property, which represents a difference compared to what previously seen with V_2O_5/ZrO_2 catalysts, probably derives from the combination of a relatively large catalyst surface area and a lower contribution of heat-transfer limitations phenomena.

We also undertook a more detailed investigation of the reaction network. As already discussed in the Section dealing with literature analysis, some authors hypothesize the existence of both a direct reaction from 3-picoline to NAc, and the two-step reaction where NAl is the intermediate. The direct reaction clearly implies that NAl, once formed, is immediately oxidised to NAc before it can desorb into the gas-phase; thus, in this case NAc would be identified as a kinetically primary compound.

Another important point concerns the role of steam; as already discussed in previous sections, steam might play several different roles. A “catalytic” role might be that of providing an additional route for NAc formation; the hydration of the carbonyl bond in NAc and the successive oxidative dehydrogenation of the geminal glycol might contribute to NAc formation, thus providing an alternative pathway to the classical oxidation mechanism with generation of a radical species on the carbonyl and successive oxidation of this intermediate species with O_2. In order to clarify these aspects, we carried out experiments in function of contact time, and some tests by feeding directly NAl as well, both in the absence and in the presence of steam.

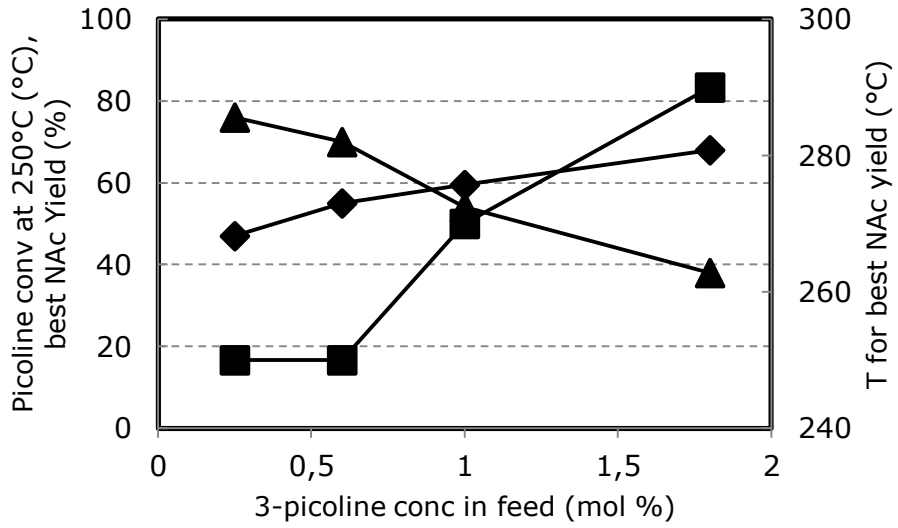

Figure 116. Effect of picoline concentration in the inlet feed on best NAc yield (◆), temperature at which the best NAc yield is achieved (■), and picoline conversion at 250°C (▲).Reaction conditions: feed composition (molar %): picoline/oxygen/steam/inert varied/16.6/24/remainder; contact time 2.0 s. Catalyst 20VTZ:

Figure 117 shows the effect of contact time, at 270°C. Results demonstrate that the formation of NAc occurs exclusively via NAl as the intermediate; in fact, selectivity to NAc extrapolated to nil conversion was equal to zero. NAc also underwent a consecutive combustion to CO_2; the latter compound, however, was also a primary product, and therefore it was also obtained by direct combustion of 3-picoline. All the other by-products were kinetically consecutive compounds; their selectivity extrapolated to nil conversion was zero, but it increased along with an increase of picoline conversion; therefore, they formed by oxidative degradation of NAl. An exception was cyanopyridine (CP), whose selectivity first increased, but then declined, an event which suggests a consecutive transformation of this compound also.

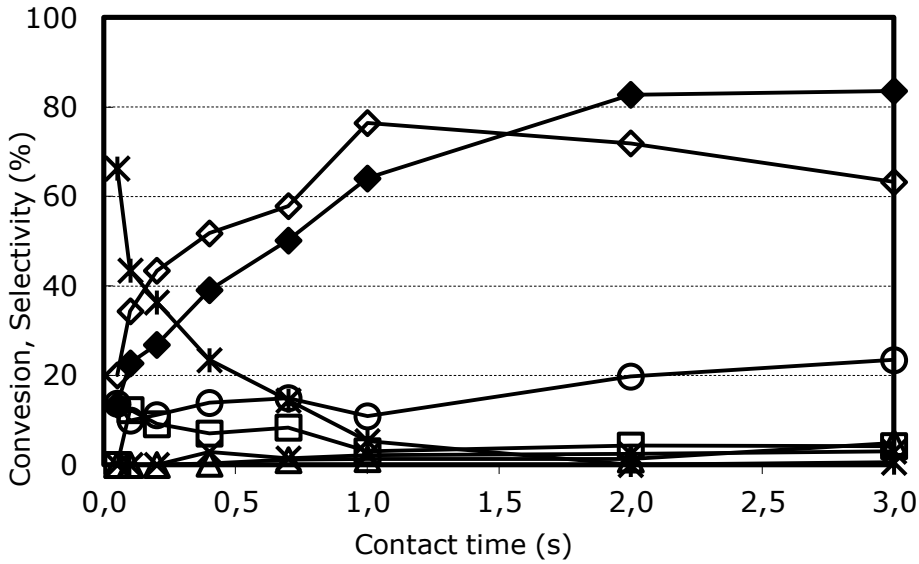

Figure 117. Effect of contact time on 3-picoline conversion and on yield to products. Reaction conditions: feed composition (molar %): picoline/oxygen/steam/inert 1.0/16.6/20.0/remainder; temperature 270°C. Symbols: picoline conversion (◆), yield to: nicotinic acid NAc (◇), nicotinic aldehyde NAl (✳), pyridine PY (△), cyanopyridine CP (□), CO (✕), and CO_2 (○). Catalyst 20VTZ.

Results of experiments carried out with NAl (nicotinic aldehyde) as the reactant are shown in figures 118 (without steam) and 119 (with steam). Results demonstrate that the aldehyde is very reactive (especially in the presence of steam); this explains the very low NAl yield generally observed in experiments with picoline, carried out with V_2O_5-based catalysts. Besides NAc, by-products were the same already observed from picoline. However, the selectivity to CO_2 was lower than that one from picoline, which supports the hypothesis above formulated that CO_2 also forms by direct combustion of picoline. It is also important to notice that selectivity to NAc was similar both in the presence and in the absence of steam (in both cases in the range 75-80%). This suggests that the presence of steam does not provide an alternative reaction pathway to NAc formation; the prevailing mechanism is likely the direct oxidation of the carbonyl moiety. The remarkable difference of conversion observed in the two cases can be ascribed, once again, to the role of steam of facilitating the desorption of adsorbed reactants and intermediates, thus increasing both the

availability of free sites deputed to the adsorption of reactants, and the TOF value as well.

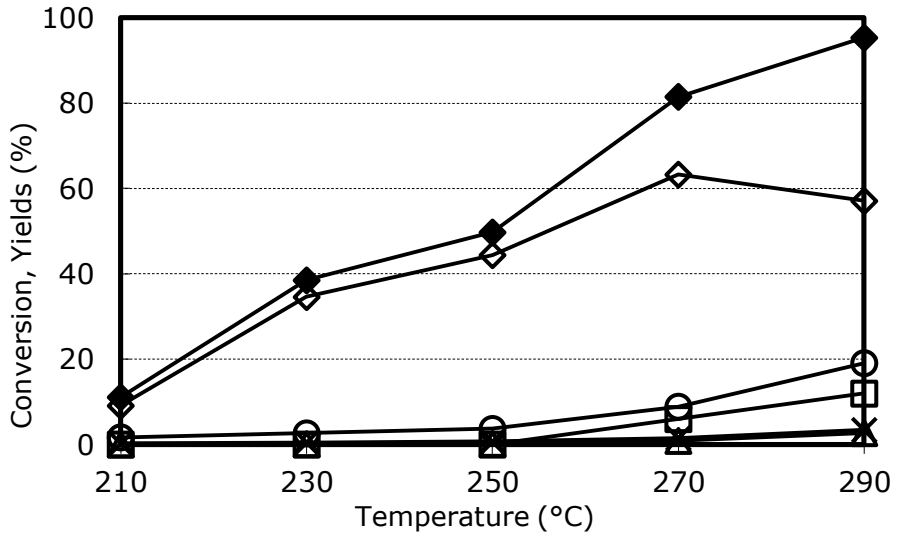

Figure 118. Effect of temperature on NAl (nicotinic aldehyde) conversion and on yield to products. Reaction conditions: feed composition (molar %): NAl/oxygen/steam/inert 1.0/20.8/0.0/remainder; contact time 2 s. Symbols: NAl conversion (◆), yield to: nicotinic acid NAc (◇),pyridine PY (△), cyanopyridine CP (□), CO (×), and CO2 (○). Catalyst 20VTZ.

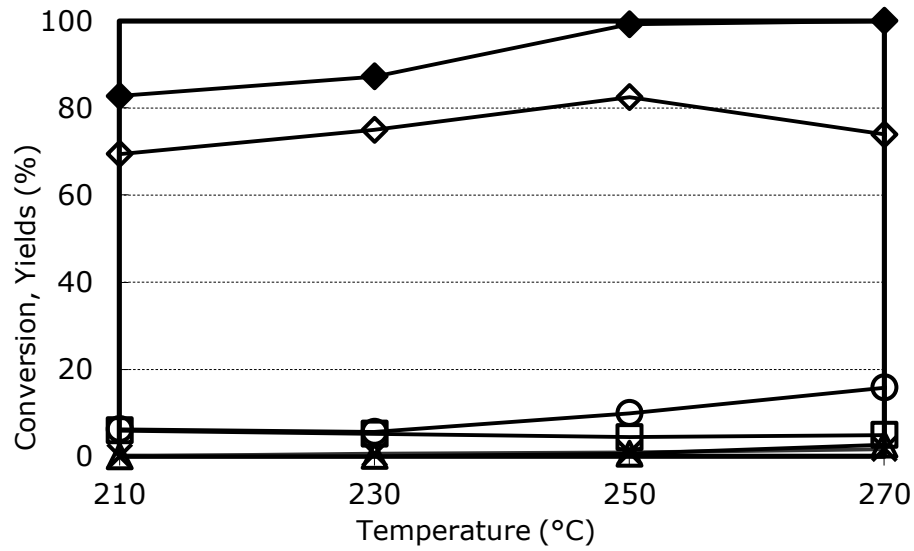

Figure 119. Effect of temperature on NAl (nicotinic aldehyde) conversion and on yield to products. Reaction conditions: feed composition (molar %): NAl/oxygen/steam/inert 1.0/16.6/20.0/remainder; contact time 2 s. Symbols: NAl conversion (◆), yield to: nicotinic acid NAc (◇), pyridine PY (△), cyanopyridine CP (□), CO (×), and CO2 (○). Catalyst 20VTZ.

A final experiment was carried to check for the stability of the catalyst (short-term lifetime test). Results are plotted in figure 120; we used conditions at which NAc yield recorded for the fresh catalyst was 59.5%, with 3-picoline conversion 83.5%. We first stabilised the catalyst for a few hours, and then we started to record the performance; an initial decline of conversion and NAc yield was shown. Then, NAc yield stabilised at ca 51%, with picoline conversion at 67-69%. We then carried out an in-situ regeneration treatment with air for 3 h at 450°C, and we noticed an immediate recovery of the catalytic behaviour, with turned out to be closer to that one of the fresh catalyst.

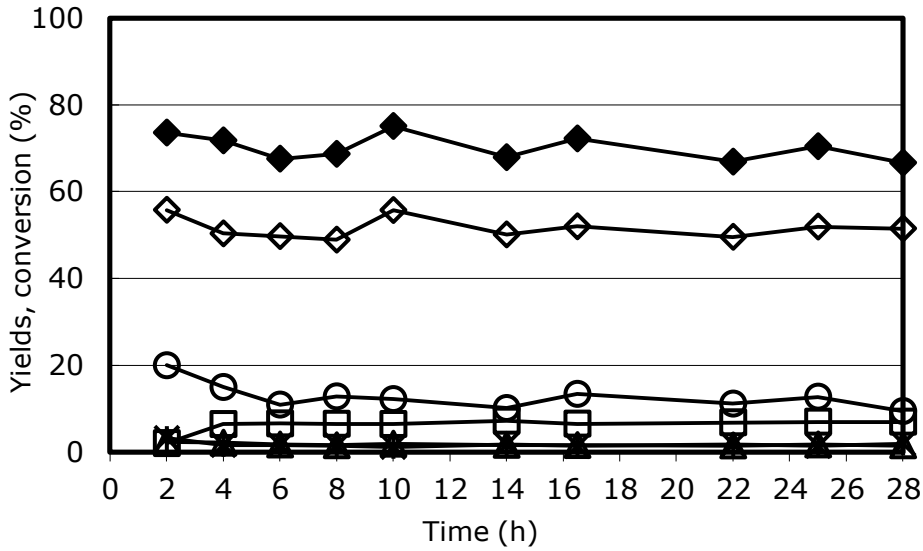

Figure 120. Effect of time-on-stream on 3-picoline conversion and on yield to products. Reaction conditions: feed composition (molar %): picoline/oxygen/steam/inert 1.0/15.0/20.0/remainder; contact time 2.0 s, temperature 270°C. Symbols: picoline conversion (◆), yield to: nicotinic acid NAc (◇), nicotinic aldehyde NAl (✳), pyridine PY (△), cyanopyridine CP (□), CO (✕), and CO_2 (○). Catalyst 20VTZ. The increase of conversion and NAc yield observed after 8 h reaction time was due to the fact that during the night the reaction was stopped and the hot catalyst was left under N_2 stream.

In conclusion, the catalyst made of V_2O_5 supported over ZrO_2-TiO_2 offers some advantages compared to the V_2O_5/ZrO_2 catalyst. The main one is that due to the better heat-conductive properties of the support, it presents fewer problems associated to heat transfer. This allows to operate with a

higher-surface area support, which is less prone to undergo surface saturation effects due to reactant adsorption; thus it seems that even the use of relatively high picoline partial pressures in feed is not detrimental for catalytic performance, provided an excess of O_2 is furnished. This finally leads to a slightly better yield to NAc. Also with this catalyst type the best performance is obtained under picoline-lean conditions, with a large excess of O_2 and H_2O in feed; however, even under picoline-rich conditions it is possible, through a proper control of the picoline/O_2 ratio, to achieve good catalytic performance.

Productivity was still an issue for the process. Therefore we tried to compare the best results obtained with catalysts used during my research work, with performances of catalysts reported in the literature. Various performance indicators were calculated in order to have a complete and fair comparison.

Catalyst [ref]	wt %V_2O_5	As_s (m^2/g)	T (°C)	3-pic (%)	O_2/3-pic	H_2O/3-pic	τ (s)	N° Vatom/nm^2
V_2O_5/TiO_2 [32]	20	29	250	0.4	40	70	1.5	45.7
V_2O_5/TiO_2 [38]	19	40	265	0.42	35	70	1.44	31.5
2VZC [figure 56]	2	4.2	330	0.24	17.5	333	1.2	31.5
2VZC [figure 72]	2	4.2	330	0.5	14	133	1.4	31.5
20VTZ [figure 106]	20	21	270	0.24	17.5	333	1.2	63.1

Table 7a. Reaction conditions for catalysts showing the best results in literature and our best results.

Catalyst [ref]	Conv (%)	NAc Sel (%)	NAc Yield (%)	WHSV (h^{-1},pic)	Productivity (gNAc/gcat*h)	Vanadium based productivity (gNAc/gV_2O_5*h)	Rate of NA production (mol/m^2*s)	TOF (s^{-1})
V_2O_5/TiO_2 [32]	91	93.7	85.3	0.0365	0.0412	0.2058	$3.20*10^{-9}$	$4.22*10^{-5}$
V_2O_5/TiO_2 [38]	98	98	96.0	0.0400	0.0508	0.2673	$2.86*10^{-9}$	$5.48*10^{-5}$
2-VZC [figure 56]	93.2	88.5	82.5	0.0137	0.0149	0.7464	$8.02*10^{-9}$	$1.53*10^{-4}$
2-VZC [figure 72]	80.5	86.0	69.2	0.0249	0.0228	1.1379	$1.22*10^{-8}$	$2.33*10^{-4}$
7VZC-TT [figure 106]	98.7	86.1	85.7	0.0180	0.0202	0.1011	$2.17*10^{-9}$	$2.07*10^{-5}$

Table 7b. Performance indicators for catalysts showing the best results in literature and our best results.

Table 7a summarizes the operative conditions used for performance indicators reported in table 7b.

In regard to NAc yield, we can see how results obtained in this thesis are comparable to those reported by Andruskevich et al. [32], while the outstanding yield reported in [38] was not achieved.

Comparison of productivity in term of WHSV and of $g_{NAc}/(g_{CAT}*h)$ are ambiguous because of the higher bulk density of zirconia-supported catalysts compared to those based on titania support; a fairer comparison can be done by taking into account either productivity based on Vanadium oxide content or TOF, calculated under the hypothesis that all of the Vanadium atoms are available for the reaction. In this case it is shown that zirconia-based catalysts were more active. The major drawback of zirconia as a support probably lies in its low thermal conductivity, which might cause surface overheating and finally result in a slight increase in selectivity to deep oxidation products.

6 The oxidation of 3-picoline to nicotinic acid with vanadyl pyrophosphate catalyst

In the search for a new and better catalyst for the oxidation of 3-picoline, we decided to test the reactivity of vanadyl pyrophosphate (VPP), the industrial catalyst for *n*-butane oxidation to maleic anhydride. The main reason for this choice is that catalyst acidity is claimed to play an important role in the reaction (see the section dealing with literature analysis), and VPP is well known to possess intrinsic acidity because of the presence of P-OH pending moieties on the surface. Moreover, VPP is one of the best performing catalysts in gas-phase selective oxidations.

The effect of temperature on picoline conversion and selectivity to products is shown in figure 121.

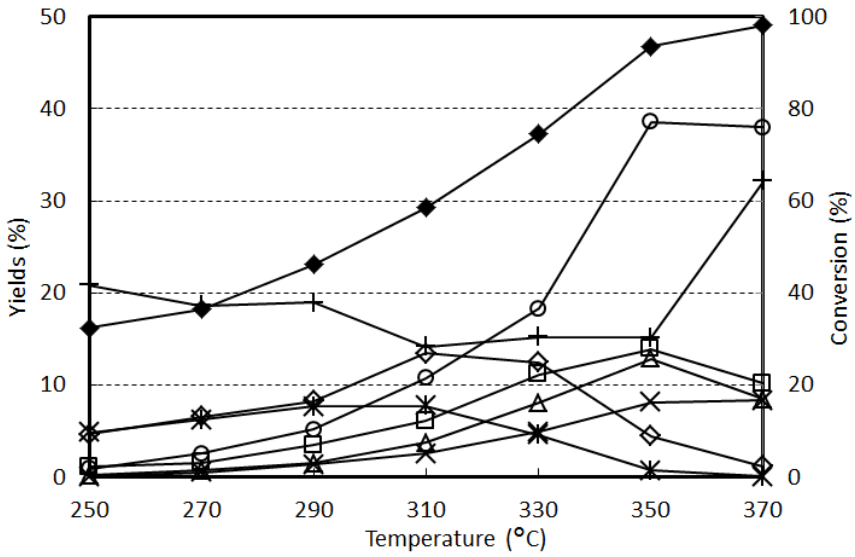

Figure 121. Effect of temperature on 3-picoline conversion and on yield to products. Reaction conditions: feed composition (molar %): picoline/oxygen/inert 1/20/79; contact time 2 s. Symbols: picoline conversion (◆), selectivity to: nicotinic acid (◇), nicotinic aldehyde (✳), pyridine (△), cyanopyridine (□), CO (×), CO_2 (○), and heavy compounds (+). Catalyst VPP.

Experiments were first carried out using 1.0 mol% of picoline in air, at contact time of 2 s; in fact, these are typical conditions for VPP when used as catalyst

for gas-phase oxidations; thus, we decided not to co-feed steam, because it is known that VPP under certain circumstances may undergo hydrolysis of V-O-P moieties and hydrothermal recrystallization phenomena which may have detrimental effect on its catalytic performance.

Also with this catalyst type, main products of the reaction were nicotinic acid (NAc), nicotinaldehyde (NAl), pyridine (PY), cyanopyridine (CP), CO and CO_2; traces of nicotinamide and bipyridine were also found, with selectivity which however was far less than 0.2%.

Figure 121 shows that the C balance at low temperature was very low, close to 30%, and improved when the temperature was raised, but was never better than 70%. Indeed, heavy compounds were formed, which accumulated on the catalyst surface but also deposited on the reactor walls. NAc maximum yield was 14% only, at 310°C; at lower temperatures, NAl also formed, with traces of CO and CO_2, whereas at temperatures higher than 310°C CO_2 became the predominant product, but also other by-products were formed in considerable amount (CP, PY and CO).

The formation of heavy compounds, especially at low temperatures, is attributable to the strong adsorptive interaction of reactants and products with the catalyst surface, due to both the high boiling temperature of these compounds and the acidity of the VPP; the protonation of the N atom in the pyridine ring may be responsible for the strong adsorption of the reactant. Thus, it may be concluded that very likely steam is necessary also with this catalyst type.

We repeated the experiment by co-feeding 20 mol% water; results are plotted in figure 122.

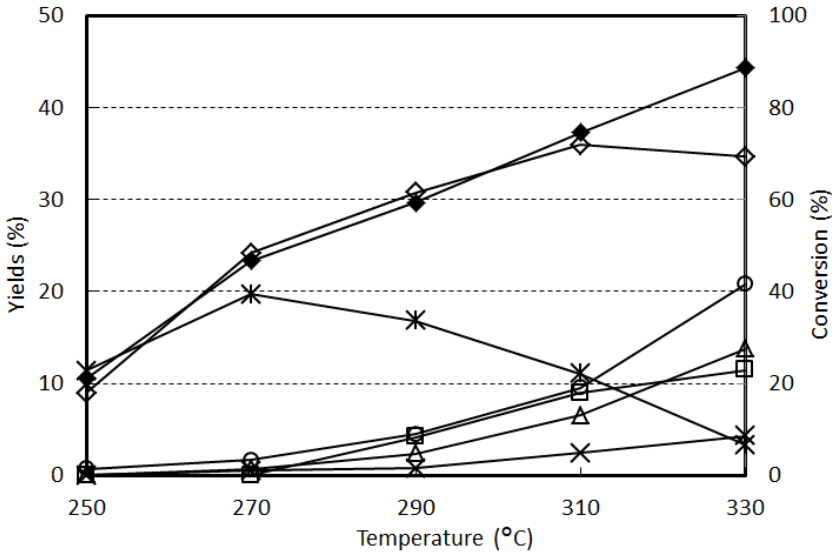

Figure 122. Effect of temperature on 3-picoline conversion and on yield to products. Reaction conditions: feed composition (molar %): picoline/oxygen/steam/inert 1/20/20/59; contact time 2 s. Symbols: picoline conversion (◆), selectivity to: nicotinic acid (◇), nicotinic aldehyde (✳), pyridine (△), cyanopyridine (□), CO (✕), and CO_2 (○). Catalyst VPP.

It is shown that in the presence of steam catalytic performance was considerably improved; best yield to NAc now was 36%, again at 310°C, whereas the selectivity to the other by-products was similar to that observed in the absence of steam. However, the more important effect was on C balance, which was close to 100% over the entire range of temperature investigated, with no formation of heavy compounds. It is also important to note that picoline conversion was greater in the presence of water (for example, at 310°C it was 75%, but only 60% in the absence of water at the same conditions). Overall, the role of water was not only to facilitate the desorption of NAc while keeping a clean surface and facilitate the adsorption of picoline, but also to limit the consecutive unselective transformation of either NAc or NAl to heavier condensation compounds, and accelerate the consecutive oxidation of NAl to NAc.

Figure 123 plots the effect of contact time on catalytic performance (picoline conversion and selectivity to products), for experiments carried out with co-

feeding of H_2O, at 310°C; figure 124 plots the results obtained in the absence of steam.

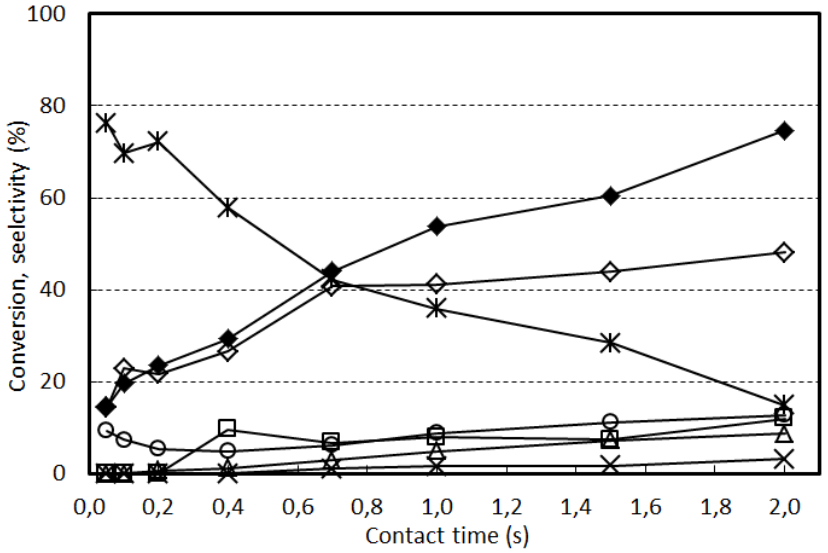

Figure 123. Effect of contact time on 3-picoline conversion and on selectivity to products. Reaction conditions: feed composition (molar %): picoline/oxygen/steam/inert 1/20/20/59; temperature 310°C. Symbols: picoline conversion (◆), selectivity to: nicotinic acid (◇), nicotinic aldehyde (✳), pyridine (△), cyanopyridine (□), CO (✕), and CO_2 (○). Catalyst VPP.

The kinetic relationship between NAl and NAc is evident; the aldehyde was the main primary product, and its selectivity rapidly declined when the contact time was increased, with a corresponding increase of selectivity to NAc and, to a minor extent, to the other by-products. CO_2 was also a primary product, in fact its selectivity extrapolated to zero contact time was higher than zero. In the case of experiments carried out without steam (figure 124), some important differences were shown. In fact, the main primary products were heavy compounds (initial C-loss was around 70%), an event which suggests that at low picoline conversion, the fraction of catalyst surface covered by the adsorbed reactant is very high, and that under these conditions adsorbed species are mainly transformed into heavy compounds. The increase of contact time and of picoline conversion led to a progressive decline of the C-loss value, and a corresponding increase of selectivity to all products, including NAc. These

experiments confirm that under the conditions employed the saturation of the catalyst surface is responsible for the low selectivity to NAc; this phenomenon may be limited by using either high temperature or high contact time, conditions which however are also leading to the formation of by-products derived from oxidative degradation. Conversely, more efficient is the use of co-fed steam, which allows to achieve higher selectivity to NAc even under relatively milder conditions.

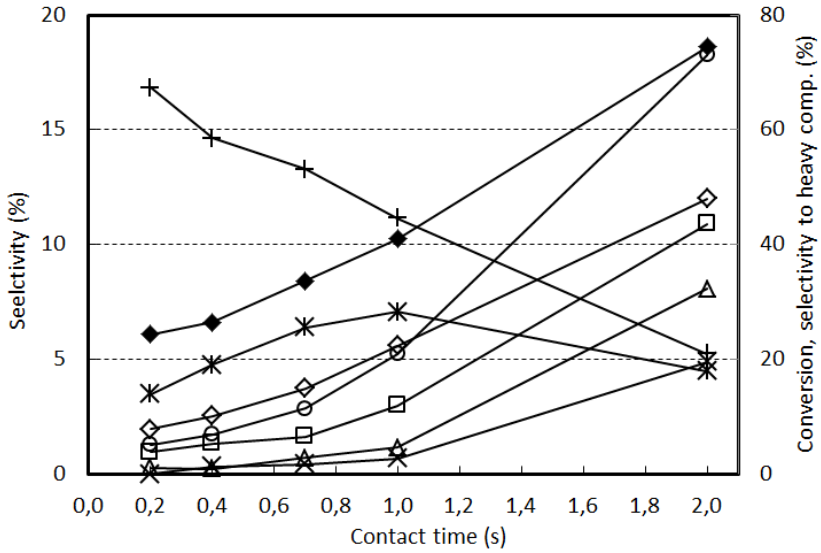

Figure 124. Effect of contact time on 3-picoline conversion and on selectivity to products. Reaction conditions: feed composition (molar %): picoline/oxygen/inert 1/20/79; temperature 330°C. Symbols: picoline conversion (◆), selectivity to: nicotinic acid (◇), nicotinic aldehyde (✳), pyridine (△), cyanopyridine (□), CO (×), CO_2 (○) and heavy compounds (+). Catalyst VPP.

We decided to carry out the reaction under conditions which in principle should be more favourable for NAc formation: lower molar fraction of picoline and higher molar fraction of steam in the reactor feed (picoline-lean conditions).

Figure 125 shows the effect of temperature with 0.2 mol% picoline and 7% O_2 (in order to keep the same picoline/O_2 ratio as for previous experiments), and 67% steam (contact time 1.4 s). At these conditions, selectivity to NAc was greatly enhanced; max yield of 59% was obtained at 350°C, with low yields to by-products.

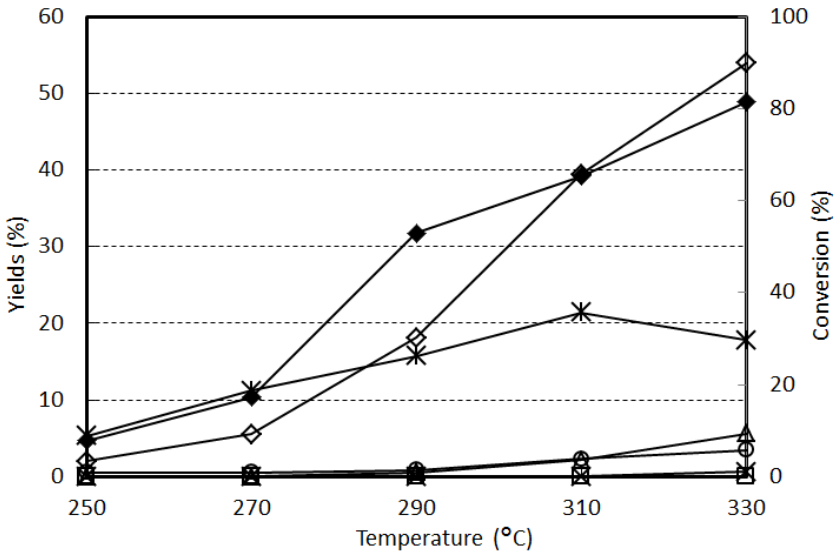

Figure 125. Effect of temperature on 3-picoline conversion and on yield to products. Reaction conditions: feed composition (molar %): picoline/oxygen/steam/inert 0.2/7/67/25.8; contact time 1.4 s. Symbols: picoline conversion (◆), selectivity to: nicotinic acid (◇), nicotinic aldehyde (✳), pyridine (△), cyanopyridine (□), CO (✕), and CO_2 (○). Catalyst VPP.

The max yield to NAc experimentally observed, even under the optimised reaction conditions, was lower than that reported in literature for catalysts based on V_2O_5/TiO_2, and of that one obtained with our V_2O_5/ZrO_2 catalysts. The comparatively lower performance of the VPP catalyst is attributable to the poor catalyst efficiency in the consecutive oxidation of NAl to NAc; in fact, results show that the selectivity to NAl still was relatively high even at high contact time or temperature, when the conversion of picoline was over 60-70%. With supported V_2O_5 catalyst, conversely, the efficient transformation of the intermediate NAl to NAc led to an excellent selectivity to the latter compound; with these catalyst types, the selectivity to NAl at high picoline conversion was virtually zero.

This hypothesis was confirmed by experiments carried out by feeding directly NAl; results are reported in figure 126 (conditions: 0.2 mol% Nal, O_2 7%, 67% steam, contact time 1.4 s). It is shown that the reactivity of the aldehyde was not much different from that one of picoline, under the same experimental

conditions, which is an unexpected result; even though NAc is the prevailing product, considerable yields to CO_2, CO and pyridine were also observed.

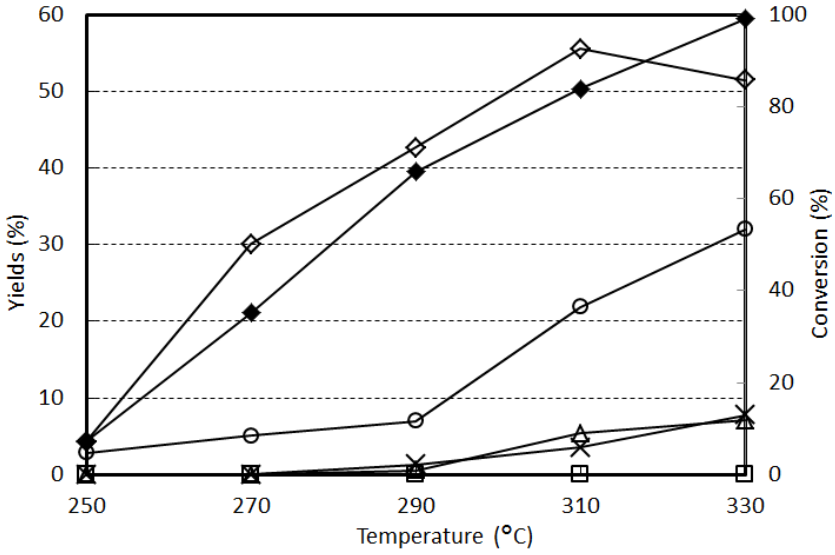

Figure 126. Effect of temperature on nicotinic aldehyde conversion and on yield to products. Reaction conditions: feed composition (molar %): NAl/oxygen/steam/inert 0.2/7/67/25.8; contact time 1.4 s. Symbols: nicotinic aldehyde conversion (◆), selectivity to: nicotinic acid (◇), pyridine (△), cyanopyridine (□), CO (✕), and CO2 (○). Catalyst VPP.

Concluding, VPP is not a good catalyst for 3-picoline oxidation to nicotinic acid; main drawbacks are its intrinsic acidity, which is clearly excessive for this reaction, and its scarce activity in the transformation of the intermediate aldehyde into nicotinic acid.

6.1 VPP catalyst characterization

Raman spectroscopy was used to study catalyst modifications occurring under reaction conditions.

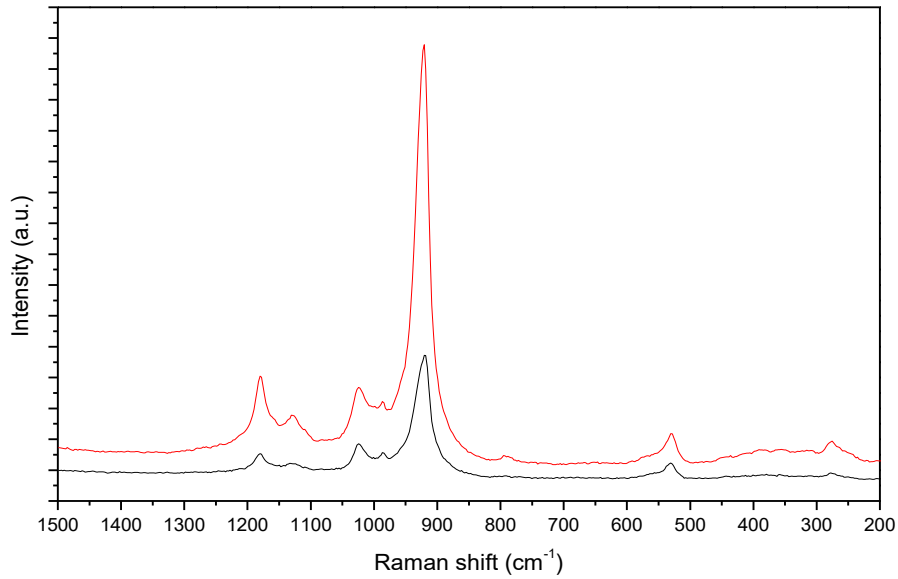

Figure 127. Raman spectra of fresh VPP catalyst; powder = red line, pressed powder = black line.

Spectra collected at r.t. for the catalyst in the powder form and in the form of granules (obtained by pressing the powder), clearly show that the VPP structure was not affected by the procedure used for granules preparation (figure 127). In both cases, bands shown correspond to those typical of the VPP. After reaction at picoline-lean conditions, Raman spectra were collected at r.t. focusing the laser beam over different particles (figure 128); these spectra show that used catalyst particles were not homogeneous. Blue and red spectra were similar to that one of fresh VPP, with bands at 1183 cm^{-1}, 1133 cm^{-1}, 1042 cm^{-1} and 924 cm^{-1}. The purple spectrum is attributable to the VPO_4 compound, with bands at 1060 cm^{-1}, 985 cm^{-1},886 cm^{-1}, 642 cm^{-1}, 426 cm^{-1} and 284 cm^{-1} [166]. The black spectrum showed bands attributable to both compounds above mentioned, but those of VPP were more intense.

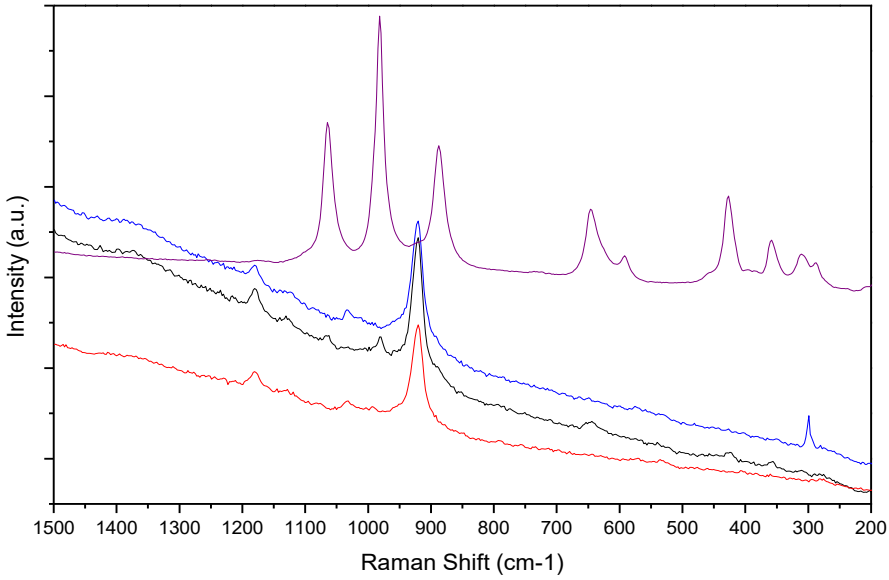

Figure 128. Raman spectra of spent VPP catalyst, taken by focusing the laser beam over different particles.

The presence of the V^{3+} phosphate demonstrates that the conditions used were "reducing" for the VPP; despite the large excess of oxygen present in the inlet feed, the very strong interaction of picoline with the VPP led to catalyst over reduction and generation of the V^{3+} compound, which could no longer be reoxidised.

7 Conclusions

The research work carried out during my PhD thesis was aimed at investigating new processes for nicotinic acid production.

The first part of the work was focused on 2-methylglutaronitrile cyclization; a catalyst screening study was carried out using different operative conditions and catalyst types. We concluded that radicalic fragmentation of the reactant severely affected the process performance in the absence of oxygen, while in the presence of oxygen complete oxidation prevailed. In any case, the desired product was not formed. Oxidative demethylation to glutaronitrile was observed, but yield achieved was too low to be of interest for industrial application.

Afterwards, attention was focused on acetaldehyde/acetonitrile condensation to picolines. A small amount of 2- and 4-picoline was produced when acetaldehyde was made react with acetonitrile, but again yields were very low. When formaldehyde was added in order to produce 3-picoline, the very high reactivity of the aldehydes compared to acetonitrile led to the formation of several by-products but no heterocycle compound was formed.

Oxidation of picoline to niacin has been the main topic of my research work; a new class of catalysts made of V_2O_5/ZrO_2 has been proposed for this reaction. This catalyst type was more active than reference catalysts reported in the literature, but yield to nicotinic acid was lower than the best literature values.

Vanadium oxide content and support surface area were found to be important parameters affecting catalysts behaviour; best performance was shown by catalysts characterised by very low surface area and low Vanadium oxide loading.

Conclusions

Highly diluted inlet feed, the so-called picoline-lean conditions, had to be used in order to obtain a selective process; more concentrated feedstock resulted in catalyst surface saturation, even though the use of a large excess of both steam and oxygen allowed to decrease the saturation effect. Steam facilitated the desorption of products, while the excess oxygen was needed to permit Vanadium reoxidation. Moreover, the poor heat conductivity of zirconia posed serious limitations to catalyst performance because of overheating effects and heat-transfer limitations.

XRD and Raman techniques were used for the characterization of catalysts. Changes of catalyst chemical-physical features occurred during reaction, as revealed by the characterisation of used catalysts. In some cases, the presence of ZrV_2O_7 was observed in spent catalysts; in-situ Raman experiments revealed the reversible formation of this phase at moderate temperatures, and its irreversible formation after treatment at temperatures higher than 400°C. However, the amount and stability of Zr pyrovanadate were greatly affected by catalyst features such as Vanadium oxide loading and surface area.

A catalyst made of ZrV_2O_7/ZrO_2 was found to be less active than V_2O_5/ZrO_2, but highly selective towards nicotinic aldehyde at low temperature.

A catalyst made of V_2O_5 supported on ZrO_2-TiO_2 was prepared in order to overcome problems related to heat dispersion limitations. Yield to niacin was slightly higher compared to that one achieved with the V_2O_5/ZrO_2 catalyst.

A vanadyl pyrophosphate catalyst was also tested, but unfortunately its high acidity and scarce activity in the transformation of the intermediate aldehyde into nicotinic acid limited its performance.

8 Ringraziamenti

Prima di tutto è doveroso un sentito ringraziamento al prof Fabrizio Cavani, che tanto ha fatto nei quattro anni precedenti e che si è superato nell'impegno che ha profuso insieme a me in questa tesi che corona tre anni sicuramente impegnativi da un punto di vista fisico e morale ma molto ripaganti per tutto ciò che ho ricevuto.

Grazie anche a tutti i colleghi di laboratorio perchè sanno essere soprattutto amici, per le discussioni "scientifiche" davanti a youtube e soprattutto per le pause pranzo in biblioteca incluso il book fotografico sul divano. Ringrazio in particolare Mugno che per sfortuna sua ha condiviso con me la scrivania e più camere ai congressi fino a farmi diventare la Sig.ra Malmusi.

Ci sono tanti amici da ringraziare, per primo Lele, compagno di seratine, seratone e seratacce; che mi ha accompagnato durante i duri anni del dottorato insegnandomi tante cose, tra cui anche un mestiere: il tassista.

Nonostante i momenti di fallimento generalizzato un grazie di cuore va ai decrescita o one direction che dir si voglia, Ciok, Fantu, Rolli, e Zac. Per i momenti di svago, le discussioni serie, le produzioni artigianali,il passatello, gli igloo, maxi seizure e tutto quello che mi hanno trasmesso in questi anni. Grazie al Supra compagno di tante serate in cantina.

Un pensiero va anche a Lesy in Festa e a tutti coloro che la rendono possibile perchè ogni anno continua a mostrare la parte più bella delle persone che collaborano e fa sentire tutti uniti ed importanti.

Dopo questi tre anni bisogna ricordare anche i tre mesi trascorsi a Rostock che mi hanno insegnato quanto è bello partire e l'indipendenza ma anche quanto è bello tornare a casa. Grazie anche alle mie gambe che mi hanno supportato durante il ritorno da Monaco e alla bicicletta che insegna tante cose sui propri limiti e libertà.

Ringraziamenti

Con questa tesi si chiude un periodo di tre anni molto intenso ma iniziato idealmente ventidue anni fa, per questo ho tenuto per ultima la mia famiglia perchè merita un posto di rilievo, sono loro che hanno sempre fatto di tutto e di più per mettermi nelle migliori condizioni per studiare o far ricerca, seguendo ed assecondando il mio percorso che non è fatto solo di studi ma anche di crescita personale.

Grazie a tutti!!!!

9 References

[1] Portney, Paul R., and Robert N. Stavins, eds., *Public Policies for Environmental Protection, 2nd ed*. (Washington: RFF Press, 2000).

[2] Tol, Richard S. J., "The Marginal Damage Costs of Carbon Dioxide Emissions: An Assessment of the Uncertainties, "Energy Policy, vol. 33, pp. 2064-74, 2005.

[3] Cox, Michael; Lehninger, Albert L; Nelson, David R. (2000). Lehninger principles of biochemistry. New York: Worth Publishers. ISBN 1-57259-153-6.

[4] Frostig, J. P., and Spies, T. D.: *The initial syndrome of pellagra and associated deficiency diseases*. American Journal of Medical Science 199:268, 1940

[5] E. Kodicek, Nutr. Dieta 4, 109 (1962)

[6]Prakash R, Gandotra S, Singh LK, Das B, Lakra A (2008). "Rapid resolution of delusional parasitosis in pellagra with niacin augmentation therapy". General Hospital Psychiatry 30 (6): 581–4

[7]Bruckert E, Labreuche J, Amarenco P (2010). "Meta-analysis of the effect of nicotinic acid alone or in combination on cardiovascular events and atherosclerosis". Atherosclerosis210 (2): 353–61

[8] Duggal JK, Singh M, Attri N, Singh PP, Ahmed N, Pahwa S, Molnar J, Singh S, Khosla S, Arora R (2010). "Effect of niacin therapy on cardiovascular outcomes in patients with coronary artery disease". Journal of cardiovascular pharmacology and therapeutics 15 (2): 158–66

[9] Gille A, Bodor ET, Ahmed K, Offermanns S (2008). "Nicotinic acid: Pharmacological effects and mechanisms of action". Annual review of pharmacology and toxicology 48 (1): 79–106

[10] Wanders D, Judd RL (2011). "Future of GPR109A agonists in the treatment of dyslipidaemia". Diabetes, obesity & metabolism **13** (8): 685–91

[11] Cavani F, Centi G, Perathoner S, Trifirò F, Sustainable Industrial Chemistry (2009), ISBN: 978-3-527-62912-1

[12]W. Ramsay, Ber. Dtsch. Chem. Ges. 10 (1877) 736

[13]A. Hanzsch, Justus Liebigs Ann. Chem. 215 (1882) 72.

[14] A. E. Chichibabin, Zh. Russ. Fiz. Khim. O-va. 37 (1905) 1229

[15] R. Chuck, Applied Catalysis A: General 280 (2005) 75-82

[16] Mc. Ateer C. Calvin J. Davis R. WO 98/32737 30/07/1998 to Reilly industries, INC

[17] W. Rebafka, G. Heilen, K. Halbritter, W. Franzischka, US 4,521,602 A1985.06.04 (1985) to BASF AG, Germany

[18] S. Lanini, R. Prins, Appl. Catal. A, 1996, 137, 287-306

[19] S. Lanini, R. Prins, Appl. Catal. A, 1996, 137, 307-326

[20] R. Di Cosimo, J. D. Burrington, R. K. Grasselli, US 4,721,789 A1988.01.26 (1988) To The Standard Oil Company, USA

[21]Y. Ishii, T. Nakano, S. Hirai, JP2,001,253,838 A2001.09.18 (2001) To Daicel Chemical Industries, Ltd. Japan

[22]H. Watanabe, S. Hirai, M. Terada,
JP2,002,053,556 A2002.02.19 (2002) To Daicel Chemical Industries, Ltd. Japan

[23] T. Hashimoto, K. Nakamura, M. Takagawa, JP 09,202,773 A1997.08.05 (1997), to Mitsubishi Gas Chemical Co. Inc. Japan

[24]T. Hashimoto, K. Nakamura, M. Takagawa, JP 09,202,772 A1997.08.05 (1997), to Mitsubishi Gas Chemical Co. Inc. Japan

[25]T. Hashimoto, K. Nakamura, M. Takagawa, JP 08,311,030 A1996.11.26 (1996), to Mitsubishi Gas Chemical Co. Inc. Japan

[26]T. Hashimoto, K. Nakamura, M. Takagawa, JP 08,311,031 A1996.11.26 (1996), to Mitsubishi Gas Chemical Co. Inc. Japan

[27] M. Hatanaka, N.Tanaka, WO 9,305,022 A1993.03.18 (1993), to Nissan Chemical Industries, Ltd. Japan

[28] Y. Asamidori, I. Hashiba, S. Takigawa, JP 07,233,150 A1995.09.05 (1995), to Nissan Chemical Industries, Ltd. Japan

[29] Y. Asamidori, I. Hashiba, S. Takigawa, Jpn Patent 94,26,603 (1994), to Nissan Chem. Ind. Ltd., Japan

[30] F. E. Cislak, W. R. Wheeler, GB 563274 A1944.08.08 (1944), to Reilly Tar & Chemical Corporation, USA

[31] R. J. Chuck, U. Zacher, EP 919,548 A11999.06.02 (1999), to Lonza AG, Switzerland

[32] E. M. Alkaeva, T. V. Andrushkevich, G. A. Zenkovets, M. G. Makarenko, WO9,520,577 A11995.08.03 (1995), to Institut Kataliza Imeni G. K. Boreskova Sibirskogo, Russia

[33] B. V. Suvorov, A. D. Kagarlitskii, T. A. Afanas'eva, I. I.Kan, chem. Of heterocyclic compounds 1969, 5(6), 858-860

[34] R. Prasad, A. K. Kar, Ind. Eng. Chem. Process Des. Dev. 1976, 15(1), 170-175

[35] S. Lars, T. Andersson, S. Järås, J. Catal. 1980, 64, 51-67

[36] S. Järås, S. T. Lundin J. Appl. Chem. Biothechnol. 1977, 27, 499-509

[37] S. T. Lundin, S. Järås, DE 2,647,712 1976, to Bofors AB, Germany

[38] D. Heinz, W Hoelderich, S. Krill, W. Boeck, K. Huthmacher, DE 19,839,559 A12000.03.02 (2000), to Degussa-Huels AG, Germany

[39] T. V. Andrushkevich, B. S. Bal'zhinimaev, V. N. Kashkin, V. B. Nakrokin, E. V. Ovchinnikova, I. A. Zolotarskii, RU 2,371,247 (2009), to Bor Inst. of Catalysis

[40] C. Lu, C. Lee, S. Hsiung, EP 1,584,618 (2005), to Chang Chun Petrochemical Co.

[41] W. Yuan, H. Lu, B. Zhang, Y. Chen, Chinese J. Molecular Catal. 2011, 25 (4), 322-327

[42] Z. Song, Z. Matsushita, T. Shishido, K. Takehira, J. Catal 2003, 218, 32-41

[43] T. Shishido, Z. Song, E. Kadowaki, Y. Wang, K. Takehira, Appl. Catal. A 2003, 239, 287-296

[44] T. Shishido, Z. Song, T. Matsushita, K. Takaki, K. Takehira, Phys. Chem. Chem. Phys. 2003, 5, 2710-2718

[45] P. V. Vorobyev, L. I. Saurambaeva, T. P. Mikhailovskaya. Rus. J. of Gen. Chem. 2013, 83 (5), 972-978

[46] P. V. Vorobyev, L. I. Saurambaeva, T. P. Mikhailovskaya, O. K. Yugay, A. P. Serebryanskaya, I. A. Shlygina, Rus. J. of Appl. Chem. 2014, 87 (7), 887-894

[47] A. Martin, Topics in Catalysis 2004, 29 (3-4), 201-206

[48] T. V. Andrushkevich, Catal. Rev. 1993, 35 (2), 213-259

[49] T. V. Andrushkevich, Kinet. Catal. 1997 38 (2), 266-276

[50] V. M. Bondareva, E. V. Ovchinnikova, T. V. Andrushkevich, React. Kinet. Catal. 2008, 93 (2), 327-336

[51] B. Grzybowska-Swierkosz, Appl. Catal. A 1997, 157, 263-310

[52] B. M. Weckhuysen, D. E. Keller, Catal. Today 2003, 218, 25-46

[53] G. C. Bond, Appl. Catal. A 1997, 157, 91-103

[54] G. Centi, Appl. Catal. A 1996, 147 (2,3), 267-298

[55] M. Jose, N. Lopez, Topics Catal. 2006, 41 (1-4), 3-15

[56] G. C. Bond, S. F. Tahir, Appl Catal A 1991, 71, 1-31

[57] D. A. Bulushev, F. Rainone, F. Kiwi-Minsker, Catal. Today 2004, 96, 195-203

[58] G. Ya. Popova, T. V. Andrushkevich, E. V. Semionova, E. V. Chesalov, L. S. Dovlitova, V. A. Rogov, V. N. Parmon, J. Molecular Catal. A 2008, 283 (1-2), 146-152

[59] A. Andersson, J. O. Bovin, P. Walter, J. Catal 1986, 98, 204-220

[60] E. M. Al'kaeva, T. V. Andrushkevich, G. A. Zenkovets, G. N. Kryukova, S. V. Tsybulya, E. B. Burgina, Stud. In Surf. Sci. and Catalysis, 1997, 110, 939-946

[61] T. V. Andrushkevich, E. V. Ovchinnikova, Catal. Reviews: Sci. and Eng, 2012, 54, 399-436

[62] E. M. Al'kaeva, T. V. Andrushkevich, G. A. Zenkovets, G. N. Kryukova, S. V. Tsybulya, Catal. Today 2000, 61, 249-254

[63] D. Srinivas, W Höelderich, S. Kujath, M. H. Valkemberg, T. Raja, L. Saika, R. Hinze, V. Ramaswamy, Pure Appl. Chem. 2000, 72, 1273-1287

[64] E. V. Ovchinnikova, T. V. Andrushkevich, L. A. Shadrina React. Kinet. Catal. Lett. 2004, 82, 191-197

[65] E. V. Ovchinnikova, T. V. Andrushkevich, G. Y. Popova, V. D. Meshcheryakov, V. A. Chumachenko, Chem. Eng. J. 2009, 154, 60-68

[66]D. Heinz, W Höelderich, S. Krill, W. Boeck, K. Huthmacher J. Catal 2000, 192, 1-10

[67] Y. A. Chesalov, G. Y. Popova, G. B. Chernobay, T. V. Andrushkevich, React. Kinet. Catal. Lett. 2009, 98, 43-50

[68] A. Martin, B. Lücke, Catal. Today 200,57, 61-70

[69] Y. Zhang, A. Martin, H. Berndt, B. Lücke, M. Meisel, J. Molecular Catal. A 1997, 118, 205-214

[70] A. Martin, V. N. Kalevaru, B. Lücke, A. Brückner, Appl. Catal. A, 2008, 335, 196-203

[71] G. B. Chernobay, Y. A. Chesalov, V. P. Baltakhinov, G. Y. Popova, T. V. Andrushkevich, Catal. Today, 2011, 164, 58-61

[72] G. Y. Popova, T. V. Andrushkevich, Y. A. Chesalov, E. V. Ovchinnikova, React. Kinet. Catal. Lett. 2006, 87, 387-394

[73] V. I. Avdeev, V. N. Parmon, J. Phys. Chem C, 2009, 11(7), 2873-2880

[74] G. Deo, I. E. Wachs, J. Haber, Crit. Rev. Surf. Chem. 1994, 4, 141-187

[75] G. Centi, Appl. Catal A, 1996, 147 (2-3), 267-298

[76] G. Deo, I. E. Wachs, J. Catal. 1994, 146 (2), 323-334

[77] F. Arena, F. Frusteri, A. Parmaliana, Appl. Catal. A, 1999, 176 (2), 189-199

[78] G. Martra, F. Arena, S. Coluccia, F. Frusteri, A. Parmaliana, Catal. Today, 2000, 63 (2), 197-207

[79] E. V. Ovchinnikova, T. V. Andrushkevich, G. Y. Popova, V. D. Meshcheryakov, V. A. Chumachenko, Chem. Eng. J. 2009, 154, 60-68

[80] A. Andersson, S. T. Lundin, J. Catal. 1980, 65, 9-15

[81] K. Takehira, T. Shishido, Z. Song, T. Matsushita, T. Kavabata, K. Takaki, Catal. Today, 2004, 91-92, 7-11

[82] S. Luciani, N. Ballarini, F. CAvani, C. Cortelli, F. Cruzzolin, A. Frattini, R. Leanza, B. Panzacchi, Catal. Today, 2009, 142(3-4), 132-137

[83] B. Olthof, A. Khodakov, A. T. Bell, E. Iglesia, J. Phis. Chem. B, 2000, 104, 1516-1528

[84] V. A. Ranea, J. L. Vicente, E. E. Mola, P. Arnal, H. Thomas, L. Gamboro Surf. Sci. 2000, 463, 115-124

[85] J-M. Jehng, G. Deo, B. M. Weckhuysen, I. E. Wachs, J. Molecular Catal. A, 1996, 110, 41-54

[86] K. V. R. Chary, C. P. Kumar, T. Rajiah, C. S. Srikanth, J. Mol. Catal. A Chem. 2006, 258, 313–319

[87]K. V. R. Chary, C. P. Kumar, D. Naresh, T. Bhaskar, Y. Sakata, J. Mol. Catal. A Chem. 2006, 243, 149–157

[88] M. Sanati, a. Andersson, L. R. Wallenberg, B. Rebenstorf, Appl. Catal. A Gen. 1993, 106, 51–72

[89] B. Beck, M. Harth, N. G. Hamilton, C. Carrero, J. J. Uhlrich, A. Trunschke, J. Catal. 2012, 296, 120–131

[90] L. J. Lakshmi, Z. Ju, E. C. Alyea, Langmuir, 1999, 15, 3521–3528

[91]L. J. Burcham, G. Deo, X. Gao, I. E. Wachs, Top. Catal. 2000, 11-12, 85–100

[92] R. Z. Khaliullin, A. T. Bell, J. Phys. Chem. B. 2002, 106, 7832–7838

[93] P. R. Shah, I. Baldychev, J. M. Vohs, R. J. Gorte, Appl. Catal. A Gen. 2009, 361, 13–17

[94] A. Adamski, Z. Sojka, K. Dyrek, M. Che, G. Wendt, S. Albrecht, Langmuir 1999, 15, 5733–5741

[95] A. Khodakov, J. Yang, S. Su, E. Iglesia, A. Bell, J. Catal. 1998, 177, 343–351

[96] R. Sasikala, V. Sudarsan, T. Sakuntala, Jagannath, C. Sudakar, R. Naik, et al., Appl. Catal. A Gen. 2008, 350, 252–258

[97] S. T. Oyama, G. A. Somorjai, J. Phys. Chem. 1990, 94, 5022–5028

[98] R. Tesser, V. Maradei, M. Di Serio, E. Santacesaria, Ind. Eng. Chem. Res. 2004, 43, 1623–1633

[99] E. Santacesaria, A. Sorrentino, R. Tesser, M. Di Serio, A. Ruggiero, J. Mol. Catal. A Chem. 2003, 204-205, 617–627

[100] N. E. Quaranta, J. Soria, V. Cortés Corberán, J. L. G. Fierro, J. Catal. 1997, 171, 1–13

[101] J. M. Miller, L. J. Lakshmi, N. J. Ihasz, J. M. Miller, J. Mol. Catal. A Chem. 2001, 165, 199–209

[102] L. J. Lakshmi, Z. Ju, E. C. Alyea, Langmuir, 1999, 15, 3521–3528.

[103] A. Christodoulakis, M. Machli, A. A. Lemonidou, S. Boghosian, J. Catal. 2004, 222, 293–306.

[104] I. E. Wachs, J.-M. Jehng, G. Deo, B. M. Weckhuysen, V. V Guliants, J. B. Benziger, J. Catal. 1997, 170, 75–88

[105] G. Deo, I. E. Wachs, J. Phys. Chem. 1991, 95, 5889–5895

[106] H. Tian, E. I. Ross, I. E. Wachs, J. Phys. Chem. B. 2006, 110, 9593–9600

[107] D. I. Enache, E. Bordes, A. Ensuque, F. Bozon-Verduraz, Appl. Catal. A Gen. 2004, 278, 103–110

[108] D. I. Enache, E. Bordes-Richard, A. Ensuque, F. Bozon-Verduraz, Appl. Catal. A Gen. 2004, 278 93–102

[109] S.C. Su, A.T. Bell, J. Phys. Chem. B. 1998, 102, 7000–7007

[110] A. Chieregato, J.M. López Nieto, F. Cavani, Coord. Chem. Rev. 2015, 301-302, 3–23

[111] A. Caldarelli, M.A. Bañares, C. Cortelli, S. Luciani, F. Cavani, Catal. Sci. Technol. 2014, 4, 419–427.

[112] F. Cavani, J.H. Teles, ChemSusChem. 2009, 2, 508–34.

[113] I.E. Wachs, K. Routray, ACS Catal. 2012, 2, 1235–1246

[114] N. Ballarini, F. Cavani, C. Cortelli, S. Ligi, F. Pierelli, F. Trifirò, et al, Top. Catal. 2006, 38, 147–156

[115] F. Cavani, N. Ballarini, S. Luciani, Top. Catal. 2009, 52, 935–947

[116] N.F. Dummer, J.K. Bartley, G.J. Hutchings, Adv. Catal. 2011, 54, 189–247

[117] D. Lesser, G. Mestl, T. Turek, Appl. Catal. A Gen. 2016, 510, 1–10

[118] M. Eichelbaum, M. Hävecker, C. Heine, A.M. Wernbacher, F. Rosowski, A. Trunschke, et al., Angew. Chem. Int. Ed. Engl. 2015, 54, 2922–6

[119] A. Shekari, G.S. Patience, Can. J. Chem. Eng. 2013, 91, 291–301

[120] F. Cavani, D. De Santi, S. Luciani, A. Löfberg, E. Bordes-Richard, C. Cortelli, et al, Appl. Catal. A Gen. 2010, 376, 66–75

[121] F. Cavani, S. Luciani, E.D. Esposti, C. Cortelli, R. Leanza, Chemistry. 2010, 16, 1646–55

[122] N. Ballarini, F. Cavani, C. Cortelli, M. Ricotta, F. Rodeghiero, F. Trifiro, et al., Catal. Today. 2006, 117, 174–179

[123] G.J. Hutchings, J. Mater. Chem. 2004, 14, 3385

[124] J.T. Cleaves, G. Centi, Catal. Today. 1993, 16, 69–78

[125] G. Centi, Catal. Letters. 1993, 22, 53–66

[126] V.A. Zazhigalov, J. Haber, J. Stoch, B.D. Mikhajluk, A.I. Pyatnitskaya, G.A. Komashko, et al., Catal. Letters. 1996, 37, 95–99

[127] F. Cavani, A. Colombo, F. Giuntoli, E. Gobbi, F. Trifirò, P. Vazquez, Catal. Today. 1996, 32, 125–132

[128] F. Cavani, A. Colombo, F. Trifirò, M.T. Sananes Schulz, J.C. Volta, G.J. Hutchings, Catal. Letters. 1997, 43, 241–247

[129] G. Bignardi, F. Cavani, C. Cortelli, T. De Lucia, F. Pierelli, F. Trifirò, et al., J. Mol. Catal. A Chem. 2006, 244, 244–251

[130] J. Haber, J. Stoch, V.A. Zazhigalov, I. V. Bacherikova, E. V. Cheburakova, Pol. J. Chem. 2008, 82, 1839–1852

[131] G. Landi, L. Lisi, J.-C. Volta, J. Mol. Catal. A Chem. 2004, 222, 175–181

[132] G. Landi, L. Lisi, G. Russo, J. Mol. Catal. A Chem. 2005, 239, 172–179

[133] Y.H. Taufiq-Yap, C.S. Saw, R. Irmawati, Catal. Letters. 2005, 105, 103–110

[134] S. Ieda, S. Phiyanalinmat, S. Komai, T. Hattori, A. Satsuma, J. Catal. 2005, 236, 304–312

[135] Y. Zhang, A. Martin, H. Berndt, B. Lücke, J. Mol. Catal. A Chem. 1997,118, 205–214

[136] A. Martin, U. Steinike, S. Rabe, B. Lücke, F.K. Hannour, J. Chem. Soc. - Faraday Trans. 1997, 93, 3855–3862

[137] A. Martin, React. Kinet. Catal. Lett. 1997, 60, 3–8

[138] A. Martin, L. Wilde, U. Steinike, J. Mater. Chem. 2000, 10, 2368–2374

[139] A. Martin, C. Janke, V.N. Kalevaru, Appl. Catal. A Gen. 2010, 376, 13–18

[140] E. Mikolajska, E.R. Garcia, R.L. Medina, A.E. Lewandowska, J.L.G. Fierro, M.A. Bañares, Appl. Catal. A Gen. 2011, 404, 93–102

[141] P.R. Makgwane, N.I. Harmse, E.E. Ferg, B. Zeelie, Chem. Eng. J. 2010, 162, 341–349

[142] V. Mahdavi, H.R. Hasheminasab, S. Abdollahi, J. Chinese Chem. Soc. 2010, 57, 189–198

[143] D.J. Upadhyaya, S.D. Samant, Catal. Today. 2013, 208, 60–65

[144] V. Mahdavi, H.R. Hasheminasab, Appl. Catal. A Gen. 2014, 482, 189–197

[145] C. Santra, S. Shah, A. Mondal, J.K. Pandey, A.B. Panda, S. Maity, et al., Microporous Mesoporous Mater. 2016, 223, 121–128

[146] N. P. Rajan, G. S. Rao, B. Putrakumar, K.V.R. Chary, RSC Adv. 2014, 4, 53419–53428

[147] N. P. Rajan, G. S. Rao, V. Pavankumar, K.V.R. Chary, Catal. Sci. Technol. 2014, 4, 81–92

[148] F. Wang, J.-L. Dubois, W. Ueda, J. Catal. 2009, 268, 260–267

[149] F. Wang, J.-L. Dubois, W. Ueda, Appl. Catal. A Gen. 2010, 376, 25–32

[150] J. Deleplanque, J.-L. Dubois, J.-F. Devaux, W. Ueda, Catal. Today. 2010, 157, 351–358

[151] G. Pavarelli, J. Velasquez Ochoa, A. Caldarelli, F. Puzzo, F. Cavani, J.-L. Dubois, ChemSusChem. 2015, 8, 2250–2259

[152] G. Busca, G. Centi, F. Trifirò, V. Lorenzelli, J. Phys. Chem. 1986, 90, 1337–1344

[153] G. Centi, G. Golinelli, F. Trifiro', Appl. Catal. 1989,48, 13–24

[154] L.M. Cornaglia, E.A. Lombardo, J.A. Andersen, J.L.G. Fierro, Appl. Catal. A Gen. 1993, 100, 37–50

[155] A. Martin, U. Bentrup, B. Lücke, A. Brückner, Chem. Commun. 1999, 1169–1170

[156] A. Brückner, Appl. Catal. A Gen. 2000, 200, 287–297

[157] K. Aït-Lachgar-Ben Abdelouahad, M. Roullet, M. Brun, A. Burrows, C.. Kiely, J.. Volta, et al., Appl. Catal. A Gen. 2001, 210, 121–136

[158] I. Sádaba, S. Lima, A.A. Valente, M. López Granados, Carbohydr. Res. 2011, 346, 2785–2791

[159] F. Cavani, F. Trifirò, A. Vaccari, Catal. Today 1991, 11 (2), 173-301

[160] F. Cavani, F. Folco, L. Ott, J. Riegler, L. Schmid, M. Janssen, WO 2014147161, A2013.03.05 (2014) to Lonza ltd, Swiss

[161] M. T. Weller, J. Chem. Soc. Dalton Trans, 2000, 23, 4227-4240

[162] S. Brauner, P. H. Emmet, E. Teller, J. Am. Chem. Soc. 1938, 60 (2), 309-319

[163] S. Gregg, K. S. W. Sing, Adsorption, Surface Area and Porosity 2nd edition, (1982)

[164] E. Y. Yakovleva, V. Y. Belotserkovskaya, O. V. Skrypnik, J. Of Anal. Chem. 2008, 63 (9), 863-866

[165]U.L.C. Hemamala, F. El-Ghusseina, D.V.S. Muthua, A.M. Krogh Andersen, S. Carlson, L. Ouyang, M.B. Kruger, Solid State Communication, 2007, 141, 680-684

[166]W-S. Dong, J. K. Bartley, F. Girgsdies, R. Schlöglb, G. J. Hutchings, J. Mater. Chem. 2005, 15, 4147–4153